

A generalized Bayesian approach for high-dimensional robust regression with serially correlated errors and predictors

Saptarshi Chakraborty¹, Kshitij Khare² and George Michailidis³ *

Abstract

This paper presents a loss-based generalized Bayesian methodology for high-dimensional robust regression with serially correlated errors and predictors. The proposed framework employs a novel scaled pseudo-Huber (SPH) loss function, which smooths the well-known Huber loss, achieving a balance between quadratic and absolute linear loss behaviors. This flexibility enables the framework to accommodate both thin-tailed and heavy-tailed data effectively. The generalized Bayesian approach constructs a working likelihood utilizing the SPH loss that facilitates efficient and stable estimation while providing rigorous estimation uncertainty quantification for all model parameters. Notably, this allows formal statistical inference without requiring ad hoc tuning parameter selection while adaptively addressing a wide range of tail behavior in the errors. By specifying appropriate prior distributions for the regression coefficients—e.g., ridge priors for small or moderate-dimensional settings and spike-and-slab priors for high-dimensional settings—the framework ensures principled inference. We establish rigorous theoretical guarantees for the accurate estimation of underlying model parameters and the correct selection of predictor variables under sparsity assumptions for a wide range of data generating setups. Extensive simulation studies demonstrate the superiority of our approach compared to traditional quadratic and absolute linear loss-based Bayesian regression methods, highlighting its flexibility and robustness in high-dimensional and challenging data contexts.

1 Introduction

In many applications, the available data for estimating statistical models may be *corrupted* due to various mechanisms, including measurements being incorrectly recorded due to device malfunction (Woodard et al., 2015; Lapinsky and Easty, 2006), erroneous record keeping (De Mingo and Cerrillo-i Martínez, 2018; Georgiou, 2021) and self-reported inaccuracies (Rosenman et al., 2011; Ezzati et al., 2006), inclusion of small distinct sub-populations incorporated in the core data set (Rosenberg et al., 2002; Li et al., 2008) and increasingly due to data poisoning attacks by malicious adversaries (Fan et al., 2022; Ahmed and Kashmoola, 2021; Steinhardt et al., 2017).

A number of concepts and techniques have been developed in the field of *robust statistics* to both assess and mitigate the impact of such corruptions to the estimators of the parameters of the statistical model under consideration; see, e.g., Tukey (1960); Huber (1964, 1972); Rousseeuw (1991); Hampel (2001); Maronna et al. (2019); Huber (1981); Maronna et al. (2006); Huber and Ronchetti (2009). The focus of this paper is to develop a robust estimator procedure for the

¹University at Buffalo, ²University of Florida, and ³University of California, Los Angeles

regression coefficient of the linear model under *high dimensional scaling*, wherein the number of predictors can exceed that of the sample size. Specifically, consider the stochastic linear regression model for data $\{(y_i, \mathbf{x}_i)\}_{i=1}^n$, wherein $y_i \in \mathbb{R}$ and $\mathbf{x}_i \in \mathbb{R}^p$ denote the response and the predictor vector for the i -th observation, respectively, given by

$$y_i = \mathbf{x}_i^T \boldsymbol{\beta} + \varepsilon_i \quad 1 \leq i \leq n, \quad (1)$$

with $\boldsymbol{\beta} \in \mathbb{R}^p$ denoting the vector of regression coefficients, and $\{\varepsilon_i\}_{i=1}^n$ denoting the errors. Note that we allow for both the errors and the predictors to exhibit *dependence*; specifically, (a) the errors $\{\varepsilon_i\}_{i=1}^n$ are identically distributed, but not necessarily independent, (b) the predictor vectors $\{\mathbf{x}_i\}_{i=1}^n$ are identically distributed, but not necessarily independent, but (c) the error process is independent of the predictor process.

The key objective of the paper is to develop flexible Bayesian methodology and provide rigorous theoretical guarantees for the parameters of model (1) when the responses y_i are corrupted or heavy-tailed (as specified in the sequel) in the following two high-dimensional regimes: (i) p is comparable to n (the “large p large n ” setting), or (ii) p is much larger than n (the “large p small n ” setting). In this general and challenging setting, it is prudent to avoid specifying a likelihood, or making other detailed assumptions regarding the error process (such as existence of moments, etc.).

In the frequentist domain, a popular approach to estimate the regression coefficient vector in model (1) in a robust manner, is to employ the Huber loss function Huber (1964), given by

$$\ell_{H,\alpha}(t) = \begin{cases} 2\alpha^{-1}|t| - \alpha^2 & |t| > \alpha^{-1}, \\ t^2 & |t| \leq \alpha^{-1}. \end{cases} \quad (2)$$

The loss $\ell_{H,\alpha}$ corresponds to the widely used ℓ_2 loss function for smaller values of t , and to the ℓ_1 loss for larger values, with the parameter α controlling the balance of the linear and quadratic components. As discussed in the sequel, this balance/combination of the ℓ_2 and ℓ_1 losses has attractive properties. Minimizing the average Huber loss $\frac{1}{n} \sum_{i=1}^n \ell_{H,\alpha}(y_i - \mathbf{x}_i^T \boldsymbol{\beta})$ with respect to $\boldsymbol{\beta}$ leads to a robust estimator for the regression coefficients. With a focus on modern high-dimensional settings, Lambert-Lacroix and Zwald (2011) and Fan et al. (2017) consider M -estimation problems that combine the Huber loss with lasso type penalty functions (see also Rosset and Zhu (2004)). High-dimensional asymptotic properties of the resulting estimators are established assuming independent and identically distributed errors (and predictors), and under suitable moment assumptions on the error distribution. In cases where the data corruption is deemed particularly severe, the ℓ_1 loss function that forgoes the quadratic component in $\ell_{H,\alpha}$ altogether is a popular choice. Methodology and theory using the ℓ_1 (also referred to as least absolute) loss function is developed in Wang (2013) (see also Hansheng Wang and Jiang (2007)).

Our goal is to develop Bayesian methodology which would come with the natural benefit of providing uncertainty quantification for the regression parameter. However, a Bayesian approach requires exact specification of the likelihood. This would require us to make specific and strong assumptions regarding the data generating process that as discussed previously, we would like to avoid. In recent work, Bissiri et al. (2016) propose a generalized Bayesian framework, which in absence of a likelihood, uses relevant loss functions to capture information in the data about the parameter(s) of interest. The exponential of the negative loss is then used as a *generalized likelihood* or a data based weight function, which after combining with the prior, produces a *generalized posterior* belief function for the parameter of interest. For the regression model with a Huber loss function and a prior belief distribution with density $\pi(\boldsymbol{\beta})$ with respect to the

Lebesgue measure on \mathbb{R}^p , the generalized posterior density is given by

$$\pi_{H,\alpha}(\boldsymbol{\beta} \mid \{(y_i, \mathbf{x}_i)\}_{i=1}^n) = \frac{\exp(-\sum_{i=1}^n \ell_{H,\alpha}((\mathbf{x}_i, y_i), \boldsymbol{\beta})) \pi(\boldsymbol{\beta})}{\int_{\mathbb{R}^p} \exp(-\sum_{i=1}^n \ell_{H,\alpha}((\mathbf{x}_i, y_i), \boldsymbol{\beta}')) \pi(\boldsymbol{\beta}') d\boldsymbol{\beta}'} \quad \forall \boldsymbol{\beta} \in \mathbb{R}^p, \quad (3)$$

assuming that the integral in the denominator is finite. This generalized posterior distribution is both intuitive and also supported by a rigorous decision-theoretic justification in Bissiri et al. (2016), wherein it is established that it minimizes a relevant (derived) loss function over the set of all distributions on the parameter space (see discussion in Section 1 of Bissiri et al. (2016)).

The non-smooth nature of the Huber loss $\ell_{H,\alpha}$ can create computational challenges for inference based on the generalized posterior distribution (3). The pseudo-Huber loss function (Hartley and Zisserman, 2003) is a smooth variant/approximation of the Huber loss, defined as

$$\ell_{PH,\alpha}(t) = \alpha^2 \left(\sqrt{1 + \frac{t^2}{\alpha^2}} - 1 \right). \quad (4)$$

It can be shown to be quadratic for small values of t , and approaches linearity for large values of t , with the parameter α controlling the transition point between these two regimes. In the context of linear regression, Park and Casella (2008) consider a two parameter version of $\ell_{PH,\alpha}$, and show that the exponential of the negative pseudo-Huber loss function (added over all observations) corresponds, up to a multiplicative factor, to the data likelihood, if the errors are assumed to be independent and identically drawn from a distribution which corresponds to a specific Generalized Inverse Gaussian (GIG) scale mixture of Gaussian distributions. With all the entries of $\boldsymbol{\beta}$ endowed with independent Laplace prior distributions, a generalized posterior distribution similar to (3) can be obtained with $\ell_{H,\alpha}$ replaced by $\ell_{PH,\alpha}$. The GIG mixture of Gaussians representation mentioned above can be leveraged to derive a Gibbs sampler (with easy to sample from conditional distributions) for the corresponding generalized posterior distribution, termed the Bayesian Huberized lasso (BHL) in Park and Casella (2008). Extensions of the BHL are provided in Kawakami and Hashimoto (2023), wherein hierarchical and empirical Bayes approaches for estimating and leveraging α are proposed.

However, the pseudo-Huber loss function has the following critical drawback: while its limit is indeed t^2 for $\alpha \rightarrow \infty$, its other limit is *not* $|t|$ for $\alpha \rightarrow 0$ as desired and hence can not act as a bridge between the ℓ_2 and ℓ_1 loss functions the way the standard Huber loss does. This discrepancy can lead to substantively inferior performance as shown in Section 2.4.

The *first key contribution* of the paper is proposing a subtle, but critical variant of the pseudo-Huber loss function that provably admits the ℓ_2 and ℓ_1 ones as its respective limits for $\alpha \rightarrow \infty$ and $\alpha \rightarrow 0$, and developing comprehensive high-dimensional generalized Bayesian methodology based on it. Specifically, we define the scaled pseudo-Huber (SPH) loss function as

$$\ell_{SPH,\alpha}(t) = \alpha \sqrt{\alpha^2 + 1} \left(\sqrt{1 + \frac{t^2}{\alpha^2}} - 1 \right). \quad (5)$$

It can easily be shown that $\lim_{\alpha \rightarrow \infty} \ell_{SPH,\alpha}(t) = t^2/2$ while $\lim_{\alpha \rightarrow 0} \ell_{SPH,\alpha}(t) = |t|$. Further, as illustrated in Proposition 1, the corresponding SPH-based generalized likelihood can still be interpreted as the actual likelihood, when the errors are independently and identically distributed according to a GIG scale mixture of Gaussian distributions (see Proposition 1). This is critical for developing scalable sampling procedures from corresponding generalized posterior distributions. Since Laplace prior distributions for the entries of $\boldsymbol{\beta}$ have well-documented issues with posterior coverage etc. Castillo et al. (2015); Bhadra et al. (2019), we focus on two alternative prior

distributions for β : (a) a standard multivariate Gaussian “ridge” prior for β for “large p , large n ” settings, and (b) spike-and-slab priors to introduce exact sparsity in β for “large p , small n ” settings. For both alternatives, we develop efficient Gibbs sampling algorithms (see Section B) which leverage the aforementioned Gaussian scale mixture representation of the scaled pseudo-Huber loss $\ell_{SPH,\alpha}$. This mixture representation assigns a scale parameter to each observation in the dataset. We utilize the marginal posterior distributions of these scale parameters to develop an approach for diagnosing outliers/contaminated observations in the data (see Section 2.3). Specifically, we monitor the posterior dispersion – e.g., the posterior standard deviation to identify the observations

The *second key contribution* of the paper is establishing consistency results for the resulting generalized posterior distributions under the ridge and the spike-and-slab priors under high dimensional scaling. Note that many of the optimization based estimators can be regarded as posterior modes under an appropriate data model and an appropriate prior distribution for β . While high-dimensional asymptotic properties of posterior mode estimators in robust regression have been established in, e.g., Lambert-Lacroix and Zwald (2011); Nevo and Ritov (2016); Fan et al. (2017); Loh (2017); Sun et al. (2020); Loh (2021), **no high-dimensional results regarding consistency of the entire posterior distribution** are available in extant literature for any of the relevant methods (see remark following Theorem 3). Further, even these posterior mode consistency results required (a) independent and identically distributed errors (and predictors), and (b) suitable moment assumptions on the error distribution. With a focus on applications of interest where the error process does not admit any integer moments, and may exhibit *temporal* correlation, we allow the errors (in the true data generating model) to form a *serially correlated second order stationary process* (with no moment assumptions whatsoever), and the predictors to form a mean zero covariance stationary Gaussian process, with mild mixing type assumptions for both processes (see Assumptions A2-A3 or B2-B3 in Section 3). For the ridge prior setting, we establish that the (sequence of) $\ell_{SPH,\alpha}$ based generalized posterior distribution concentrates on an appropriately shrinking neighborhood of the (sequence of) true regression coefficient vector (see Theorem 2). In this setting, no sparsity is assumed and we allow p to grow with n with the constraint $p_n \log p_n = o(n)$. For the spike-and-slab prior setting, we assume sparsity in the (sequence of) true regression coefficient vector corresponding to the data generating model. Further, we allow p to grow sub-exponentially with n , and show that the induced posterior distribution on the space of 2^p possible sparsity patterns in β in the limit places all of its mass on the “true” sparsity pattern (Theorem 3).

The scaled pseudo-Huber loss based methodology is developed in Section 2. Estimation and sparsity selection consistency results are presented in Section 3. Extensive empirical analysis to study the performance of the proposed method is undertaken in Section 4. Additional details related to the methodological developments in Section 2 and proofs of the consistency results in Section 3 are provided in an Appendix.

Notation: The notation for the various probability distributions used in our model and methodology are displayed in Table 1.

2 Robust generalized Bayesian regression based on the scaled Pseudo-Huber Loss

We start the exposition by providing a key normal scale-mixture representation for the pseudo-Huber loss function that is used in the sequel.

Proposition 1. Suppose $\varepsilon \mid \lambda \sim \mathcal{N}(0, \lambda)$ with $\lambda \mid \alpha \sim \text{GIG}(a = 1 + \alpha^2, b = \alpha^2, p = 1)$ for any

Table 1: Notation and density/mass functions for various probability distributions used in this paper.

Notation	Probability density/mass function
$x \sim \text{Inv-Gaussian}(\mu, \sigma)$	$\sqrt{\frac{\sigma}{2\pi}} x^{-3/2} \exp\left(-\frac{\sigma(x-\mu)^2}{2\mu^2 x}\right); \quad x > 0, \mu > 0, \sigma > 0$
$x \sim \text{GIG}(a, b, p)$	$\frac{(a/b)^{p/2}}{2K_p(\sqrt{ab})} x^{p-1} \exp\left[-\frac{1}{2}\left(ax + \frac{b}{x}\right)\right], \quad x > 0, a > 0, b > 0, -\infty < p < \infty$
$x \sim \text{Inv-Gamma}(a, b)$	$f(x) = \frac{b^a}{\Gamma(a)} (1/x)^{a+1} \exp(-b/x); \quad x > 0; a > 0, b > 0$
$x \sim \text{Beta}(a, b)$	$\frac{\Gamma(a+b)}{\Gamma(a)\Gamma(b)} x^{a-1} (1-x)^{b-1}; \quad 0 < x < 1; a > 0; b > 0$
$x \sim \text{Exponential}(\lambda)$	$\frac{1}{\lambda} \exp(-x/\lambda); \quad x > 0; \lambda > 0$
$x \sim \mathcal{N}(\mu, \sigma^2)$	$\frac{1}{\sqrt{2\pi}\sigma} \exp\left[-\frac{1}{2\sigma^2} \left(\frac{x-\mu}{\sigma}\right)^2\right]; \quad -\infty < x < \infty; \lambda > 0$
$\mathbf{x} \sim \mathcal{N}_p(\boldsymbol{\mu}, \Sigma)$	$\frac{1}{\sqrt{2\pi}^{ \Sigma }} \exp\left[-\frac{1}{2} (\mathbf{x} - \boldsymbol{\mu})^T \Sigma^{-1} (\mathbf{x} - \boldsymbol{\mu})\right]; \quad \mathbf{x} \in \mathbb{R}^p; \boldsymbol{\mu} \in \mathbb{R}^p, \Sigma \in \mathbb{S}^{p \times p}$
$x \sim \text{Bernoulli}(p)$	$p^x (1-p)^{1-x} \quad x \in \{0, 1\}; \quad 0 \leq p \leq 1$

fixed $\alpha > 0$. Then, the λ -marginalized density $f_\varepsilon(\varepsilon | \alpha)$ of ε at a fixed $\alpha > 0$ has the form:

$$f_\varepsilon(\varepsilon | \alpha) \propto \exp\left[-\alpha\sqrt{1+\alpha^2} \left(\sqrt{1+\left(\frac{\varepsilon}{\alpha}\right)^2} - 1\right)\right],$$

which is the generalized density associated with the scaled pseudo-Huber loss function with tuning parameter $\alpha \in (0, \infty)$.

Within the framework of the generalized Bayes approach discussed in the introduction, the above λ -marginalized density $f_\varepsilon(\varepsilon | \alpha)$ can be thought of as the error distribution producing the *generalized likelihood* associated with a scaled pseudo-Huber loss-based linear regression. Consequently, the Proposition enables the construction of the following hierarchical/multilevel (generalized) likelihood layer for robust pseudo-Huber regression:

$$y_i | \boldsymbol{\beta}, \lambda_i \sim \mathcal{N}(\mathbf{x}_i^T \boldsymbol{\beta}, \lambda_i), \quad \lambda_i | \alpha \sim \text{GIG}(a = 1 + \alpha^2, b = \alpha^2, p = 1) \quad (6)$$

wherein the parameters $\{\lambda_i\}$ are treated as latent/augmented data.

Remark A in Section A in the Appendix shows that for $\alpha \rightarrow 0$, $f_\varepsilon(\varepsilon | \alpha)$ converges to the density of the standard Laplace distribution, while for $\alpha \rightarrow \infty$ to that of the standard normal distribution, the two error distributions associated with the ordinary ℓ_2 and the robust ℓ_1 (median) regression respectively. Thus the proposed framework (6) enables an amalgamation of the standard ℓ_2 and the ℓ_1 regression models. The former can be recovered by setting $\lambda_i \equiv \sigma^2$ (i.e., setting a degenerate $\mathbb{1}_{\{\sigma^2\}}$ mixing distribution for λ_i) for some *common* parameter $\sigma^2 > 0$ for all i while the latter can be obtained by fixing the parameters of the GIG distribution to $\text{GIG}(a = 2, b = 0, p = 1) \equiv \text{Exponential}(1)$ for λ_i .

Remark. The parameter α can be thought of as a “*global*” *contamination* parameter in the following sense. The closer α is to 0, the closer is the pseudo-Huber loss function to the ℓ_1 loss, and consequently the larger the degree of contamination of the responses. At the other end of the spectrum, as $\alpha \rightarrow \infty$, the pseudo-Huber loss approaches the ℓ_2 loss and hence the degree of contamination of the responses is rather limited. Consequently, in the proposed Bayesian formulation, the posterior distribution of α would provide an assessment of the amount of “*global* contamination” present in the data under consideration.

Remark. Throughout, we assume the predictor variables to be centered and, therefore, ignore an additional intercept parameter μ in the model. If needed, a straightforward generalization of the model of the form

$$y_i \mid \mu, \boldsymbol{\beta}, \lambda_i \sim \mathcal{N}(\mu + \mathbf{x}_i^T \boldsymbol{\beta}, \lambda_i), \quad \lambda_i \mid \alpha \sim \text{GIG}(a = 1 + \alpha^2, b = \alpha^2, p = 1)$$

will allow incorporation of intercept terms.

Remark. Similar to Kozumi and Kobayashi (2011), one can consider an additional *global* scaling parameter $\sigma > 0$ in the model:

$$y_i \mid \boldsymbol{\beta}, \lambda_i, \sigma \sim \mathcal{N}(\mathbf{x}_i^T \boldsymbol{\beta}, \sigma^2 \lambda_i), \quad \lambda_i \mid \alpha \sim \text{GIG}(a = 1 + \alpha^2, b = \alpha^2, p = 1)$$

This can potentially aid some additional flexibility for the model to permit modeling of a richer set of data.

To complete the specification of the generalized Bayes posterior distribution of the model, the key model (regression) parameter $\boldsymbol{\beta}$ and the tuning parameter α – and additionally the intercept parameter μ and/or the global scaling parameter σ , if present, are endowed with prior distributions. We discuss some specific choices for the prior distribution next.

2.1 Specification of distributions for the parameters $\boldsymbol{\beta}$ and α of the scaled pseudo-Huber regression model

We consider independent prior distributions for the regression parameter $\boldsymbol{\beta}$ and the pseudo-Huber tuning/balance parameter α . Two specifications for the prior distribution of $\boldsymbol{\beta}$ are considered: the first is better suited for a low-dimensional setting wherein the number of predictors is of the order of the sample size ($p = O(n)$), and the second is suited for high-dimensional data ($p \gg n$). We list the two prior distributions for $\boldsymbol{\beta}$ as follows.

(1) A *Gaussian, weakly informative prior distribution* of the form:

$$\boldsymbol{\beta} \sim \mathcal{N}(\boldsymbol{\beta}_0, Q^{-1}), \tag{7}$$

where $\boldsymbol{\beta}_0$ is a fixed prior mean and Q is a fixed prior precision matrix for the regression parameter $\boldsymbol{\beta}$. Commonly, $\boldsymbol{\beta}_0$ is set to the zero vector, and Q is set to a diagonal matrix with some moderately small diagonal entries such as 0.01, effectuating independent vague priors for the coordinates of $\boldsymbol{\beta}$.

(2) A *hierarchical spike-and-slab prior distribution* of the form:

$$\begin{aligned} \beta_j \mid \gamma_j = 0 &\sim \mathbb{1}_{\{0\}}, & \beta_j \mid \gamma_j = 1 &\sim \mathcal{N}(0, \tau^2) \\ \gamma_j &\sim \text{Bernoulli}(q), & q &\sim \text{Beta}(a_q, b_q), \end{aligned} \tag{8}$$

where γ_j is a Bernoulli 0-1 random variable with $[\gamma_j = 1]$ implying that the j -th predictor is “active”. Conditional on $\gamma_j = 1$, β_j is endowed with a “slab” prior $\mathcal{N}(0, \tau^2)$ with some reasonably large τ such as $\tau = 100$. On the other hand, when $\gamma_j = 0$, β_j is fixed (has a degenerate distribution) at zero. The a priori proportion q of “active” predictors can be specified; we consider a $\text{Beta}(a_q, b_q)$ prior on q for its data-driven estimation.

For the tuning/balance parameter α , a Gamma prior distribution is considered:

$$\alpha^2 \sim \text{Gamma}(a_\alpha, b_\alpha).$$

In addition, if the model includes an intercept term μ , a vague normal prior such as $\mu \sim N(0, \tau_\mu^2)$ can be used for some reasonably large τ_μ such as $\tau_\mu = 100$. In addition, if the model includes an additional global scaling parameter σ , one may use an inverse gamma prior of the form $\sigma^2 \sim \text{Inv-Gamma}(a_\sigma, b_\sigma)$.

2.2 Posterior Distribution Computation

The complicated structures of the likelihood and the prior distribution – for both low/moderate dimensional and high-dimensional cases – render the resulting posterior distributions intractable, precluding independent random drawing from the posterior. Since principled uncertainty quantification is a key motivation of this paper, we focus on Markov chain Monte Carlo (MCMC) sampling from the posterior, which permits theoretically guaranteed computation for the posterior distribution. Below, we summarize an efficient Gibbs-type algorithm for MCMC sampling from the target posterior distribution. We first describe MCMC sampling of model parameters given a fixed value of the tuning parameter α . Then, we describe an approach for MCMC sampling for α for a full Bayesian inference.

MCMC sampling from the posterior distribution given α . (1) With the weakly informative Gaussian prior (7) on β , the form of the posterior distribution is given in Section B in the Appendix. The conditional (posterior) distributions for the model parameters for a fixed value of the balance parameter α have closed-form expressions involving standard probability distributions, namely, Gaussian (for β and the intercept μ , if exists), generalized inverse Gaussian (for $\{\lambda_i\}$) and inverse gamma (for σ^2 , if exists) that permit efficient random sampling. Hence, a standard Gibbs sampling algorithm can be devised for MCMC drawing from the α -conditioned posterior distribution.

(2) With the hierarchical spike-and-slab prior in (8) for β , the (full) conditional posterior distributions of the model parameters given a fixed value of α still have analogous closed-form expressions, with similar conditional distributions as in the weakly informative Gaussian prior case for β , $\{\lambda_i\}$, μ (if exists) and σ^2 (if exists). In addition, the full conditional distribution for each spike and slab “active” predictor indicator γ_i each has a Bernoulli structure, and the corresponding prior proportion parameter q has a full conditional beta distribution. Therefore another Gibbs sampling scheme yields draws from the α -conditioned posterior distribution. Detailed steps for the Gibbs samplers for the settings (1) and (2) are provided in Section B in the Appendix.

MCMC sampling for α . The integral producing the marginal posterior density of α is unavailable in closed form, and the conditional posterior density of α , given the remaining model parameters, does not have a standard form for efficient random sampling. A rejection sampler can be constructed using analytical upper bounds for the modified Bessel function-based terms to draw samples from the conditional posterior distribution of α given $\{\lambda_i\}$. However, the general non-tightness of these bounds can lead to substantial inefficiency in practice. Instead, we suggest using slice sampling (Neal, 2003) for Markov chain sampling from the $\{\lambda_i\}$ -integrated conditional posterior density of α given β (and μ , and σ^2 , if exists). Integrating out $\{\lambda_i\}$ from the full conditional distribution for sampling α results in a blocked/collapsed MCMC sampler; such blocking/collapsing can lead to improved mixing for the resulting Markov chain.

Remark. Instead of drawing posterior samples for α for full Bayesian inference, one may use a point estimate of α for *empirical Bayes inference* for the remaining model parameters. Leveraging the conditional posterior distribution of the model parameters as described, an iterative Gibbs expectation maximization (Gibbs EM) algorithm (Casella, 2001) may be constructed that alternates between maximizing the posterior conditional density of α and MCMC sampling from the remaining model parameters. The consequent algorithm will be computationally faster than the complete MCMC algorithm described above if the maximization step for α is limited only to burn-in iterations of the Gibbs EM algorithm. The resulting empirical Bayes estimators for the model parameters will still permit rigorous β inference, variable selection (for the high dimensional setup), and prediction, thanks to the strong theoretical guarantees for the model presented

in Section 3. However, as discussed in Section 2.3 below, the shape of the posterior distribution of α , as opposed to only a single point estimate, provides valuable diagnostic information about the contamination levels present in the data and hence can be insightful in exploratory data analyses.

Remark. The computational complexity for each iteration of the proposed slice-within-Gibbs sampler can be derived in terms of n and p , and additionally, the sparsity level $\sum_{j=1}^p \gamma_j$ (for the spike and slab case). For the normal (ridge) prior model, the computational complexity for each MCMC iteration is $O(n) + O(p^3)$ owing to the $O(n)$ -operations for $\{\lambda_i; i = 1, \dots, n\}$ sampling and $O(p^3)$ operations for β sampling which requires an inversion of a $p \times p$ matrix for multivariate normal generation. A regular *stepping out* slice sampling with a pre-specified maximum number of *window*s (Neal, 2003) for α is done in constant $O(1)$ operations and thus does not change the overall cost complexity of the sampler in terms of n and p . In the spike and slab prior model, sampling β reduces into an $O((\sum_{j=1}^p \gamma_j)^3)$ operation which can be substantially smaller than $O(p^3)$ if the sparsity level is high, i.e., $\sum_{j=1}^p \gamma_j \ll p$. However, sampling from the full conditional distribution of each γ_j requires $O((1 + \sum_{j' \in \{1, \dots, p\} \setminus \{j\}} \gamma_{j'})^3)$ operations owing to the computation of the determinants (see Appendix B) in its Bernoulli mass function. Collectively for all $\{\gamma_j\}$ this leads to a computation complexity of $O(p(1 + \sum_{j=1}^p \delta_j)^3)$ which can be substantial, e.g., near $O(p^4)$ if the sparsity level is low, i.e., $\sum_j^p \delta_j$ is nearly in the same order as p . The overall cost complexity for each iteration of the MCMC sampler for the spike and slab model is thus $O(n) + O(p(1 + \sum_{j=1}^p \delta_j)^3)$.

2.3 Diagnosis of contaminated observations through the micro-level contamination parameters

Based on the hierarchical model structure, the parameter λ_i serves as the individualized Gaussian scale parameter for the response y_i , with independent Generalized Inverse Gaussian (GIG) priors assigned to λ_i . The posterior distribution is influenced by both the working model and the data; hence, for contaminated observations with heavy-tailed errors, the marginal posterior distribution of the corresponding λ_i is expected to exhibit higher variability. We propose using this heuristic to identify contaminated observations. Specifically, we suggest examining the marginal posterior standard deviations $s_i = \text{sd}(\lambda_i \mid \text{data})$ or their scaled variants $\tilde{s}_i = s_i / \min_{i'=1, \dots, n} s_{i'}$ to determine the contaminated observations. In practice, observations with significantly large s_i or \tilde{s}_i can be determined using standard outlier detection methods based on empirical quantiles and interquartile ranges for s_i or \tilde{s}_i (Chambers, 2018; McGill et al., 1978) as implemented in typical boxplot computation routines, including the default boxplot method in R. This heuristic is expected to perform well in applications with low-to-moderate contamination proportions.

To visualize the heuristic's performance as the contamination proportion varies, we performed two simulation experiments. In each experiment, data were generated from a linear regression model with $p = 5$ predictors and regression coefficients $\beta = (2, 2, 0, 0, 0)^T$. Predictors were generated from autoregressive AR(1) processes with a standard normal base distribution and a serial correlation coefficient of 0.4. The first two predictors, corresponding to the non-zero regression coefficients, had a correlation of 0.9, while the remaining three predictors were independent of each other and the first two.

In the first simulation, residual errors were generated from a 90%-10% mixture of (a) an AR(1) process with a standard normal base distribution and a serial correlation of 0.2 (the uncontaminated distribution) and (b) an independent Cauchy(0, 5) distribution (the contaminant distribution). Contaminated observations were labeled. In the second experiment, a 50%-50%

mixture of the same distributions was used to generate the residual errors. In each setting we generated datasets with $n = 20$ (small), $n = 50$ (medium), and $n = 500$ (large) and fit the proposed scaled pseudo-Huber model with a ridge prior on the regression coefficients using the proposed MCMC sampler (10,000 final draws after discarding the initial 10,000 draws as burn-in).

We then obtained the marginal posterior standard deviations $\{\tilde{s}_i\}$ of the micro-level contamination parameter $\{\lambda_i\}$ and their scaled variants for each dataset. These values are shown as boxplots in Figure 1—with separate boxplots for the contaminated and non-contaminated observations (true labels). As illustrated, there is a clear distinction between $\{\tilde{s}_i\}$ values for contaminated and non-contaminated observations across all data sizes and contamination proportions. The $\{\tilde{s}_i\}$ values for contaminated observations are notably higher. Thus, a standard empirical quantile-based outlier detection method applied to these $\{\tilde{s}_i\}$ values is expected to identify the truly contaminated observations with reasonable precision.

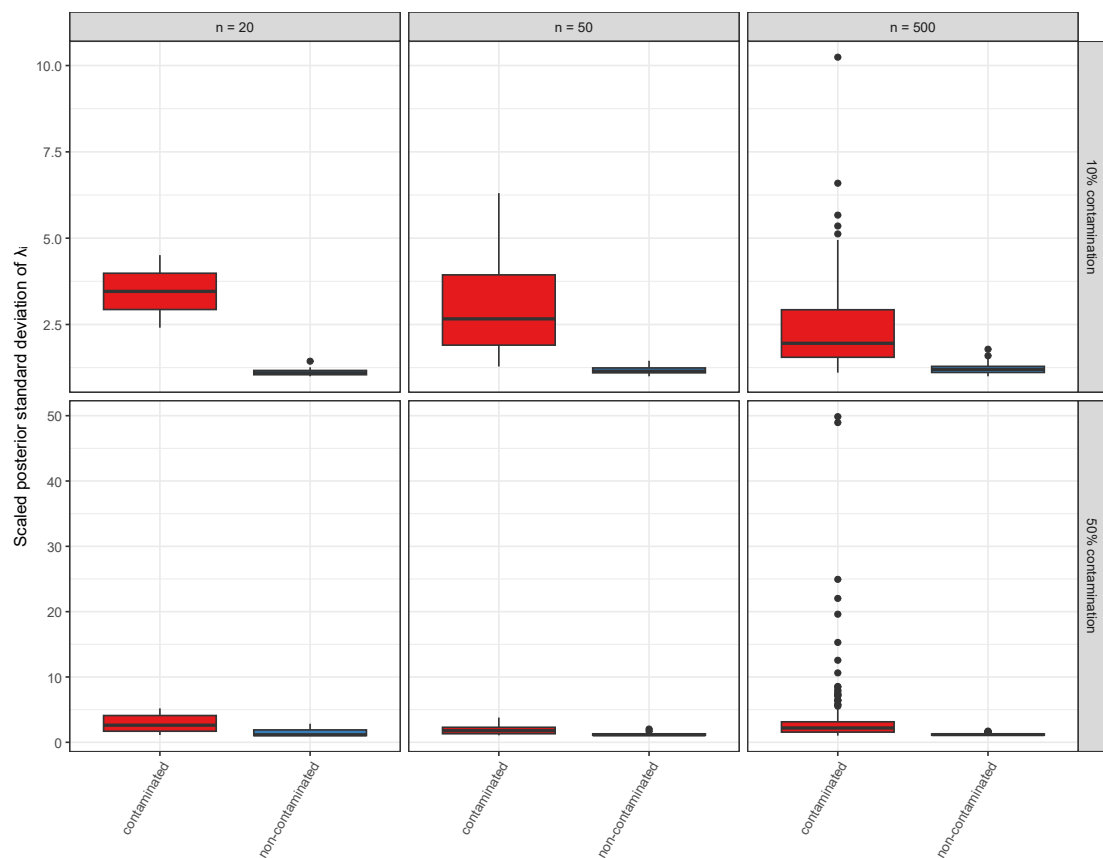


Figure 1: Boxplots of scaled posterior standard deviations of $\{\lambda_i\}$ (y axis) obtained separately for contaminated and non-contaminated observations.

2.4 Empirical assessment of the effect of ‘scaling’ the pseudo-Huber loss

As noted in the Introduction, a key novelty of our approach is the proposed scaling of the pseudo-Huber loss, which ensures that the loss asymptotically becomes the *exact* ℓ_1 and ℓ_2 losses as $\alpha \rightarrow 0$ and $\alpha \rightarrow \infty$ respectively. The unscaled pseudo-Huber loss, by contrast, does not converge to ℓ_1 when $\alpha \rightarrow 0$ and thus is not guaranteed to provide robust Bayesian inference in the presence of heavy contamination—precisely where the ℓ_1 loss is preferred over the ℓ_2 loss.

To assess the impact of this non-convergence of the unscaled pseudo-Huber loss on inference, we considered the first simulation experiment described in Section 2.3 with a 90%-10% mix of contaminated and non-contaminated observations in each of the three simulated datasets of sizes $n = 20$ (small), $n = 50$ (medium), and $n = 500$ (large). On each dataset, we fitted two generalized Bayesian pseudo-Huber models: one with a scaled pseudo-Huber loss and one with an unscaled loss, using the proposed MCMC algorithm and its modification (analogous to) to handle the unscaled loss, respectively. For comparison, we also fitted Bayesian ℓ_1 and ℓ_2 regression models using MCMC sampling. Each MCMC was run for 10,000 iterations after discarding the initial 10,000 iterations as burn-in.

To alongside assess the contamination diagnostic method proposed in Section 2.3, we obtained the scaled posterior standard deviations $\{\tilde{s}_i\}$ of $\{\lambda_i\}$ from each scaled pseudo-Huber fit and applied an empirical quantile-based outlier detection approach on these $\{\tilde{s}_i\}$ values using the default boxplot function in R. The observations $\{i\}$ corresponding to the identified outliers in $\{\tilde{s}_i\}$ were deemed contaminated and were subsequently discarded from the original training datasets. We then reran the Bayesian scaled pseudo-Huber model on these *filtered* datasets using MCMC sampling.

Posterior draws for $\boldsymbol{\beta} = (\beta_1, \dots, \beta_5)^T$ were collected from each model fit on each dataset, and the first two coordinates of these draws were visualized as scatterplots. These scatterplots are displayed in Figure 2 with overlaid contour lines (red curves) showing the 50%, 80%, and 95% highest posterior density regions for (β_1, β_2) computed from the posterior MCMC draws. The figure also visualizes the corresponding true value $(2, 2)$ (yellow dot) of (β_1, β_2) .

We make the following observations from Figure 2. First, the scaled pseudo-Huber Bayesian model demonstrates impressive estimation performance for (β_1, β_2) , with the posterior closely aligning with the true values across all dataset sizes (small, medium, and large). The posteriors concentrate well around the true values, with the degree of concentration increasing with the sample size. Second, the posteriors for the scaled pseudo-Huber model resemble those of the ℓ_1 model, which is expected given the substantial contamination in the generated data, causing the scaled pseudo-Huber fit to trace the ℓ_1 model fit.

Third, the unscaled pseudo-Huber fits exhibit a highly sporadic pattern, with no clear concentration of the posterior around the true values, contrasting sharply with the scaled pseudo-Huber posteriors. This sporadicity limits the utility of the unscaled pseudo-Huber model for inference in high contamination settings. The ℓ_2 fits also appear sporadic, though to a lesser degree than the unscaled pseudo-Huber fits. Finally, the contamination filtering (based on the diagnostic proposed in Section 2.3) and subsequent refitting strategy result in a small but positive improvement in the posterior, aligning it more closely with the true values.

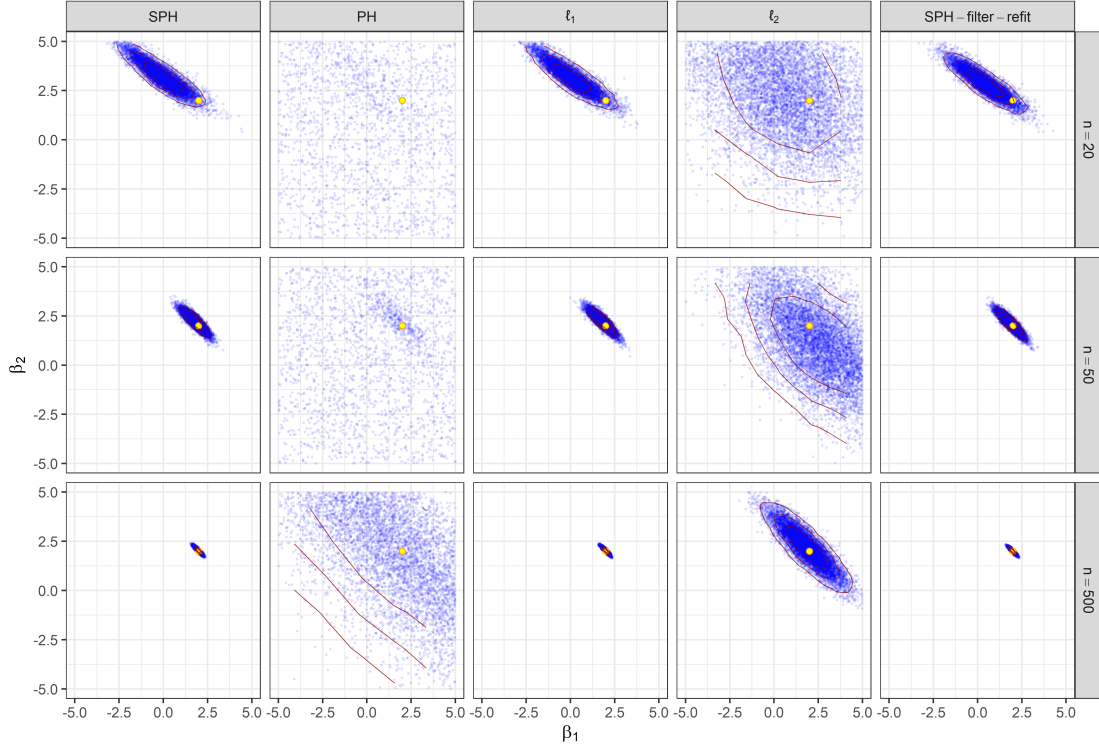


Figure 2: Visualizing the joint generalized posterior distributions of the first two coordinates (β_1, β_2) of β , under different losses and a weakly informative Gaussian prior belief distribution for β , through point clouds and density contours. The contour lines represent the joint highest posterior density sets for (β_1, β_2) at 50%, 80%, 90%, and 95% probability levels.

3 Theoretical guarantees: consistency of pseudo-Huber based robust estimators for linear regression

Consider the linear regression model in (1). As discussed in Section 2, we consider two settings, the first wherein the number of predictors is of the order of the sample size and the second corresponding to high-dimensional scaling.

For both settings, we consider the generalized likelihood function $\mathcal{L}(\beta) := \exp(-nH_\alpha(\beta))$, with

$$H_\alpha(\beta) := \frac{1}{n} \sum_{i=1}^n \ell_\alpha(Y_i - \mathbf{x}_i^T \beta), \quad (9)$$

and ℓ_α corresponding to the scaled pseudo-Huber loss function

$$\ell_\alpha(x) = \alpha \sqrt{1 + \alpha^2} \left(\sqrt{1 + \left(\frac{x}{\alpha}\right)^2} - 1 \right). \quad (10)$$

3.1 Consistency in the $p = \mathcal{O}(n)$ setting

As discussed in Section 2.1, for this setting a Gaussian prior distribution on the regression coefficients is imposed, given by

$$\pi_{ridge}(\boldsymbol{\beta}) \propto \exp(-\tau^2 \boldsymbol{\beta}^T \boldsymbol{\beta}) \quad \forall \boldsymbol{\beta} \in \mathbb{R}^p, \quad (11)$$

for some $\tau^2 > 0$. The posterior density for the posited working Bayesian model is given by

$$\pi_{ridge}(\boldsymbol{\beta} | Y) \propto \exp(-nH_\alpha(\boldsymbol{\beta}) - \tau^2 \boldsymbol{\beta}^T \boldsymbol{\beta}) \quad \forall \boldsymbol{\beta} \in \mathbb{R}^p. \quad (12)$$

We consider an asymptotic setting wherein the number of regressors $p = p_n$ grows with the sample size n . For the purposes of asymptotic evaluation, we allow $\alpha = \alpha_n$ to vary with n as well, but consider it to be fixed/known and do not place a prior distribution on α in the working model. The true data generating model is given by

$$Y_{i,n} = \mathbf{x}_{i,n}^T \boldsymbol{\beta}_{0,n} + \epsilon_{i,n} \quad i = 1, 2, \dots, n. \quad (13)$$

for every $n \geq 1$, with $\boldsymbol{\beta}_{0,n}$ denoting the vector of true regression coefficients. In particular, we make the following regularity assumptions regarding the data generating model and the prior precision parameter τ^2 .

- (Assumption A1) - $p_n \log p_n = o(n)$, $p_n \rightarrow \infty$, $\alpha_n \rightarrow \infty$ and $\alpha_n \sqrt{\frac{p_n}{n}} \rightarrow 0$. Here \tilde{M} is an appropriately chosen constant.

The growth rate of p_n in this setting is constrained by the lack of any low dimensional structure, such as sparsity on $\boldsymbol{\beta}_{0,n}$. Note that p_n would be allowed to grow at a much faster rate (sub-exponentially) in the spike-and-slab based consistency analysis (Section 3.2).

- (Assumption A2) - For every $n \geq 1$, the predictor vectors $\{\mathbf{x}_{i,n}\}_{i=1}^n$ are independent of the errors $\{\epsilon_{i,n}\}_{i=1}^n$, and form a covariance stationary Gaussian sequence with $\Gamma_n(h) := Cov(\mathbf{x}_{i,n}, \mathbf{x}_{i+h,n})$ for every $-(n-1) \leq h \leq n-1$ and $1 \leq i, i+h \leq n$. There exists $\kappa_1 > 0$ (not depending on n) such that

$$0 < \kappa_1 < \lambda_{\min}(\Gamma_n(0)) \leq \lambda_{\max}(\Gamma_n(0)) < \kappa_1^{-1} < \infty,$$

and

$$\kappa_2 := \sup_{n \geq 1} \sum_{h=0}^{n-1} \|\Gamma_n(h)\|_2 < \infty.$$

- (Assumption A3) - For every $n \geq 1$, the errors $\{\epsilon_{i,n}\}_{i=1}^n$ form a second order stationary sequence. Also, for the uniformly bounded function $g(x) := E[(1+x^2 + (1/\kappa_1)Z^2)^{-3/2} Z^2]$ (with Z standard normal), we have

$$K_\epsilon := \sup_{n \geq 1} \left\{ Var(g(\epsilon_{1,n})) + 2 \sum_{i=2}^n |Cov(g(\epsilon_{1,n}), g(\epsilon_{i,n}))| \right\} < \infty.$$

Some standard and common settings where Assumption A3 is satisfied are presented next.

- The error process forms an m -dependent second order stationary sequence (such as a moving average process); in this case $Cov(g(\epsilon_{1,n}), g(\epsilon_{i,n})) = 0$ for every $i > m$.

- The errors form a second order stationary α -mixing sequence (see for example Jones (2004)) with $\sum_{k=1}^{\infty} \alpha_{\epsilon}(k) < \infty$. Since g is uniformly bounded by κ_1 , it follows by (Ibragimov, 1962, Theorem A.5) that $|Cov(g(\epsilon_{1,n}), g(\epsilon_{i,n}))| \leq 4\kappa_1^2 \alpha_{\epsilon}(i-1)$ for every $i \geq 2$, and hence Assumption A3 is satisfied.
- In particular, Assumption A3 is satisfied if the errors form a stationary and geometrically ergodic Markov chain (since such a Markov chain is exponentially fast α -mixing and g is uniformly bounded, see Chan and Geyer (1994)).
- (Assumption A4) - The prior distribution's precision parameter τ_n^2 satisfies

$$\tau_n^2 = O(\alpha\sqrt{np_n}/\|\beta_{0,n}\|).$$

Note that under a Gaussian likelihood based working model, the posterior mode for β (with the prior distribution specified in (11)) is given by the ridge regression estimator $\hat{\beta}_{ridge} = (X^T X + \tau^2 I_p)^{-1} X^T \mathbf{y}$. It is clear that some upper bound on the parameter τ^2 (depending also on $\beta_{0,n}$) is needed for consistency of $\hat{\beta}_{ridge}$. To see this, consider the special case when X is semi-orthogonal, in particular, $X^T X = nI_p$. In this case

$$\hat{\beta}_{ridge} = \frac{n}{n + \tau^2} \beta_{0,n} + \frac{1}{n} X^T \epsilon.$$

The $\|\ell_2\|$ -norm of the second (error) term on the right-hand-side can be shown to converge to zero (in probability) by routine arguments assuming Gaussian errors, and it is clear that the condition $\frac{\tau^2}{n + \tau^2} \|\beta_{0,n}\|$ is necessary for consistency of $\hat{\beta}_{ridge}$. Assumption A4 can be thought as its counterpart in the current setting (with possibly non-Gaussian and correlated errors).

Let P_0 denote the underlying probability measure corresponding to the true data generating model, and E_0 the expectation with respect to P_0 . In the subsequent analysis, we will often refer to $Y_{i,n}, \epsilon_{i,n}, \mathbf{x}_{i,n}, Q_n, \beta_{0,n}$ by $Y_i, \epsilon_i, \mathbf{x}_i, Q, \beta_0$ for notational convenience. Since $\ell''_{\alpha}(x) = \sqrt{1 + \alpha^{-2}}(1 + (x/\alpha))^{-3/2} > 0$ for every $x \in \mathbb{R}$, it follows that the Hessian matrix of H given by

$$\nabla^2 H_{\alpha}(\beta) = \frac{1}{n} \sum_{i=1}^n \ell''_{\alpha}(Y_i - \mathbf{x}_i^T \beta) \mathbf{x}_i \mathbf{x}_i^T$$

is positive definite for every $\beta \in \mathbb{R}^p$. It follows that

$$Q_{\alpha}(\beta) := \alpha^{-1} H_{\alpha}(\beta) + \frac{\tau^2}{n\alpha} \beta^T \beta$$

is strictly convex and has a unique minimizer. This minimizer is of course, also the posterior mode, and will be denoted by $\hat{\beta}_{pm,ridge}$. The first task is to study the asymptotic properties of $\hat{\beta}_{pm,ridge}$ under the high-dimensional setting described above.

Theorem 1 (Posterior mode consistency with ridge prior). Under Assumptions A1-A4

$$P_0 \left(\|\hat{\beta}_{pm,ridge} - \beta_0\| > \tilde{M} \alpha_n \sqrt{\frac{p_n}{n}} \right) \rightarrow 0$$

as $n \rightarrow \infty$, for an appropriate constant \tilde{M} .

With the consistency of the posterior mode in hand, we proceed to establish the consistency of the *entire posterior distribution*. For this result, we need to slightly strengthen our set of assumptions by adding the following regularity conditions.

- (Assumption A5) - (a) The prior precision parameter τ^2 satisfies $\tau^2 = O\left(\min\left(\frac{\alpha\sqrt{np}}{\|\beta_0\|}, \frac{n^2}{p}\right)\right)$, (b) the error process has a finite first moment, i.e., $E|\epsilon_1| < \infty$, and (c) there exists a constant $\kappa_3 > 0$ such that $\lambda_{\min}(\Theta_n) \geq \kappa_3$ for every $n \geq 1$. Recall that Θ_n denote the $n \times n$ block partitioned matrix whose $(i, j)^{th}$ block is given by $\Gamma_n(i - j)$ for $1 \leq i, j \leq n$.

The following result shows that the posterior distribution asymptotically places all of its mass on a neighbourhood of radius $O(\alpha_n \sqrt{\frac{p_n}{n}})$ around the true parameter β_0 .

Theorem 2 (Posterior distribution consistency with ridge prior). Let $\Pi_{\text{ridge}}(\cdot | \mathbf{Y})$ denote the posterior distribution for the Bayesian working model based on the likelihood in (9) and prior distribution in (11). Under Assumptions A1-A5, there exists a constant \tilde{M}^* such that

$$E_0 \left[\Pi \left(\|\beta - \beta_0\| > \tilde{M}^* \alpha_n \sqrt{\frac{p_n}{n}} \mid \mathbf{Y} \right) \right] \rightarrow 0$$

as $n \rightarrow \infty$.

Remark. With a Gaussian likelihood based working model, a ridge prior distribution on β , and serially correlated *Gaussian errors and predictors* in the data generating model (with relevant regularity assumptions on their respective spectral densities), minor modifications to arguments in Ghosh et al. (2021) lead to a posterior convergence rate of $\sqrt{\frac{p}{n}}$, when *no low-dimensional structure* is imposed on $\beta_{0,n}$ and $p_n \log p_n = o(n)$. In the current setting, where minimal assumptions are placed on the error process (existence of first moment and weak dependence outlined in Assumption A3) in the data generating model, Theorem 2 establishes a convergence rate of $\alpha_n \sqrt{\frac{p}{n}}$. To summarize, the rate in Theorem 2 contains an extra factor of α_n as compared to the Gaussian error setting, but is obtained under *significantly weaker assumptions* on the error process (and of course using a different, pseudo-Huber based, working model).

3.2 Sparsity selection consistency in the high-dimensional setting

Next, we focus on the high-dimensional setting where sparsity is induced in β by the use of independent spike-and-slab prior distributions on the entries of β as in (8). The spike-and-slab posterior can be obtained by combining this prior with the generalized likelihood in (9). We begin by defining relevant sparsity-based notation.

Note that every element of the set $\{0, 1\}^p$ represents a possible sparsity pattern in the regression coefficient vector β . In particular, $\mathbf{s} \in \{0, 1\}^p$ represents the sparsity pattern where the coefficients with indices in $\text{ind}(\mathbf{s}) := \{\mathbf{j} : \mathbf{s}_{\mathbf{j}} = \mathbf{1}\}$ are deemed significant and other coefficients are deemed insignificant. Given a sparsity pattern \mathbf{s} , for any $\mathbf{a} \in \mathbb{R}^p$, define the sub-vector $\mathbf{a}_{\mathbf{s}}$ as $\mathbf{a}_{\mathbf{s}} = (a_j)_{j \in \text{ind}(\mathbf{s})}$. Similarly, for any $p \times p$ matrix A , define the submatrix $A_{\mathbf{s}}$ as $A_{\mathbf{s}} = ((a_{jk}))_{j,k \in \text{ind}(\mathbf{s})}$. Finally, we define $|s| := |\{j : s_j = 1\}|$, and for any $\mathbf{b} \in \mathbb{R}^{|s|}$, $Q_{\alpha}(\mathbf{b})$ will implicitly stand for the function $Q_{\alpha}(\mathbf{b}_{\text{fill},s})$, where the $b_{\text{fill},s,s_j} = 1$ for $1 \leq j \leq |s|$ and all other entries of $\mathbf{b}_{\text{fill},s}$ are zero.

Note that the spike-and-slab posterior distribution induces a probability distribution over the space of all possible sparsity patterns, or equivalently $\{0, 1\}^p$. Let $\Pi_{SS}(\mathbf{s} | \mathbf{Y})$ denote the probability mass assigned to the sparsity pattern \mathbf{s} by the spike-and-slab posterior distribution.

Routine calculations show that

$$\Pi_{SS}(\mathbf{s} \mid \mathbf{Y}) \propto \left(\frac{q\tau}{(1-q)\sqrt{2\pi}} \right)^{|\mathbf{s}|} \int \exp(-n\alpha Q_\alpha(\boldsymbol{\beta}_s)) d\boldsymbol{\beta}_s \quad (14)$$

for every $\mathbf{s} \in \{0, 1\}^p$.

Consider the true data generating model described in (13). Recall that P_0 denotes the underlying probability measure corresponding to the true data generating model, and E_0 the expectation with respect to P_0 . Further, let $\mathbf{s}_0 \in \{0, 1\}^p$ represent the sparsity pattern corresponding to $\boldsymbol{\beta}_0$ (the ‘‘true’’ sparsity pattern). The first task will be to establish *strong selection consistency*, i.e.,

$$\Pi_{SS}(\mathbf{s}_0 \mid \mathbf{Y}) \xrightarrow{P_0} 1$$

as $n \rightarrow \infty$. In other words, we want to show that with P_0 -probability tending to 1, the posterior distribution (on the sparsity patterns) places almost all of its mass on the true sparsity pattern \mathbf{s}_0 . This will be achieved by examining the ratio

$$\frac{\Pi_{SS}(\mathbf{s} \mid \mathbf{Y})}{\Pi_{SS}(\mathbf{s}_0 \mid \mathbf{Y})} = \left(\frac{q\tau}{(1-q)\sqrt{2\pi}} \right)^{|\mathbf{s}|-|\mathbf{s}_0|} \frac{\int \exp(-n\alpha Q_\alpha(\boldsymbol{\beta}_s)) d\boldsymbol{\beta}_s}{\int \exp(-n\alpha Q_\alpha(\boldsymbol{\beta}_{\mathbf{s}_0})) d\boldsymbol{\beta}_{\mathbf{s}_0}} \quad (15)$$

for different choices of the sparsity pattern \mathbf{s} . The authors in Narisetty and He (2014) establish strong selection consistency for linear regression with spike-and-slab prior distribution, when the errors in both the true and the working model are assumed to be independent and identically normally distributed. Further, in their setting, the non-zero components of the true parameter $\boldsymbol{\beta}_0$ do not change with n . We too assume that *the set of indices which are 1 for the true sparsity pattern \mathbf{s}_0 do not change with n* , and impose the following regularity conditions. These regularity conditions are very similar to Assumptions A1-A4, with appropriate adaptations for the spike-and-slab setting.

- (Assumption B1) - $p_n \rightarrow \infty$, $\alpha_n \rightarrow \infty$ and $\alpha_n^{2+\delta} \log p = o(n)$ for some $\delta > 0$.
- (Assumption B2) - For every $n \geq 1$, the predictor vectors $\{\mathbf{x}_{i,n}\}_{i=1}^n$ are independent of the errors $\{\epsilon_{i,n}\}_{i=1}^n$, and are a covariance stationary Gaussian sequence with $\Gamma_n(h) := \text{Cov}(\mathbf{x}_{i,n}, \mathbf{x}_{i+h,n})$ for every $-(n-1) \leq h \leq n-1$ and $1 \leq i, i+h \leq n$. There exists $\kappa_1 > 0$ (not depending on n) such that

$$0 < \kappa_1 < \lambda_{\min}(\Gamma_n(0)) \leq \lambda_{\max}(\Gamma_n(0)) < \kappa_1^{-1} < \infty,$$

and

$$\kappa_2 := \sup_{n \geq 1} \sum_{h=0}^{n-1} \|\Gamma_n(h)\|_2 < \infty.$$

- (Assumption B3) - For every $n \geq 1$, the errors $\{\epsilon_{i,n}\}_{i=1}^n$ form a second order stationary sequence which is either m -dependent or is α -mixing with $\sum_{k=1}^{\infty} \alpha_\epsilon(k) < \infty$.
- (Assumption B4) - The prior mixture probability $q = q_n$ satisfies $q_n = p_n^{-\alpha^{2+\delta}}$. The prior slab precision parameter $\tau^2 > 0$ does not vary with n .

Remark. In Ghosh et al. (2021), the authors consider a linear regression with a spike-and-slab prior distribution and a Gaussian likelihood based working model. They extend the strong selection results of Narisetty and He (2014) to a setting where the true error and predictor processes are stationary Gaussian processes with serial correlation. Leaving minor modifications involving boundedness of eigenvalues of spectral densities and fixing \mathbf{s}_0 with n aside, the key differences/tradeoffs in the assumptions required by Ghosh et al. (2021) and Assumptions B1-B4 above are as follows: (a) Assumption B3 does not require Gaussianity and is significantly weaker than the corresponding assumption on the error process in Ghosh et al. (2021), but (b) $\log p = o(n/\alpha^{2+\delta})$ in Assumption B1 as opposed to $\log p = o(n)$ in Ghosh et al. (2021), and $q_n = p_n^{-\alpha^{2+\delta}}$ as opposed to $q_n = p_n^{-C}$ (for an appropriate constant C) in Ghosh et al. (2021). Again, it should be noted that a pseudo-Huber loss based working model is used here, as compared to the Gaussian likelihood based working model in Ghosh et al. (2021).

With Assumptions B1-B4 in hand, we proceed to analyze and bound the ratio $\frac{\Pi(\mathbf{s}|\mathbf{Y})}{\Pi(\mathbf{s}_0|\mathbf{Y})}$ under different cases - the sparsity pattern \mathbf{s} is a superset of the true one \mathbf{s}_0 , \mathbf{s} is a subset of \mathbf{s}_0 , and finally none is a subset of the other one, but with some additional requirements on their size - to establish the following result.

Theorem 3 (Strong selection consistency with spike-and-slab prior). Consider the spike-and-slab prior distribution based working model in Section 2.1, with the true data generating mechanism given by (13). Under Assumptions B1-B4, and restricting to *realistic* sparsity patterns, whose cardinality is less than or equal to $n/(\log(\max(n, p)))^{1+\delta}$, the working model posterior distribution on the space of sparsity patterns satisfies

$$\Pi_{SS}(\mathbf{s}_0 | \mathbf{Y}) \xrightarrow{P_0} 1$$

as $n \rightarrow \infty$.

Remark. We carefully review relevant high-dimensional consistency results in the robust regression literature. To the best of our knowledge, existing high-dimensional analyses focus *only on consistency of posterior modes* for various robust Bayesian models (note that most optimization based estimators can be regarded as posterior modes under an appropriate Bayesian model), and do not establish consistency/convergence of the entire posterior distribution. In Lambert-Lacroix and Zwald (2011), consistency and asymptotic normality of penalized estimators based on Huber loss and the lasso/adaptive lasso penalty is established in the i.i.d. error and fixed p setting. Fan et al. (2017) extend the consistency results in the high-dimensional setting where p is allowed to grow sub-exponentially with n , but consider independent errors with bounded second moments (under the data generating model). The predictor process is assumed to be i.i.d sub-Gaussian, and Sun et al. (2020) considers truncation based adaptations and extensions to the setting when the predictors are heavy-tailed (with finite fourth moments) under the data generating model. Loh (2017) considers generalized M -estimators obtained by minimizing an objective which combines a ‘robust’ loss function (convex, bounded derivatives etc.) and a separable penalty function (with suitable regularity) and establish consistency allowing p to grow sub-exponentially with n . The errors in the data generating model are assumed to be independent. In Nevo and Ritov (2016), the authors establish consistency of the Bayes estimator under a bounded loss function under spike-and-slab prior distributions on the components of β . The working model and the data generating models *both* assume i.i.d. errors with a common log-concave density.

4 Simulation study

This section summarizes results from extensive simulation experiments conducted to assess the frequentist statistical properties of our approach and compare them with Bayesian ℓ_1 and ℓ_2 regressions under both the ridge prior and the spike-and-slab prior. We considered a wide range of data-generating settings for regression, varying n , p , sparsity levels, residual error distributions, and error and predictor correlations. The data-generating setups were segmented into two broad categories: one representing a low/moderate-dimensional setup with $p = O(n)$, and the other representing a sparse, high-dimensional setup. The true data-generating model was specified as

$$y_i = \mathbf{x}_i^T \boldsymbol{\beta}^{\text{true}} + \epsilon_i,$$

with randomly generated $\mathbf{x}_i = (x_{i1}, \dots, x_{ij})^T \in \mathbb{R}^p$, $y_i \in \mathbb{R}$, and $\epsilon_i \in \mathbb{R}$ for $i = 1, \dots, n$ in each dataset, and a prespecified “true” regression parameter $\boldsymbol{\beta}^{\text{true}}$ common across datasets (the frequentist replication setup). We generated $\{\epsilon_i\}$ using an autoregressive(1) process with serial correlation $\rho_\epsilon \in \{0, 0.2, 0.4\}$ for $i = 1, \dots, n$, and drew $\{\mathbf{x}_i\}$ using a vector autoregressive(1) process with serial (over i) correlation ρ_x and the same predictor-coordinate (over j) correlation $\rho_x \in \{0, 0.4, 0.6\}$.

We used the standard normal distribution as the underlying marginal distribution (across both i and j) for the vector autoregressive(1) process used to generate the predictors $\{x_{ij}\}$ across all simulation settings. For the marginal distribution of the residual error ϵ_i , we considered a wide range of distributions across simulations, comprising the normal distribution and its continuous scale mixtures—specifically, the student t distribution—as well as discrete mixtures. We considered four broad categories for the marginal distributions of ϵ_i : (a) *thin-tailed*, comprising the standard normal distribution; (b) *moderate-tailed*, consisting of the student t distributions with 4 and 8 degrees of freedom, and 99%-1% and 95%-5% discrete mixtures of standard normal-standard Cauchy and standard normal- $\mathcal{N}(0, 10^2)$ distributions; (c) *heavy-tailed*, covering the student t distribution with 1 (i.e., the standard Cauchy) and 2 degrees of freedom, and 90%-10% discrete mixtures of standard normal-standard Cauchy and standard normal- $\mathcal{N}(0, 10^2)$ distributions; and (d) *extremely heavy-tailed*, comprising 90%-10% and 50%-50% discrete mixtures of standard normal and Uniform($-10^{10}, 10^{10}$) distributions.

Collectively, we considered a large range of values for the sample size n , ranging between 50 and 20,000, and the predictor dimension p , ranging between 10 and 250. We ensured $n > p$ for the low/moderate-dimensional $p = o(n)$ setups, and $n \leq p$ for the sparse high-dimensional setups. The “true” regression coefficient $\boldsymbol{\beta}^{\text{true}} = (\beta_j^{\text{true}} : j = 1, \dots, p)$ was created using the rule:

$$\beta_j^{\text{true}} = 0.5 + (j - 1) \frac{2}{p - 1},$$

for the low/moderate-dimensional $p = o(n)$ setups, and the rule:

$$\beta_j^{\text{true}} = \begin{cases} 2 & j \leq \lceil p/20 \rceil, \\ 0 & j > \lceil p/20 \rceil, \end{cases}$$

for the sparse high-dimensional setups, where $\lceil x \rceil$ denotes the smallest positive integer greater than or equal to x . A detailed description of all individual data-generating settings considered in our simulation study is provided in Supplementary Tables ??-??.

For each data-generating setting corresponding to a specific choice of n , p , correlation (for ϵ and x), and error distribution, we generated $R = 200$ independent data replicates. Subsequently,

for each replicated dataset, we fit the Bayesian SPH model alongside ℓ_1 and ℓ_2 regressions to compare their performances. For the low/moderate-dimensional setups, we used the ridge prior while fitting the models, whereas, for the sparse high-dimensional setups, we employed the spike-and-slab prior. The models included an intercept term but did not include an additional common variance parameter σ^2 beyond $\{\lambda_i\}$ except for ℓ_2 which included a common variance λ^2 for all observations.

All model parameters, including the prior hyperparameters and the SPH tuning parameter α , were estimated in a fully Bayesian way through posterior MCMC sampling. Specifically, we used the proposed MCMC sampler (Algorithm ??) to generate 10,000 approximate posterior draws for model inference after discarding the initial 5,000 draws as burn-in. We subsequently focused on the posterior draws for the regression parameters β to quantify and assess Bayesian estimation, prediction, and credible interval estimation performances. For the sparse high-dimensional setups, we also examined the spike-and-slab indicator parameters γ to evaluate variable selection performances. The subsections below summarize our evaluation results.

4.1 Estimation performance

To aid a holistic assessment of the Bayesian estimation of the regression parameters β^{true} in each replicated dataset, we focused on the posterior mean squared error (posterior MSE), defined as

$$M_{j,\text{data}} = \text{posterior MSE}(j, \text{data}) = E [(\beta_j - \beta_j^{\text{true}})^2 \mid \text{data}],$$

which utilizes the *entire posterior distribution* obtained for a model in each given dataset. The posterior MCMC draws for β were used to compute/approximate the integral underlying this MSE. Separately for each of the three models SPH, ℓ_1 , and ℓ_2 , we computed posterior MSE coordinate-wise for β in each dataset, yielding a separate MSE $M_{j,r}^{\text{model}}$ for each data-generating setting (combining all setups; see Supplementary Tables xx-yy), where $r = 1, \dots, R = 200$ indexes the data replicates for the setting, and $j = 1, \dots, p_1$ indexes the β coordinates, where p_1 denotes the number of non-zero (“signal”) coefficients in β^{true} ; i.e., $p_1 = p$ in all low/moderate dimensional settings with $n > p$ while $p_1 = \lceil p/20 \rceil$ under all high dimensional settings with $n \leq p$. Subsequently, as a summary measure for each model in each data-generating setting, we focused on the median posterior MSE, defined as

$$\text{median}_{j=1, \dots, p_1} \left(\text{median}_{r=1, \dots, R} M_{j,r}^{\text{model}} \right),$$

where $\text{median}(\cdot)$ denotes the empirical median operator.

Figure 3 visualizes these median posterior MSEs obtained for the different simulation settings for the three models as vertical line/bar plots. Simulation settings are shown along the horizontal axis, with the median posterior MSE (relative to SPH for that setting) plotted along the vertical setting separately under low/moderate-dimensional setups (panels A, C) and sparse high-dimensional setups (panels B, D). Different error distribution groups—specifically, heavy, moderate, and thin—are considered within each setup and labeled as facets within each panel.

The figure demonstrates that across all simulation settings—both low/moderate-dimensional setups using a ridge prior for estimation (panels A, C) and high-dimensional setups involving a spike-and-slab prior for estimation (panels B, D)—the proposed SPH model strikes an impressive balance between ℓ_1 and ℓ_2 in terms of model estimation accuracy. It closely approximates the better of the two in extreme situations, such as those involving heavy tails (where ℓ_1 is expected to be superior) or thin tails (where ℓ_2 is expected to perform better). In contrast, in the intermediate setups involving moderate tails, the SPH outperforms both ℓ_1 and ℓ_2 .

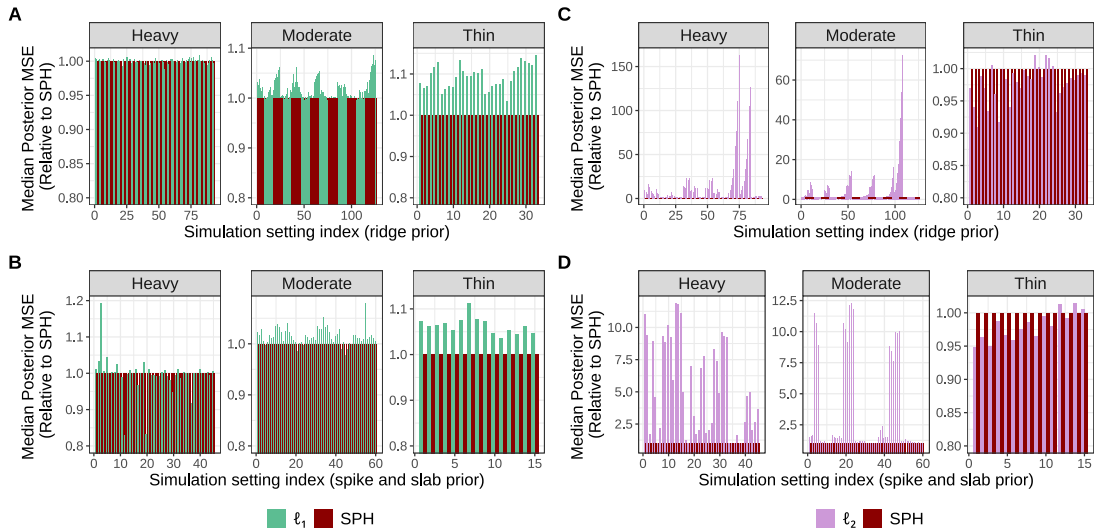


Figure 3: Median (over replicates and β coordinates) posterior MSEs for Bayesian ℓ_1 , ℓ_2 , and SPH regression across simulation settings. Panels A and C show low/moderate-dimensional setups with the ridge prior, while panels B and D depict sparse high-dimensional setups with the spike-and-slab prior. Each panel is grouped by error distributions— heavy, moderate, and thin tails—displayed as subplots/facets. Median posterior MSE values are scaled relative to SPH in each setting, with results for SPH, ℓ_1 , and ℓ_2 shown in red, green, and purple, respectively.

4.2 Prediction performance

For prediction assessment, we first generated an independent “test dataset” for each replicated training dataset used to fit the models. The test dataset shared the same n , p , β^{true} , predictor and error correlation structure, and error model as the training data but differed in the random elements, namely ϵ_i , \mathbf{x}_i , and y_i . Subsequently, we focused on the expected (over the data distribution) posterior predictive distribution to predict y_i^{test} given $\mathbf{x}_i^{\text{test}}$ and obtained the prediction (posterior) MSE:

$$\tilde{M}_{i,\text{data}} = \text{prediction MSE}(i, \text{data}) = E \left[(y_i^{\text{test}} - \mu - \beta^T \mathbf{x}_i^{\text{test}})^2 \mid \text{training data} \right].$$

Analogous to the steps involved in estimation performance assessment, the prediction MSE was first computed using posterior MCMC draws for each fitted model and every observation i (i.e., \mathbf{y} coordinate) within each replicate of the training-test dataset pair, yielding $\tilde{M}_{i,r}^{\text{model}}$ for each individual data-generating setting (see Supplementary Tables xx–yy), where $r = 1, \dots, R = 200$ indexes the data replicates for the setting, and $i = 1, \dots, n$ indexes the observation/ y coordinates. As a summary measure for each model in each simulation setting, we then computed the median posterior MSE, defined as

$$\text{median}_{i=1,\dots,n} \left(\text{median}_{r=1,\dots,R} \tilde{M}_{i,r}^{\text{model}} \right).$$

Figure 4 visualizes these median prediction MSEs for the different simulation settings for the three models as vertical line/bar plots. Simulation settings are plotted along the horizontal axis, with the median posterior MSE (relative to SPH for that setting) shown separately under

low/moderate-dimensional setups (panels A, C) and sparse high-dimensional setups (panels B, D). Different error distribution groups—specifically, heavy, moderate, and thin—are considered within each setup and labeled as facets within each panel.

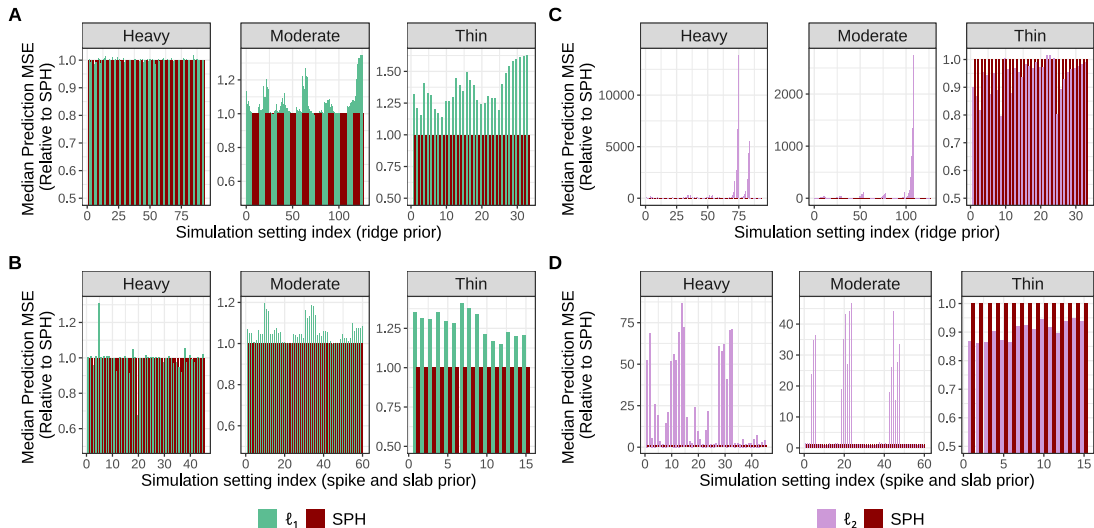


Figure 4: Median (over replicates and \mathbf{y} coordinates) prediction MSEs for Bayesian ℓ_1 , ℓ_2 , and SPH regression across simulation settings. Panels A and C show low/moderate-dimensional setups with the ridge prior, while panels B and D depict sparse high-dimensional setups with the spike-and-slab prior. Each panel is grouped by error distributions— heavy, moderate, and thin tails—displayed as subplots/facets. Median prediction MSE values are scaled relative to SPH in each setting, with results for SPH, ℓ_1 , and ℓ_2 shown in red, green, and purple, respectively.

The figure conveys a message similar to that obtained in the estimation performance assessment shown in Figure 3. Across all simulation settings—both low/moderate-dimensional setups using a ridge prior for estimation (panels A, C) and high-dimensional setups involving a spike-and-slab prior for estimation (panels B, D)—the proposed SPH model achieves an impressive balance between ℓ_1 and ℓ_2 in terms of prediction accuracy. SPH closely approximates the better of ℓ_1 and ℓ_2 in extreme situations, such as those involving heavy tails where SPH tracks ℓ_1 , which performs better than ℓ_2 , or thin tails where SPH resembles ℓ_2 , which is superior to ℓ_1 . However, in the intermediate setups involving moderate tails, SPH outperforms both ℓ_1 and ℓ_2 .

4.3 Interval Estimation Performance: Frequentist coverages of uncertainty (posterior credible) intervals

To assess the uncertainty (credible) interval performance of the models, we focused on settings with independent errors (i.e., zero serial correlation) and a low dimensional β ($p = 10$). Within this setup, we considered a large range of error distributions categorized into four groups: extremely heavy, heavy, moderate, and thin (see Supplementary Tables xx - yy), and generated replicated datasets of a wide range of sample size n ranging between 50 and 20,000. In each replicate, we fit the three models using the ridge prior. From each fitted model in each replicated dataset, we obtained the (marginal) uncertainty/Bayesian credible interval for each β coordinate

using equi-tailed posterior quantiles (computed using the MCMC draws). We then evaluated the frequentist replication-based coverage, defined as

$$\text{coverage}(j, \text{model}) = \frac{1}{R} \sum_{r=1}^R \mathbb{1} \left(\hat{\beta}_{j,r}^{L, \text{model}} \leq \beta_j^{\text{true}} \leq \hat{\beta}_{j,r}^{U, \text{model}} \right),$$

and the mean length of credible intervals, defined as

$$\text{mean length}(j, \text{model}) = \frac{1}{R} \sum_{r=1}^R \left(\hat{\beta}_{j,r}^{U, \text{model}} - \hat{\beta}_{j,r}^{L, \text{model}} \right),$$

where $(\hat{\beta}_{j,r}^{L, \text{model}}$ and $\hat{\beta}_{j,r}^{U, \text{model}})$ denote the 90% equi-tailed posterior credible interval for β_j , computed using the posterior MCMC draws for the model and separately for each data-generating setting, for data replicate r .

Posterior credible intervals obtained from Bayesian ℓ_1 regression with a fixed/low p and vague priors on β are known to suffer from poor frequentist coverage under high error contamination and model misspecification. This issue arises from the resulting non-standard asymptotic structures of the Bayesian ℓ_1 posteriors, leading to a mismatch between the asymptotic (in n) sampling variance of a point estimate of β —such as the posterior mean or mode—and the asymptotic form of the posterior covariance of β commonly used to obtain Bernstein–von Mises-type asymptotic normal approximations for a β posterior. Adjustments to the asymptotic posterior covariance of β under these settings have been suggested to address this mismatch in Bayesian ℓ_1 regression. Specifically, it has been established that for Bayesian ℓ_1 regression with a known σ , an asymptotic normal approximation of the form $\mathcal{N}_p(E(\beta | \text{data}), V_n)$ matches the asymptotic frequentist sampling distribution of $E(\beta | \text{data})$, through the approximate asymptotic covariance matrix:

$$V_n = \frac{1}{\sigma^2} \left(\text{var}(\beta | \text{data}) \mathbf{X}^T \mathbf{X} \text{var}(\beta | \text{data}) \right),$$

where $\text{var}(\beta | \text{data})$ denotes the posterior covariance matrix for β , which can be computed using MCMC draws from the posterior as usual. This asymptotic structure differs from that of Bayesian ℓ_2 regression, where both the asymptotic posterior distribution of β and the asymptotic sampling distribution of $E(\beta | \text{data})$ has the approximate form $\mathcal{N}_p(E(\beta | \text{data}), \text{var}(\beta | \text{data}))$.

In our simulations, while assessing frequentist coverage performances, we implemented this adjustment to produce an adjusted ℓ_1 posterior (ℓ_1 -adj) and considered the associated posterior credible intervals. Specifically, credible/confidence intervals for the coordinates of β under ℓ_1 -adj were obtained through the corresponding approximate normal equi-tailed quantiles. Since the SPH loss converges to the ℓ_1 loss under heavy-tailed setups, we also considered analogous adjustments to the SPH-based β posteriors to yield the SPH-adj posterior and the consequent adjusted credible intervals.

The computed frequentist coverages and average lengths are plotted along the vertical axis as dots and error bars—reflecting the median and 10% and 90% empirical percentiles computed over all simulations settings specific to every sample size—for different sample size n (horizontal axis). The dots and error bars are color-coded by the models.

The figure highlights the robustness of SPH and ℓ_1 , along with their posterior variance-adjusted counterparts (SPH-adj and ℓ_1 -adj), in achieving adequate frequentist coverage and maintaining narrow uncertainty intervals across all sample sizes (n) and error distributions. SPH-adj and ℓ_1 -adj are particularly effective, achieving coverage levels close to the nominal 90% when $n \geq 200$ across all data-generating settings while maintaining small mean interval lengths.

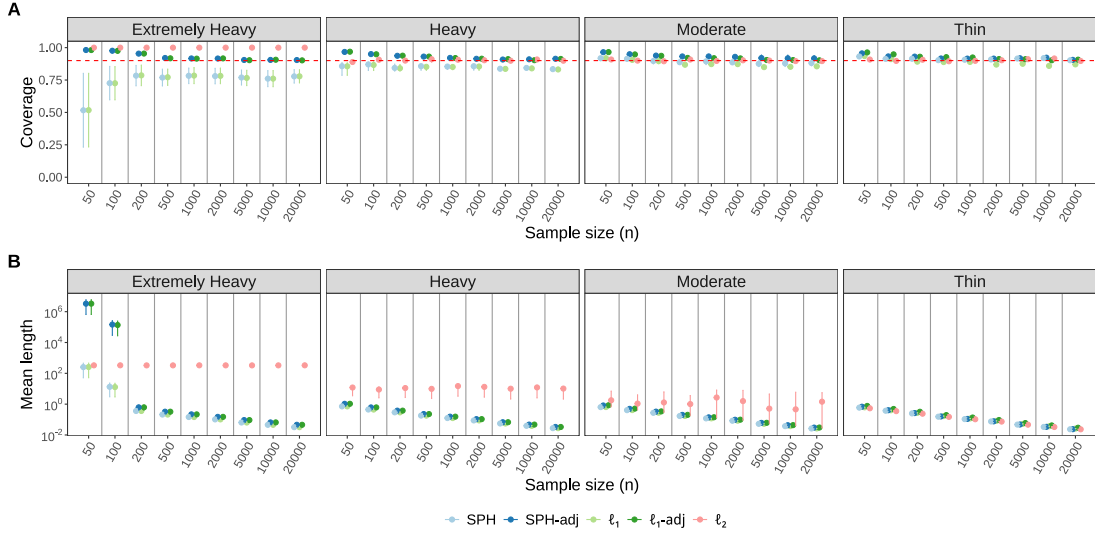


Figure 5: Replication-based coverages (Panel A) and mean lengths (Panel B) of 90% Bayesian credible (equi-tailed) intervals for Bayesian ℓ_1 , ℓ_1 -adj, ℓ_2 , SPH, and SPH-adj regression models across various error distribution categories (extremely heavy, heavy, moderate, and thin) and sample sizes (n).

However, for small to moderate sample sizes ($n \leq 100$) under extremely heavy-tailed errors, the adjustment results in overly wide intervals, but they become reasonable and effective as $n \geq 200$. Notably, the adjustment appears crucial for ℓ_1 to achieve adequate coverage under moderate and thin-tailed errors, where it would otherwise undercover. In contrast, SPH maintains adequate coverage without adjustment for moderate and thin-tailed errors (thanks to its ability to mimic ℓ_2 in these setups) but benefits from the adjustment under heavy and extremely heavy-tailed errors. Both SPH and ℓ_1 consistently outperform ℓ_2 in all setups except under thin-tailed errors in terms of mean interval lengths; ℓ_2 produces adequate coverage tracking the nominal level (except with extremely heavy-tailed errors, where it severely overcovers) but with substantially wider intervals—often more than an order of magnitude larger than SPH and ℓ_1 —in all but thin error tail setups.

4.4 Variable Selection Performance under Spike and Slab prior

Finally, to assess the variable selection performances of the three models under the spike and slab prior, we focused on simulation settings within the $n > p$ regime. For each replicated dataset generated in this regime, we obtained a Bayesian point estimate of the variable selection indicator vector $\hat{\gamma}^{\text{model}} = (\hat{\gamma}_j^{\text{model}} : j = 1, \dots, p)$, defined separately for each model and each coordinate j of β as

$$\hat{\gamma}_j^{\text{model}} = \mathbb{1} [\Pr(\gamma_j^{\text{model}} = 1 \mid \text{data}) > 0.5],$$

where the posterior probabilities were computed using posterior MCMC draws for the model. Subsequently, for each dataset, the variable selection performances of the three models were measured using the Matthews Correlation Coefficient (MCC) between the estimated variable

selection indicators $\hat{\gamma}^{\text{model}}$ and the “true active” variable indicators

$$\gamma^{\text{true}} = (\mathbb{1} [\beta_j^{\text{true}} \neq 0] : j = 1, \dots, p).$$

As an overall summary of variable selection performance for each model across replications, the empirical median of these MCC values was computed across all simulation settings for each specific combination of n , p , predictor and error correlation, and error tail category (heavy, moderate, and thin). The results are presented in Table 2 below.

Correlation	n	p	Error Tail: Heavy			Error Tail: Moderate			Error Tail: Thin		
			ℓ_1	ℓ_2	SPH	ℓ_1	ℓ_2	SPH	ℓ_1	ℓ_2	SPH
None	75	100	1.00	0.08	1.00	1.00	0.88	1.00	1.00	1.00	1.00
	75	200	0.86	0.03	0.88	1.00	0.81	1.00	1.00	1.00	1.00
	75	250	0.51	0.02	0.52	0.98	0.72	0.99	1.00	0.98	1.00
Low	75	100	0.98	0.16	0.99	1.00	0.90	1.00	1.00	1.00	1.00
	75	200	0.96	0.11	0.94	1.00	0.87	1.00	1.00	1.00	1.00
	75	250	0.76	0.05	0.71	1.00	0.82	1.00	1.00	1.00	1.00
	100	100	1.00	0.16	1.00	0.99	0.94	1.00	1.00	1.00	1.00
	100	200	0.99	0.12	1.00	1.00	0.92	1.00	1.00	1.00	1.00
	100	250	0.97	0.10	0.98	1.00	0.89	1.00	1.00	1.00	1.00
Moderate	75	100	0.92	0.21	0.91	0.99	0.90	0.99	0.99	1.00	0.99
	75	200	0.89	0.25	0.88	0.99	0.88	0.99	1.00	1.00	1.00
	75	250	0.75	0.18	0.75	0.99	0.81	0.99	1.00	1.00	1.00
	100	100	0.92	0.34	0.92	0.99	0.94	0.99	0.99	1.00	0.99
	100	200	0.93	0.25	0.93	0.99	0.92	0.99	1.00	1.00	1.00
	100	250	0.93	0.24	0.93	1.00	0.93	0.99	1.00	1.00	1.00

Table 2: Overall variable selection performances as measured by MCC (summarized via medians across replicates and simulation settings) under simulation settings with models fitted using spike and slab priors. In each simulation setting with a specific combination of correlation, n , p , and error tail, the highest MCC obtained from the three models ℓ_1 , ℓ_2 , and SPH are highlighted via **bold** texts.

The table documents the impressive performance of SPH in variable selection across all simulation settings. SPH consistently achieves the highest or nearly the highest MCC values among the three models, regardless of the correlation structure, sample size (n), or predictor dimension (p). The selection performance is virtually perfect for all settings under moderate and thin error tails and remains high for most settings under heavy error tails, except in cases where $n \ll p$ (e.g., $n = 75$ and $p = 250$), where the MCC values are moderate. The performance of Bayesian ℓ_1 is very similar to SPH in most settings, providing a competitive alternative. In contrast, Bayesian ℓ_2 consistently underperforms across all settings other than the thin error-tailed setups, with low MCC values. All models show moderate declines in variable selection performance under heavy error tails when predictor and error correlations increase, which effectively reduces the datasets’ effective sample sizes.

References

- Abramowitz, M., Stegun, I. A. and Romer, R. H. (1988) Handbook of mathematical functions with formulas, graphs, and mathematical tables.
- Ahmed, I. M. and Kashmoola, M. Y. (2021) Threats on machine learning technique by data poisoning attack: A survey. In *Advances in Cyber Security: Third International Conference, ACeS 2021, Penang, Malaysia, August 24–25, 2021, Revised Selected Papers 3*, 586–600. Springer.
- Basu, S. and Michailidis, G. (2015) Regularized estimation in sparse high-dimensional time series models. *The Annals of Statistics*, **43**, 1535 – 1567. URL: <https://doi.org/10.1214/15-AOS1315>.
- Bhadra, A., Datta, J., Polson, N. G. and Willard, B. (2019) Lasso meets horseshoe. *Statistical Science*, **34**, 405–427.
- Bissiri, P. G., Holmes, C. C. and Walker, S. G. (2016) A general framework for updating belief distributions. *Journal of the Royal Statistical Society. Series B (Statistical Methodology)*, **78**, 1103–1130. URL: <http://www.jstor.org/stable/44682909>.
- Cao, X., Khare, K. and Ghosh, M. (2020) High-dimensional posterior consistency for hierarchical non-local priors in regression. *Bayesian Analysis*, **15**, 241–262.
- Casella, G. (2001) Empirical bayes Gibbs sampling. *Biostatistics*, **2**, 485–500.
- Castillo, I., Schmidt-Hieber, J. and Van der Vaart, A. (2015) Bayesian linear regression with sparse priors. *Ann. Stat.*
- Chambers, J. M. (2018) *Graphical methods for data analysis*. Chapman and Hall/CRC.
- Chan, K. S. and Geyer, C. J. (1994) Comment on “markov chains for exploring posterior distributions”. *The Annals of Statistics*, **22**, 1747–1758.
- De Mingo, A. C. and Cerrillo-i Martínez, A. (2018) Improving records management to promote transparency and prevent corruption. *International journal of information management*, **38**, 256–261.
- Ezzati, M., Martin, H., Skjold, S., Hoorn, S. V. and Murray, C. J. (2006) Trends in national and state-level obesity in the usa after correction for self-report bias: analysis of health surveys. *Journal of the royal Society of Medicine*, **99**, 250–257.
- Fan, J., Li, Q. and Wang, Y. (2017) Estimation of high dimensional mean regression in the absence of symmetry and light tail assumptions. *J R Stat Soc Series B Stat Methodol*, **79**, 247–265.
- Fan, J., Yan, Q., Li, M., Qu, G. and Xiao, Y. (2022) A survey on data poisoning attacks and defenses. In *2022 7th IEEE International Conference on Data Science in Cyberspace (DSC)*, 48–55. IEEE.
- Georgiou, A. V. (2021) The manipulation of official statistics as corruption and ways of understanding it. *Statistical Journal of the IAOS*, **37**, 85–105.
- Ghosh, S., Khare, K. and Michailidis, G. (2019) High-dimensional posterior consistency in bayesian vector autoregressive models. *Journal of the American Statistical Association*, **114**, 735–748. URL: <https://doi.org/10.1080/01621459.2018.1437043>. PMID: 31474783.

- (2021) Strong selection consistency of Bayesian vector autoregressive models based on a pseudo-likelihood approach. *The Annals of Statistics*, **49**, 1267 – 1299. URL: <https://doi.org/10.1214/20-AOS1992>.
- Hampel, F. R. (2001) Robust statistics: A brief introduction and overview. In *Research Report/Seminar für Statistik, Eidgenössische Technische Hochschule (ETH)*, vol. 94. Seminar für Statistik, Eidgenössische Technische Hochschule.
- Hansheng Wang, G. L. and Jiang, G. (2007) Robust regression shrinkage and consistent variable selection through the lad-lasso. *Journal of Business & Economic Statistics*, **25**, 347–355. URL: <https://doi.org/10.1198/073500106000000251>.
- Hartley, R. and Zisserman, A. (2003) *Multiple view geometry in computer vision*. Cambridge university press.
- Huber, P. J. (1964) Robust estimation of a location parameter. *The Annals of Mathematical Statistics*, **35**, 73–101.
- (1972) The 1972 wald lecture robust statistics: A review. *The Annals of Mathematical Statistics*, **43**, 1041–1067.
- (1981) *Robust statistics*. Wiley Series in Probability and Mathematical Statistics. John Wiley & Sons, Inc., New York.
- Huber, P. J. and Ronchetti, E. M. (2009) *Robust statistics*. Wiley Series in Probability and Statistics. John Wiley & Sons, Inc., Hoboken, NJ, second edn. URL: <https://doi.org/10.1002/9780470434697>.
- Ibragimov, I. (1962) Some limit theorems for stationary processes. *Thy. Prob. Appl.*, **7**, 349–382.
- Jones, G. L. (2004) On the Markov chain central limit theorem. *Probability Surveys*, **1**, 299 – 320. URL: <https://doi.org/10.1214/154957804100000051>.
- Kawakami, J. and Hashimoto, S. (2023) Approximate Gibbs sampler for Bayesian huberized lasso. *Journal of Statistical Computation and Simulation*, **93**, 128–162. URL: <https://doi.org/10.1080/00949655.2022.2096886>.
- Kozumi, H. and Kobayashi, G. (2011) Gibbs sampling methods for Bayesian quantile regression. *Journal of Statistical Computation and Simulation*, **81**, 1565–1578. URL: <https://doi.org/10.1080/00949655.2010.496117>.
- Lambert-Lacroix, S. and Zwald, L. (2011) Robust regression through the Huber’s criterion and adaptive lasso penalty. *Electronic Journal of Statistics*, **5**, 1015 – 1053. URL: <https://doi.org/10.1214/11-EJS635>.
- Lancaster, H. O. (1957) Some properties of the bivariate normal distribution considered in the form of a contingency table. *Biometrika*, **44**, 289—292.
- Lapinsky, S. E. and Easty, A. C. (2006) Electromagnetic interference in critical care. *Journal of critical care*, **21**, 267–270.
- Li, J. Z., Absher, D. M., Tang, H., Southwick, A. M., Casto, A. M., Ramachandran, S., Cann, H. M., Barsh, G. S., Feldman, M., Cavalli-Sforza, L. L. and Myers, R. M. (2008) Worldwide human relationships inferred from genome-wide patterns of variation. *Science*, **319**, 1100–1104.

- Loh, P.-L. (2017) Statistical consistency and asymptotic normality for high-dimensional robust M -estimators. *Ann. Statist.*, **45**, 866–896. URL: <https://doi.org/10.1214/16-AOS1471>.
- (2021) Scale calibration for high-dimensional robust regression. *Electronic Journal of Statistics*, **15**, 5933 – 5994. URL: <https://doi.org/10.1214/21-EJS1936>.
- Maronna, R. A., Martin, R. D. and Yohai, V. J. (2006) *Robust statistics*. Wiley Series in Probability and Statistics. John Wiley & Sons, Ltd., Chichester. URL: <https://doi.org/10.1002/0470010940>. Theory and methods.
- Maronna, R. A., Martin, R. D., Yohai, V. J. and Salibián-Barrera, M. (2019) *Robust statistics: theory and methods (with R)*. John Wiley & Sons.
- McGill, R., Tukey, J. W. and Larsen, W. A. (1978) Variations of box plots. *The american statistician*, **32**, 12–16.
- Narisetty, N. N. and He, X. (2014) Bayesian variable selection with shrinking and diffusing priors. *The Annals of Statistics*, **42**, 789 – 817. URL: <https://doi.org/10.1214/14-AOS1207>.
- Neal, R. M. (2003) Slice sampling. *The Annals of Statistics*, **31**, 705–767.
- Nevo, D. and Ritov, Y. (2016) On Bayesian robust regression with diverging number of predictors. *Electronic Journal of Statistics*, **10**, 3045 – 3062. URL: <https://doi.org/10.1214/16-EJS1205>.
- Park, T. and Casella, G. (2008) The Bayesian lasso. *Journal of the American Statistical Association*, **103**, 681–686. URL: <https://doi.org/10.1198/016214508000000337>.
- Rosenberg, N. A., Pritchard, J. K., Weber, J. L., Cann, H. M., Kidd, K. K., Zhivotovsky, L. A. and Feldman, M. W. (2002) Genetic structure of human populations. *science*, **298**, 2381–2385.
- Rosenman, R., Tennekoon, V. and Hill, L. G. (2011) Measuring bias in self-reported data. *International Journal of Behavioural and Healthcare Research*, **2**, 320–332.
- Rosset, S. and Zhu, J. (2004) Discussion of “least angle regression,” by b. efron, t. hastie, i. johnstone, and r. tibshirani. *The Annals of Statistics*, **32**, 469–475.
- Rousseeuw, P. J. (1991) Tutorial to robust statistics. *Journal of chemometrics*, **5**, 1–20.
- Rudelson, M. and Vershynin, R. (2013) Hanson-Wright inequality and sub-gaussian concentration. *Electronic Communications in Probability*, **18**, 1 – 9. URL: <https://doi.org/10.1214/ECP.v18-2865>.
- Steinhardt, J., Koh, P. W. W. and Liang, P. S. (2017) Certified defenses for data poisoning attacks. *Advances in neural information processing systems*, **30**.
- Sun, Q., Zhou, W.-X. and Fan, J. (2020) Adaptive Huber regression. *J. Amer. Statist. Assoc.*, **115**, 254–265. URL: <https://doi.org/10.1080/01621459.2018.1543124>.
- Tukey, J. W. (1960) A survey of sampling from contaminated distributions. *Contributions to probability and statistics*, 448–485.
- Vershynin, R. (2011) Introduction to the non-asymptotic analysis of random matrices. *arXiv*.

Wang, L. (2013) The l1 penalized lad estimator for high dimensional linear regression. *Journal of Multivariate Analysis*, **120**, 135–151. URL: <https://www.sciencedirect.com/science/article/pii/S0047259X1300047X>.

Woodard, M., Sarvestani, S. S. and Hurson, A. R. (2015) A survey of research on data corruption in cyber-physical critical infrastructure systems. *Advances in Computers*, **98**, 59–87.

Appendix

A Technical Developments for Section 2

Proof of Proposition 1:

The joint density of (ε, λ) is given by:

$$\begin{aligned} f_{\varepsilon, \lambda}(\varepsilon, \lambda) &= \frac{1}{\sqrt{2\pi}} \lambda^{-1/2} \exp\left[-\frac{1}{2} \frac{\varepsilon^2}{\lambda}\right] \times \frac{\sqrt{1+\alpha^2}/\alpha}{2K_1(\alpha\sqrt{1+\alpha^2})} \exp\left[-\frac{1}{2} \left\{(1+\alpha^2)\lambda + \frac{\alpha^2}{\lambda}\right\}\right] \\ &= C_1(\alpha) \lambda^{-1/2} \exp\left[-\frac{1}{2} \left\{(1+\alpha^2)\lambda + \frac{\alpha^2 + \varepsilon^2}{\lambda}\right\}\right]; \quad \lambda > 0, -\infty < \varepsilon < \infty, \end{aligned}$$

where $C_1(\alpha) = \frac{\sqrt{1+\alpha^2}}{2\sqrt{2\pi}\alpha K_1(\alpha\sqrt{1+\alpha^2})}$. We consider the transformation $(\varepsilon, \lambda) \mapsto (\varepsilon, \kappa)$ where $\kappa = 1/\lambda$. The absolute Jacobian of the transformation is simply $1/\kappa^2$. Therefore, in the transformed scale, the joint density of (ε, κ) is:

$$f_{\varepsilon, \kappa}(\varepsilon, \kappa) = C_1(\alpha) \kappa^{-3/2} \exp\left[-\frac{1}{2} \left\{(\alpha^2 + \varepsilon^2)\kappa + \frac{1 + \alpha^2}{\kappa}\right\}\right].$$

Note that for any fixed $\varepsilon \in (-\infty, \infty)$, the right hand side above without the proportionality constant $C_1(\alpha)$ is the kernel of an Inverse-Gaussian $\left(\mu = \frac{\sqrt{1+\alpha^2}}{\sqrt{\alpha^2 + \varepsilon^2}}, \sigma = 1 + \alpha^2\right)$ density for κ .

Thus,

$$\begin{aligned} &\int_0^\infty \kappa^{-3/2} \exp\left[-\frac{1}{2} \left\{(\alpha^2 + \varepsilon^2)\kappa + \frac{1 + \alpha^2}{\kappa}\right\}\right] d\kappa \\ &= \frac{\sqrt{2\pi}}{\sqrt{1+\alpha^2}} \exp\left[-\sqrt{1+\alpha^2}\sqrt{\alpha^2 + \varepsilon^2}\right] \\ &= \frac{\sqrt{2\pi}}{\sqrt{1+\alpha^2}} \exp\left[-\alpha\sqrt{1+\alpha^2} \left(\sqrt{1 + \left(\frac{\varepsilon}{\alpha}\right)^2}\right)\right] \\ &= \frac{\sqrt{2\pi}}{\sqrt{1+\alpha^2}} \exp\left(-\alpha\sqrt{1+\alpha^2}\right) \exp\left[-\alpha\sqrt{1+\alpha^2} \left(\sqrt{1 + \left(\frac{\varepsilon}{\alpha}\right)^2} - 1\right)\right]. \end{aligned}$$

Therefore, the marginal density of ε is obtained as

$$f_{\varepsilon}(\varepsilon | \alpha) = \int_0^\infty f_{\varepsilon, \kappa}(\varepsilon, \kappa) d\kappa = C_2(\alpha) \exp\left[-\alpha\sqrt{1+\alpha^2} \left(\sqrt{1 + \left(\frac{\varepsilon}{\alpha}\right)^2} - 1\right)\right],$$

where $C_2(\alpha) = C_1(\alpha) \frac{\sqrt{2\pi}}{\sqrt{1+\alpha^2}} \exp(-\alpha\sqrt{1+\alpha^2}) = \frac{1}{2\alpha K_1(\alpha\sqrt{1+\alpha^2})} \exp(-\alpha\sqrt{1+\alpha^2})$ is free of ε . This completes the proof. \square

Remark. Since $\lim_{\alpha \rightarrow 0} \alpha K_1(\alpha\sqrt{1+\alpha^2}) = 1$, it follows that as $\alpha \rightarrow 0$, $f_{\varepsilon}(\varepsilon | \alpha) \rightarrow \frac{1}{2} \exp(-|\varepsilon|)$ which is the density of a standard Laplace distribution. On the other hand, as $\alpha \rightarrow \infty$, $\sqrt{1+\alpha^2} \sim \alpha$ and $C_2(\alpha) \sim \tilde{C}_2(\alpha)$ where $\tilde{C}_2(\alpha) = \frac{1}{2\alpha K_1(\alpha^2) \exp(\alpha^2)}$ and “ \sim ” represents asymptotic equivalence defined for two functions $f_1(\alpha)$ and $f_2(\alpha)$ as $f_1(\alpha) \sim f_2(\alpha)$ as $\alpha \rightarrow \infty$ if

and only if $\lim_{\alpha \rightarrow \infty} \frac{f_1(\alpha)}{f_2(\alpha)} = 1$. Now for positive real $\alpha \rightarrow \infty$, $K_1(\alpha) = \sqrt{\frac{\pi}{2\alpha}} \exp(-\alpha) \left(1 + o\left(\frac{1}{\alpha}\right)\right)$ (Abramowitz et al., 1988, p. 378, 9.7.2); hence as $\alpha \rightarrow \infty$

$$\frac{1}{\bar{C}_2(\alpha)} = 2\alpha \sqrt{\frac{\pi}{2\alpha^2}} \exp(-\alpha^2) \left(1 + o\left(\frac{1}{\alpha^2}\right)\right) \exp(\alpha^2) = \sqrt{2\pi} \left(1 + o\left(\frac{1}{\alpha^2}\right)\right) \rightarrow \sqrt{2\pi}.$$

Furthermore, $\exp\left[-\alpha\sqrt{1+\alpha^2}\left(\sqrt{1+\left(\frac{\varepsilon}{\alpha}\right)^2}-1\right)\right] \sim \exp\left[-\alpha^2\left(\sqrt{1+\left(\frac{\varepsilon}{\alpha}\right)^2}-1\right)\right]$ as $\alpha \rightarrow \infty$ and

$$\lim_{\alpha \rightarrow \infty} \alpha^2 \left(\sqrt{1+\left(\frac{\varepsilon}{\alpha}\right)^2}-1\right) = \lim_{t \rightarrow 0} \frac{\sqrt{1+t\varepsilon^2}-1}{t} = \lim_{t \rightarrow 0} \frac{\varepsilon^2}{2\sqrt{1+t\varepsilon^2}} = \frac{\varepsilon^2}{2}$$

where the second last equality is a consequence of the L'Hospital rule. Together, this implies $f_\varepsilon(\varepsilon | \alpha) \rightarrow \frac{1}{\sqrt{2\pi}} \exp\left(-\frac{\varepsilon^2}{2}\right)$, the standard normal density, as $\alpha \rightarrow \infty$.

B Additional Details on Posterior Distribution Computations

B.1 Posterior MCMC sampling for the Gaussian (ridge) prior case

For the Gaussian, weakly informative prior distribution, some standard calculations lead to the following simplified form of the posterior distribution of the model parameters. Let $\boldsymbol{\lambda} = (\lambda_1, \dots, \lambda_n)^T$ and $\Lambda = \text{diag}(\boldsymbol{\lambda})$, we get:

$$\begin{aligned} & \pi(\boldsymbol{\beta}, \boldsymbol{\lambda}, \sigma^2, \alpha^2 \mid \text{data}) \\ & \propto \left\{ \prod_{i=1}^n \lambda_i^{-1/2} \right\} (\sigma^2)^{-n/2} \exp\left[-\frac{1}{2\sigma^2}(\mathbf{y} - X\boldsymbol{\beta})^T \Lambda^{-1}(\mathbf{y} - X\boldsymbol{\beta})\right] \\ & \quad \times 2^{-n} (1 + \alpha^2)^{n/2} (\alpha^2)^{-n/2} \left[K_1\left(\sqrt{\alpha^2(1 + \alpha^2)}\right) \right]^{-n} \exp\left[-\frac{1}{2} \left(\sum_{i=1}^n \frac{\alpha^2}{\lambda_i} + (1 + \alpha^2) \sum_{i=1}^n \lambda_i \right)\right] \\ & \quad \times (\sigma^2)^{-p/2} |Q|^{1/2} \exp\left[-\frac{1}{2\sigma^2}(\boldsymbol{\beta} - \boldsymbol{\beta}_0)^T Q(\boldsymbol{\beta} - \boldsymbol{\beta}_0)\right] \\ & \quad \times (\sigma^2)^{-a_\sigma - 1} \exp\left(-\frac{1}{\sigma^2} b_\sigma\right) \times \\ & \quad \times (\alpha^2)^{a_\alpha - 1} \exp(-b_\alpha \alpha^2) \\ & \propto \exp\left[-\frac{1}{2\sigma^2}(\mathbf{y} - X\boldsymbol{\beta})^T \Lambda^{-1}(\mathbf{y} - X\boldsymbol{\beta})\right] \\ & \quad \times \prod_{i=1}^n \left\{ \lambda_i^{\frac{1}{2}-1} \exp\left[-\frac{1}{2} \left(\frac{\alpha^2}{\lambda_i} + \alpha^2 \lambda_i \right)\right] \right\} \\ & \quad \times \exp\left[-\frac{1}{2\sigma^2}(\boldsymbol{\beta} - \boldsymbol{\beta}_0)^T Q(\boldsymbol{\beta} - \boldsymbol{\beta}_0)\right] \\ & \quad \times (\sigma^2)^{-\left(\frac{n+p}{2} + a_\sigma\right) - 1} \exp\left(-\frac{1}{\sigma^2} b_\sigma\right) \\ & \quad \times (\alpha^2)^{a_\alpha - 1} \exp(-b_\alpha \alpha^2) \end{aligned}$$

Then, MCMC samples from the posterior distribution can be obtained through the following Gibbs-type sampling procedure in Algorithm 1 below.

Algorithm 1:

1. $\mu \mid \text{rest} \sim \mathcal{N}(v_{\lambda;\mu} m_{\lambda;\mu}, \sigma^2 v_{\lambda;\mu})$ where $v_{\lambda;\mu} = 1 / \left(\frac{1}{\tau_\mu^2} + \sum_{i=1}^n \frac{1}{\lambda_i} \right)$ and $m_{\lambda;\mu} = \sum_{i=1}^n \frac{1}{\lambda_i} (y_i - \mathbf{x}_i^T \boldsymbol{\beta})$.
2. $\boldsymbol{\beta} \mid \text{rest} \sim \mathcal{N}(V_\lambda m_\lambda, \sigma^2 V_\lambda)$ where $V_\lambda = (X^T \Lambda^{-1} X + Q)$ and $m_\lambda = X^T \Lambda^{-1} \mathbf{y} + Q \boldsymbol{\beta}_0$.
3. $\lambda_i \mid \text{rest} \sim \text{GIG} \left(a = \alpha^2, b = \alpha^2 + \frac{1}{\sigma^2} (y_i - \mathbf{x}_i^T \boldsymbol{\beta})^2, p = \frac{1}{2} \right)$ independently for $i = 1, \dots, n$.
Sampling from this GIG distribution is efficient because $\text{GIG}(a, b, p) = \frac{1}{\text{GIG}(b, a, -p)}$ and a GIG distribution with $p = -1/2$ collapses into an ordinary inverse Gaussian distribution which permits computationally efficient random variate generation.
4. $\sigma^2 \mid \text{rest} \sim \text{Inv-Gamma} \left(a = \frac{n+p}{2} + a_\sigma, b = \frac{1}{2} \{ (\mathbf{y} - X\boldsymbol{\beta})^T \Lambda^{-1} (\mathbf{y} - X\boldsymbol{\beta}) + (\boldsymbol{\beta} - \boldsymbol{\beta}_0)^T Q (\boldsymbol{\beta} - \boldsymbol{\beta}_0) \} + b_\sigma \right)$.
5. $p(\alpha \mid \text{rest}) \propto$

Remark. Straightforward modifications can be made on the above Gibbs sampler, specifically on Step 2, to cater to the L^2 and L^1 regression problems. The steps for drawing $\boldsymbol{\beta}$ and σ^2 remain unaltered. For L^2 regression one simply sets all $\lambda_i \equiv 1$. For L^1 regression, the independent (in i) full conditional density of λ_i turns out to be of the form

$$\pi(\lambda_i \mid \text{rest}) \propto \lambda_i^{-\frac{1}{2}} \exp \left[-\frac{1}{2} \left\{ 2\lambda_i + \frac{(y_i - \mathbf{x}_i^T \boldsymbol{\beta})^2}{\sigma^2} \frac{1}{\lambda_i} \right\} \right],$$

which implies

$$\lambda_i \mid \text{rest} \sim \text{GIG} \left(a = 2, b = \frac{1}{\sigma^2} (y_i - \mathbf{x}_i^T \boldsymbol{\beta})^2, p = \frac{1}{2} \right). \quad (16)$$

B.2 Posterior MCMC sampling for the spike-and-slab prior case

For the hierarchical spike-and-slab prior distribution, we first note that the conditional on $\boldsymbol{\beta}$, the full conditional posterior densities for μ , $\boldsymbol{\lambda}$, and α remain the same as those provided in Step 3 of Algorithm 1. However, the full conditional distributions of $\boldsymbol{\beta}$ and σ^2 have a different form, and in addition there is a need to sample the predictor activation variables $\boldsymbol{\gamma} = (\gamma_1, \dots, \gamma_p)^T$ and q . The following Gibbs sampling procedure for fixed value of α summarized in Algorithm 2 below outlines how to obtain samples for the model parameters $\boldsymbol{\beta}$, $\boldsymbol{\gamma}$, q , and σ^2 .

1. **Full conditional posterior distribution of (β_j, γ_j) for each $j = 1, \dots, p$.** Due to degenerate nature of the spike distribution, the joint full conditional distributions of the entire $(\boldsymbol{\beta}, \boldsymbol{\gamma})$ vector becomes intractable. Instead, we focus on the full conditional posterior distribution of each coordinate (β_j, γ_j) for posterior Gibbs sampling. Straightforward algebra shows that

$$p(\mathbf{y} \mid \beta_j, \gamma_j = 0, \boldsymbol{\beta}_{-j}, \boldsymbol{\gamma}_{-j}, \text{rest}) \propto \mathcal{N}(y \mid X_{-j} \boldsymbol{\beta}_{-j}, \sigma^2 \Lambda)$$

and

$$p(\mathbf{y} \mid \beta_j, \gamma_j = 1, \boldsymbol{\beta}_{-j}, \boldsymbol{\gamma}_{-j}, \text{rest}) \propto \mathcal{N}(y \mid X_{-j} \boldsymbol{\beta}_{-j} + X_j \beta_j, \sigma^2 \Lambda)$$

Therefore, the β_j integrated (marginal) likelihood is:

$$p(\mathbf{y} \mid \gamma_j = 0, \beta_{-j}, \gamma_{-j}, \text{rest}) = \mathcal{N}(\mathbf{y} \mid X_{-j}\beta_{-j}, \sigma^2\Lambda)$$

and

$$p(\mathbf{y} \mid \gamma_j = 1, \gamma_{-j}, \beta_{-j}, \sigma^2) = \mathcal{N}(\mathbf{y} \mid X_{-j}\beta_{-j}, \sigma^2\Lambda + \tau^2 X_j X_j^\top).$$

Combining

2. **Full conditional distribution of q .** We have $q \mid \text{rest} \sim \text{Beta}(a_q + p_1, b_q + p - p_1)$ where $p_1 = \#\{j : \gamma_j = 1\}$.

3. **Full conditional distribution of σ^2 .** Given γ , define Γ_1 , $X^{(1)}$ and $\beta^{(1)}$ as before. Then

$$\sigma^2 \mid \text{rest} \sim \text{Inv-Gamma} \left(a = a_\sigma + \frac{n + p_1}{2}, b = b_\sigma + \frac{1}{2} \left\{ \left(\mathbf{y} - X^{(1)}\beta^{(1)} \right)^T \Lambda \left(\mathbf{y} - X^{(1)}\beta^{(1)} \right) + \frac{1}{\tau^2} \sum_{j \in \Gamma_1} \beta_j^2 \right\} \right).$$

C Proofs of Posterior Consistency Results in Section 3

C.1 Proof of Theorem 1

Suppose we have $\inf_{\mathbf{u}: \|\mathbf{u}\|=1} Q_\alpha(\beta_0 + \delta_n \mathbf{u}) > Q_\alpha(\beta_0)$. It would then imply that Q_α has a local minimum in the set $\{\beta : \|\beta - \beta_0\| \leq \delta_n\}$. Since Q_α is a strictly convex function, this would imply $\|\hat{\beta}_{pm} - \beta_0\| \leq \delta_n$. Hence to establish the result, it is enough to show that

$$P_0 \left(\inf_{\mathbf{u}: \|\mathbf{u}\|=1} Q_\alpha(\beta_0 + \delta_n \mathbf{u}) > Q_\alpha(\beta_0) \right) \rightarrow 1$$

as $n \rightarrow \infty$.

With this goal in mind, we arbitrarily fix \mathbf{u} such that $\|\mathbf{u}\| = 1$. Using the second order Taylor expansion of $f_{\mathbf{u}}(t) = Q_\alpha(\beta_0 + t\delta_n \mathbf{u})$ around $t = 0$, we get

$$\begin{aligned} Q_\alpha(\beta_0 + \delta_n \mathbf{u}) - Q_\alpha(\beta_0) &= f_{\mathbf{u}}(1) - f_{\mathbf{u}}(0) \\ &= \frac{\delta_n}{n\alpha} \sum_{i=1}^n \ell'_\alpha(\epsilon_i) \mathbf{x}_i^T \mathbf{u} + \frac{\delta_n^2}{2n\alpha} \sum_{i=1}^n \ell''_\alpha(\epsilon_i - t^* \delta_n^2 \mathbf{x}_i^T \mathbf{u}) (\mathbf{x}_i^T \mathbf{u})^2 + \\ &\quad \frac{\tau^2 \delta_n^2}{n\alpha} \mathbf{u}^T \mathbf{u} + \frac{2\tau^2 \delta_n}{n\alpha} \mathbf{u}^T \beta_0. \end{aligned} \tag{17}$$

where $t^* \in (0, 1)$. Since $(\epsilon_i - t^* \delta_n \mathbf{x}_i^T \mathbf{u})^2 \leq 2\epsilon_i^2 + 2\delta_n^2 (\mathbf{x}_i^T \mathbf{u})^2$, and $\ell''_\alpha(y) = \sqrt{1 + \alpha^{-2}} (1 + \alpha^{-2} y^2)^{-3/2}$, it follows that

$$\begin{aligned} Q_\alpha(\beta_0 + \delta_n \mathbf{u}) - Q_\alpha(\beta_0) &\geq \frac{\delta_n}{n\alpha} \sum_{i=1}^n \ell'_\alpha(\epsilon_i) \mathbf{x}_i^T \mathbf{u} - \frac{2\tau^2 \delta_n}{n\alpha} \|\mathbf{u}\| \|\beta_0\| + \\ &\quad \frac{\delta_n^2 \sqrt{1 + \alpha^{-2}}}{2n\alpha} \sum_{i=1}^n (1 + 2\alpha^{-2} \epsilon_i^2 + 2\delta_n^2 \alpha^{-2} (\mathbf{x}_i^T \mathbf{u})^2)^{-3/2} (\mathbf{x}_i^T \mathbf{u})^2. \end{aligned} \tag{18}$$

Since $2\alpha^{-2} < 1$ and $2\alpha^{-2} \delta_n^2 < 1$ for large enough n (by Assumption A1), we have

$$\inf_{\mathbf{u}: \|\mathbf{u}\|=1} (Q_\alpha(\beta_0 + \delta_n \mathbf{u}) - Q_\alpha(\beta_0))$$

$$\begin{aligned} &\geq \inf_{\mathbf{u}: \|\mathbf{u}\|=1} \frac{\delta_n^2 \sqrt{1+\alpha^{-2}}}{2n\alpha} \sum_{i=1}^n (1+\epsilon_i^2 + (\mathbf{x}_i^T \mathbf{u})^2)^{-3/2} (\mathbf{x}_i^T \mathbf{u})^2 - \sup_{\mathbf{u}: \|\mathbf{u}\|=1} \left| \frac{\delta_n}{n\alpha} \sum_{i=1}^n \ell'_\alpha(\epsilon_i) \mathbf{x}_i^T \mathbf{u} \right| - \\ &\quad \frac{2\tau^2 \delta_n}{n\alpha} \|\beta_0\|. \end{aligned} \quad (19)$$

Next, we focus on the second term on the RHS in (19). Let $K_1 > 0$ be arbitrarily fixed. Since $\{\mathbf{x}_i\}_{i=1}^n$ and $\epsilon = \{\epsilon_i\}_{i=1}^n$ are independent, it follows that for any \mathbf{u} with $\|\mathbf{u}\| \leq 1$

$$\begin{aligned} P_0 \left(\frac{1}{n\alpha} \sum_{i=1}^n \ell'_\alpha(\epsilon_i) \mathbf{x}_i^T \mathbf{u} > K_1 \sqrt{\frac{p}{n}} \right) &= E_0 \left[P_0 \left(\frac{s}{n\alpha} \sum_{i=1}^n \ell'_\alpha(\epsilon_i) \mathbf{x}_i^T \mathbf{u} > K_1 \sqrt{\frac{p}{n}} \mid \epsilon \right) \right] \\ &\leq E_0 \left[E_0 \left[\exp \left(\frac{s}{n\alpha} \sum_{i=1}^n \ell'_\alpha(\epsilon_i) \mathbf{x}_i^T \mathbf{u} - s K_1 \sqrt{\frac{p}{n}} \right) \mid \epsilon \right] \right] \end{aligned} \quad (20)$$

By Assumption A2 and $|\ell'_\alpha(\epsilon_i)| \leq \alpha \sqrt{1+\alpha^{-2}}$, it follows that conditional on ϵ , the random variable $\alpha^{-1} \sum_{i=1}^n \ell'_\alpha(\epsilon_i) \mathbf{x}_i^T \mathbf{u}$ has a Gaussian distribution with mean zero and variance v_n , where

$$\begin{aligned} v_n &= \sum_{i=1}^n \frac{\ell'^2_\alpha(\epsilon_i)}{\alpha^2} \mathbf{u}^T \Gamma_n(0) \mathbf{u} + \sum_{1 \leq i \neq j \leq n} \frac{\ell'_\alpha(\epsilon_i) \ell'_\alpha(\epsilon_j)}{\alpha^2} \mathbf{u}^T \Gamma_n(j-i) \mathbf{u} \\ &\leq (1+\alpha^{-2}) \left(n \mathbf{u}^T \Gamma_n(0) \mathbf{u} + \sum_{k=1}^{n-1} (n-k) \left| \mathbf{u}^T (\Gamma_n(k) + \Gamma_n(-k)) \mathbf{u} \right| \right) \\ &\leq (1+\alpha^{-2}) \left(n \|\Gamma_n(0)\|_2 + \sum_{k=1}^{n-1} (n-k) \|\Gamma_n(k) + \Gamma_n(-k)\|_2 \right) \\ &\leq (1+\alpha^{-2}) (2n \sum_{k=0}^{n-1} \|\Gamma_n(k)\|_2) \\ &\leq 2(1+\alpha^{-2}) \kappa_2 n. \end{aligned}$$

The last two inequalities follow from Assumption A2 and the fact that $\Gamma_n(-k) = \Gamma_n(k)^T$. It follows by (20) that

$$\begin{aligned} P_0 \left(\frac{1}{n\alpha \sqrt{1+\alpha^{-2}}} \sum_{i=1}^n \ell'_\alpha(\epsilon_i) \mathbf{x}_i^T \mathbf{u} > K_1 \sqrt{\frac{p}{n}} \right) &= E_0 \left[\exp \left(\frac{2\kappa_2 n s^2}{2n^2} - s K_1 \sqrt{\frac{p}{n}} \right) \right] \\ &= E_0 \left[\exp \left(\frac{\kappa_2 s^2}{n} - s K_1 \sqrt{\frac{p}{n}} \right) \right] \end{aligned}$$

for every $s > 0$. Choosing $s = K_1 \sqrt{np}/(2\kappa_2)$, we get

$$P_0 \left(\frac{1}{n\alpha \sqrt{1+\alpha^{-2}}} \sum_{i=1}^n \ell'_\alpha(\epsilon_i) \mathbf{x}_i^T \mathbf{u} > K_1 \sqrt{\frac{p}{n}} \right) \leq \exp \left(-\frac{K_1^2 p}{4\kappa_2} \right)$$

for every \mathbf{u} such that $\|\mathbf{u}\| \leq 1$. Since $\mathbf{x}_i^T \mathbf{u}$ has a symmetric distribution around 0, it follows that

$$P_0 \left(-\frac{1}{n\alpha \sqrt{1+\alpha^{-2}}} \sum_{i=1}^n \ell'_\alpha(\epsilon_i) \mathbf{x}_i^T \mathbf{u} > K_1 \sqrt{\frac{p}{n}} \right) \leq \exp \left(-\frac{K_1^2 p}{4\kappa_2} \right)$$

for every \mathbf{u} such that $\|\mathbf{u}\| \leq 1$, which implies

$$P_0 \left(\left| \frac{1}{n\alpha\sqrt{1+\alpha^{-2}}} \sum_{i=1}^n \ell'_\alpha(\epsilon_i) \mathbf{x}_i^T \mathbf{u} \right| > K_1 \sqrt{\frac{p}{n}} \right) \leq \exp \left(-\frac{K_1^2 p}{4\kappa_2} \right) \quad (21)$$

for every \mathbf{u} such that $\|\mathbf{u}\| \leq 1$. To get a bound on the supremum over all appropriate \mathbf{u} , we employ a technique similar to Vershynin (2011). By (Vershynin, 2011, Lemma 5.2), there exists a set S_{10} with the property that $S_{10} \subseteq \{\mathbf{u} : \|\mathbf{u}\| \leq 1\}$, $|S_{10}| \leq 21^p$, and for any \mathbf{u} with $\|\mathbf{u}\| \leq 1$, there exists $\mathbf{w}(\mathbf{u}) \in S_{10}$ such that $\|\mathbf{u} - \mathbf{w}(\mathbf{u})\| \leq 0.1$. Now, for any \mathbf{u} with $\|\mathbf{u}\| \leq 1$, we have

$$\begin{aligned} & \left| \frac{1}{n\alpha} \sum_{i=1}^n \ell'_\alpha(\epsilon_i) \mathbf{x}_i^T \mathbf{u} \right| \\ & \leq \left| \frac{1}{n\alpha} \sum_{i=1}^n \ell'_\alpha(\epsilon_i) \mathbf{x}_i^T (\mathbf{u} - \mathbf{w}(\mathbf{u})) \right| + \left| \frac{1}{n\alpha} \sum_{i=1}^n \ell'_\alpha(\epsilon_i) \mathbf{x}_i^T \mathbf{w}(\mathbf{u}) \right| \\ & \leq 0.1 \left| \frac{1}{n\alpha} \sum_{i=1}^n \ell'_\alpha(\epsilon_i) \mathbf{x}_i^T (10(\mathbf{u} - \mathbf{w}(\mathbf{u}))) \right| + \max_{\mathbf{w} \in S_{10}} \left| \frac{1}{n\alpha} \sum_{i=1}^n \ell'_\alpha(\epsilon_i) \mathbf{x}_i^T \mathbf{w} \right| \\ & \leq 0.1 \sup_{\mathbf{u} : \|\mathbf{u}\| \leq 1} \left| \frac{1}{n\alpha} \sum_{i=1}^n \ell'_\alpha(\epsilon_i) \mathbf{x}_i^T \mathbf{u} \right| + \max_{\mathbf{w} \in S_{10}} \left| \frac{1}{n\alpha} \sum_{i=1}^n \ell'_\alpha(\epsilon_i) \mathbf{x}_i^T \mathbf{w} \right|. \end{aligned}$$

It follows that

$$\sup_{\mathbf{u} : \|\mathbf{u}\| \leq 1} \left| \frac{1}{n\alpha} \sum_{i=1}^n \ell'_\alpha(\epsilon_i) \mathbf{x}_i^T \mathbf{u} \right| \leq \frac{10}{9} \max_{\mathbf{w} \in S_{10}} \left| \frac{1}{n\alpha} \sum_{i=1}^n \ell'_\alpha(\epsilon_i) \mathbf{x}_i^T \mathbf{w} \right|.$$

Using this inequality along with the union-sum inequality, and noting that (21) holds for an arbitrary $K_1 > 0$, we obtain

$$\begin{aligned} & P_0 \left(\sup_{\mathbf{u} : \|\mathbf{u}\|=1} \left| \frac{1}{n\alpha\sqrt{1+\alpha^{-2}}} \sum_{i=1}^n \ell'_\alpha(\epsilon_i) \mathbf{x}_i^T \mathbf{u} \right| > K_1 \sqrt{\frac{p}{n}} \right) \\ & \leq P_0 \left(\max_{\mathbf{w} \in S_{10}} \left| \frac{1}{n\alpha\sqrt{1+\alpha^{-2}}} \sum_{i=1}^n \ell'_\alpha(\epsilon_i) \mathbf{x}_i^T \mathbf{w} \right| > \frac{9K_1}{10} \sqrt{\frac{p}{n}} \right) \\ & \leq 21^p \exp \left(-\frac{81K_1^2 p}{400\kappa_2} \right) \\ & = \exp \left(-\left\{ \frac{81K_1^2}{400\kappa_2} - \log 21 \right\} p \right) \rightarrow 0 \text{ as } n \rightarrow \infty \end{aligned} \quad (22)$$

if K_1 is chosen to be $\frac{40\sqrt{\kappa_2 \log 21}}{9}$. We now focus our attention on the first term in (19). Again, fix \mathbf{u} with $\|\mathbf{u}\| = 1$ arbitrarily. Define the random variables

$$Z_i(\mathbf{u}) := \left(1 + \epsilon_i^2 + \frac{(\mathbf{x}_i^T \mathbf{u})^2}{\kappa_1 \mathbf{u}^T \Gamma_n(0) \mathbf{u}} \right)^{-3/2} \frac{(\mathbf{x}_i^T \mathbf{u})^2}{\mathbf{u}^T \Gamma_n(0) \mathbf{u}} \quad \forall 1 \leq i \leq n.$$

It follows by Assumptions A2 and A3 that $\{Z_i(\mathbf{u})\}_{i=1}^n$ are i.i.d. random variables and are uniformly bounded by κ_1 . Note that $G(\mathbf{u}) := \mathbf{x}_1^T \mathbf{u} / \sqrt{\mathbf{u}^T \Gamma_n(0) \mathbf{u}}$ has a standard normal distribution

and is independent of ϵ_1 . Hence

$$\begin{aligned} E_0[Z_1(\mathbf{u})] &= E_0 \left[(1 + \epsilon_1^2 + (1/\kappa_1)G(\mathbf{u})^2)^{-3/2} G(\mathbf{u})^2 \right] \\ &:= M_1. \end{aligned}$$

Based on the arguments above, it follows that M_1 is a strictly positive constant which does not depend on \mathbf{u} and n . Also, by the definition of the function g in Assumption A3, it follows that $g(\epsilon_i) = E[Z_i(\mathbf{u}) | \epsilon]$ (and $E_0[Z_i(\mathbf{u})] = E[g(\epsilon_i)]$ by tower property). Note that

$$\begin{aligned} &P_0 \left(\left| \frac{1}{n} \sum_{i=1}^n Z_i(\mathbf{u}) - E_0[Z_1(\mathbf{u})] \right| > \frac{M_1}{2} \right) \\ &\leq P_0 \left(\left| \sum_{i=1}^n Z_i(\mathbf{u}) - \sum_{i=1}^n g(\epsilon_i) \right| > \frac{nM_1}{4} \right) + P_0 \left(\left| \sum_{i=1}^n g(\epsilon_i) - nE_0[Z_1(\mathbf{u})] \right| > \frac{nM_1}{4} \right) \\ &= P_0 \left(\left| \sum_{i=1}^n Z_i(\mathbf{u}) - \sum_{i=1}^n E[Z_i(\mathbf{u}) | \epsilon] \right| > \frac{nM_1}{4} \right) + P_0 \left(\left| \sum_{i=1}^n g(\epsilon_i) - nE_0[g(\epsilon_1)] \right| > \frac{nM_1}{4} \right) \\ &= E_0 \left[P_0 \left(\left| \sum_{i=1}^n Z_i(\mathbf{u}) - \sum_{i=1}^n E[Z_i(\mathbf{u}) | \epsilon] \right| > \frac{nM_1}{4} \mid \epsilon \right) \right] + P_0 \left(\left| \sum_{i=1}^n g(\epsilon_i) - nE_0[g(\epsilon_1)] \right| > \frac{nM_1}{4} \right) \end{aligned}$$

We first derive an upper bound for $V(\sum_{i=1}^n Z_i(\mathbf{u}) | \epsilon)$. Note that $Z_i(\mathbf{u})$ is a uniformly bounded function of $\mathbf{x}_i^T \mathbf{u}$ (which has a normal distribution, even if we condition on ϵ). Using the fact that the maximal correlation between two normal random variables Z_1 and Z_2 is given by $|Corr(Z_1, Z_2)|$ (see for example Lancaster (1957)), the stationarity of the predictor process, and Assumption A2, we obtain

$$\begin{aligned} Cov(Z_i(\mathbf{u}), Z_j(\mathbf{u}) | \epsilon) &\leq 4\kappa_1^2 |Corr(\mathbf{x}_i^T \mathbf{u}, \mathbf{x}_j^T \mathbf{u} | \epsilon)| \\ &\leq \frac{4\kappa_1^2 |\mathbf{u}^T \Gamma_n(i-j)\mathbf{u}|}{\mathbf{u}^T \Gamma_n(0)\mathbf{u}} \\ &\leq 4\kappa_1 |\mathbf{u}^T \Gamma_n(i-j)\mathbf{u}| \\ &\leq 2\kappa_1 \|\Gamma_n(i-j) + \Gamma_n(i-j)\|. \end{aligned}$$

Let $\mathbf{1}_n$ denote the vector of all ones in \mathbb{R}^n . It follows by Assumption A2 that

$$\begin{aligned} V\left(\sum_{i=1}^n Z_i(\mathbf{u}) | \epsilon\right) &= \sum_{i=1}^n V(Z_i(\mathbf{u}) | \epsilon) + \sum_{1 \leq i \neq j \leq n} Cov(Z_i(\mathbf{u}), Z_j(\mathbf{u}) | \epsilon) \\ &\leq 4n\kappa_1 \sum_{h=0}^{n-1} \|\Gamma_n(h)\|_2 \\ &= 4n\kappa_1 \kappa_2. \end{aligned}$$

Using the independence of the predictors and the errors, along with Bernstein's concentration inequality for bounded random variables, we obtain

$$E_0 \left[P_0 \left(\left| \sum_{i=1}^n Z_i(\mathbf{u}) - \sum_{i=1}^n E[Z_i(\mathbf{u}) | \epsilon] \right| > \frac{nM_1}{4} \mid \epsilon \right) \right]$$

$$\begin{aligned}
&\leq E_0 \left[\exp \left(- \frac{\frac{1}{32} n^2 M_1^2}{V(\sum_{i=1}^n Z_i(\mathbf{u}) \mid \boldsymbol{\epsilon}) + \frac{n\kappa_1}{6} M_1} \right) \right] \\
&\leq \exp \left(- \frac{\frac{1}{32} n^2 M_1^2}{4n\kappa_1^2 + 16n\kappa_1\kappa_2 + \frac{n\kappa_1 M_1}{6}} \right) \\
&=: \exp(-nM_2),
\end{aligned} \tag{24}$$

where $M_2 = \frac{3M_1^2}{384\kappa_1^2 + 1536\kappa_1\kappa_2 + 16\kappa_1 M_1}$. We now focus on the second term in (23). Note that by second order stationarity of the error sequence

$$\frac{1}{n} V\left(\sum_{i=1}^n g(\epsilon_i)\right) = V(g(\epsilon_1)) + \sum_{i=2}^n \left(1 - \frac{i}{n}\right) \text{Cov}(g(\epsilon_1), g(\epsilon_i)) \leq V(g(\epsilon_1)) + \sum_{i=2}^n |\text{Cov}(g(\epsilon_1), g(\epsilon_i))| \leq K_\epsilon.$$

Again using uniform boundedness of g , Bernstein's concentration inequality and Assumption A3, it follows that

$$\begin{aligned}
P_0 \left(\left| \sum_{i=1}^n g(\epsilon_i) - nE_0[g(\epsilon_1)] \right| > \frac{nM_1}{4} \right) &\leq \exp \left(- \frac{\frac{1}{32} n^2 M_1^2}{V(\sum_{i=1}^n g(\epsilon_i)) + \frac{n\kappa_1}{6} M_1} \right) \\
&\leq \exp \left(- \frac{\frac{1}{32} n^2 M_1^2}{nK_\epsilon + \frac{n\kappa_1}{6} M_1} \right) =: \exp(-nM_3), \tag{25}
\end{aligned}$$

where $M_3 = \frac{3M_1^2}{96K_\epsilon + 16\kappa_1 M_1}$. Since

$$Z_i(\mathbf{u}) \leq (1 + \epsilon_i^2 + (\mathbf{x}_i^T \mathbf{u})^2)^{-3/2} \frac{(\mathbf{x}_i^T \mathbf{u})^2}{\kappa_1},$$

it follows by (23), (24) and (25) that

$$\begin{aligned}
P_0 \left(\frac{1}{n} \sum_{i=1}^n (1 + \epsilon_i^2 + (\mathbf{x}_i^T \mathbf{u})^2)^{-3/2} (\mathbf{x}_i^T \mathbf{u})^2 < \frac{\kappa_1 M_1}{2} \right) &\leq P_0 \left(\frac{1}{n} \sum_{i=1}^n Z_i(\mathbf{u}) < \frac{M_1}{2} \right) \\
&= P_0 \left(\frac{1}{n} \sum_{i=1}^n Z_i(\mathbf{u}) < E_0[Z_1(\mathbf{u})] - \frac{M_1}{2} \right) \\
&\leq 2 \exp(-\min(M_2, M_3)n). \tag{26}
\end{aligned}$$

We now use another covering argument to get a bound on the infimum over all appropriate \mathbf{u} . By (Vershynin, 2011, Lemma 5.2), there exists a set $S_{1/p}$ with the property that $S_{1/p} \subseteq \{\mathbf{u} : \|\mathbf{u}\| \leq 1\}$, $|S_{1/p}| \leq (2p+1)^p$, and for any \mathbf{u} with $\|\mathbf{u}\| = 1$, there exists $\mathbf{w}_{(\mathbf{u})} \in S_{1/p}$ such that $\|\mathbf{u} - \mathbf{w}_{(\mathbf{u})}\| \leq p^{-1}$. We define $\tilde{\mathbf{w}}_{(\mathbf{u})} = (1/\|\mathbf{w}_{(\mathbf{u})}\|)\mathbf{w}_{(\mathbf{u})}$ so that $\|\tilde{\mathbf{w}}_{(\mathbf{u})}\| = 1$. Since

$$\|1 - \|\mathbf{w}_{(\mathbf{u})}\|\| = \left| \|\mathbf{u}\| - \|\mathbf{w}_{(\mathbf{u})}\| \right| \leq \|\mathbf{u} - \mathbf{w}_{(\mathbf{u})}\| \leq \frac{1}{p},$$

we get

$$\|\mathbf{u} - \tilde{\mathbf{w}}_{(\mathbf{u})}\| \leq \|\mathbf{u} - \mathbf{w}_{(\mathbf{u})}\| + \left| \frac{1}{\|\mathbf{w}_{(\mathbf{u})}\|} - 1 \right| \|\mathbf{w}_{(\mathbf{u})}\| \leq \frac{2}{p}.$$

We denote the collection of all possible $\tilde{\mathbf{w}}_{(\mathbf{u})}$ (as \mathbf{u} varies over $\{\mathbf{u} : \|\mathbf{u}\| = 1\}$) by $\tilde{S}_{1/p}$. It follows that $|\tilde{S}_{1/p}| \leq (2p+1)^p$. Now, for any $a > 0$, consider the function

$$g_a(x) = \frac{x^2}{(1+a+x^2)^{-3/2}}.$$

Simple calculations show that

$$|g'_a(x)| \leq \left| \frac{2x}{(1+a+x^2)^{-3/2}} \right| + \left| \frac{3x^3}{(1+a+x^2)^{-5/2}} \right| \leq 5.$$

Hence for every \mathbf{u} , we have

$$\begin{aligned} \left\| \frac{\partial}{\partial \mathbf{u}} \left(\frac{1}{n} \sum_{i=1}^n (1 + \epsilon_i^2 + (\mathbf{x}_i^T \mathbf{u})^2)^{-3/2} (\mathbf{x}_i^T \mathbf{u})^2 \right) \right\| &= \left\| \frac{\partial}{\partial \mathbf{u}} \left(\frac{1}{n} \sum_{i=1}^n g_{\epsilon_i^2}(\mathbf{x}_i^T \mathbf{u}) \right) \right\| \\ &= \left\| \frac{1}{n} \sum_{i=1}^n g'_{\epsilon_i^2}(\mathbf{x}_i^T \mathbf{u}) \mathbf{x}_i \right\| \\ &\leq \frac{1}{n} \sum_{i=1}^n |g'_{\epsilon_i^2}(\mathbf{x}_i^T \mathbf{u})| \|\mathbf{x}_i\| \\ &\leq \frac{5}{n} \sum_{i=1}^n \|\mathbf{x}_i\| \\ &\leq 5 \sqrt{\frac{1}{n} \sum_{i=1}^n \mathbf{x}_i^T \mathbf{x}_i} \end{aligned} \quad (27)$$

The last inequality follows by Jensen's inequality, using the concavity of the square-root function. Let $\mathbf{x} \in \mathbb{R}^{np}$ be the vector obtained by stacking $\mathbf{x}_1, \mathbf{x}_2, \dots, \mathbf{x}_n$ on top of each other. Let Θ_n denote the $n \times n$ block partitioned matrix whose $(i, j)^{th}$ block is given by $\Gamma_n(i-j)$ for $1 \leq i, j \leq n$. Then by Assumption A2, \mathbf{x} has a multivariate normal distribution with mean $\mathbf{0}$ and covariance matrix Θ_n .

We next present an argument to bound the largest eigenvalue of Θ_n in terms of κ_2 . The argument below is based on the proof of Theorem 2.3 in Basu and Michailidis (2015), but is presented here for completeness. Consider the function

$$f_n(\theta) = \frac{1}{2\pi} \sum_{k=-(n-1)}^{n-1} \Gamma_n(k) e^{-ik\theta}, \quad \theta \in [-\pi, \pi].$$

The existence, boundedness and continuity of f_n follows from Assumption A2. For any $\tilde{\mathbf{u}} \in \mathbb{R}^{np}$ with $\|\tilde{\mathbf{u}}\|_2 = 1$, partition $\tilde{\mathbf{u}}$ as $((\tilde{\mathbf{u}}^1)^T, (\tilde{\mathbf{u}}^2)^T, \dots, (\tilde{\mathbf{u}}^n)^T)^T$. Define $G(\theta) = \sum_{k=1}^n \mathbf{u}^k e^{-ik\theta}$, and note that

$$\int_{-\pi}^{\pi} G^*(\theta) G(\theta) d\theta = \sum_{k=1}^n \sum_{k'=1}^n \int_{-\pi}^{\pi} (\tilde{\mathbf{u}}^k)^T \tilde{\mathbf{u}}^{k'} e^{i(k-k')\theta} d\theta = 2\pi \sum_{k=1}^n (\tilde{\mathbf{u}}^k)^T \tilde{\mathbf{u}}^{k'} = 2\pi.$$

By Assumption A2, and the triangle inequality for the $\|\cdot\|_2$ -norm (for matrices with complex valued entries), it follows that $\|f_n(\theta)\|_2 \leq \kappa_2/\pi$ for every $\theta \in [-\pi, \pi]$. Note also that $f_n(\theta)$ is

hermitian and all its eigenvalues are real for every $\theta \in [-\pi, \pi]$. Using the block partitioned form of Θ_n , and the definition of f_n , we obtain

$$\begin{aligned}
\tilde{\mathbf{u}}^T \Theta_n \tilde{\mathbf{u}} &= \sum_{k=1}^n \sum_{k'=1}^n (\tilde{\mathbf{u}}^k)^T \Gamma_n(k-k') \tilde{\mathbf{u}}^{k'} \\
&= \sum_{k=1}^n \sum_{k'=1}^n \int_{-\pi}^{\pi} (\tilde{\mathbf{u}}^k)^T f_n(\theta) e^{i(k-k')\theta} \tilde{\mathbf{u}}^{k'} d\theta \\
&= \int_{-\pi}^{\pi} G(\theta)^* f_n(\theta) G(\theta) d\theta \\
&\leq \frac{\kappa_2}{\pi} \int_{-\pi}^{\pi} G(\theta)^* G(\theta) d\theta \\
&= 2\kappa_2.
\end{aligned}$$

We conclude that $\|\Theta_n\|_2 \leq 2\kappa_2$.

Let $C_n := \{\frac{1}{n} \sum_{i=1}^n \mathbf{x}_i^T \mathbf{x}_i \leq 4p\kappa_2\}$. Since $\mathbf{x}^T \mathbf{x} = \sum_{i=1}^n \mathbf{x}_i^T \mathbf{x}_i$ and $\|\Theta_n\|_2 \leq 2\kappa_2$, the event $\{\mathbf{x}^T \Theta_n^{-1} \mathbf{x} \leq 2np\}$ is a subset of C_n . Note that $\mathbf{x}^T \Theta_n^{-1} \mathbf{x}$ has a χ_{np}^2 distribution under P_0 . Using standard tail concentration bounds for χ^2 random variables (see for example (Cao et al., 2020, Lemma 4.1)), it follows that

$$\begin{aligned}
P_0(C_n^c) &\leq P_0(\mathbf{x}^T \Theta_n^{-1} \mathbf{x} \geq 2np) \\
&\leq 2 \exp\left(-\frac{4n^2 p^2}{4np + 2np}\right) \\
&= 2 \exp\left(-\frac{2np}{3}\right) \rightarrow 0
\end{aligned}$$

as $n \rightarrow \infty$. It follows by the mean value theorem and (27) that for every \mathbf{u} with $\|\mathbf{u}\| = 1$

$$\begin{aligned}
&\left| \frac{1}{n} \sum_{i=1}^n (1 + \epsilon_i^2 + (\mathbf{x}_i^T \mathbf{u})^2)^{-3/2} (\mathbf{x}_i^T \mathbf{u})^2 - \frac{1}{n} \sum_{i=1}^n (1 + \epsilon_i^2 + (\mathbf{x}_i^T \tilde{\mathbf{w}}(\mathbf{u}))^2)^{-3/2} (\mathbf{x}_i^T \tilde{\mathbf{w}}(\mathbf{u}))^2 \right| \\
&\leq 10\sqrt{p\kappa_2} \|\mathbf{u} - \tilde{\mathbf{w}}(\mathbf{u})\| \\
&\leq \frac{20\kappa_2}{\sqrt{p}}
\end{aligned} \tag{28}$$

on C_n . Hence

$$\inf_{\mathbf{u}: \|\mathbf{u}\|=1} \frac{1}{n} \sum_{i=1}^n (1 + \epsilon_i^2 + (\mathbf{x}_i^T \mathbf{u})^2)^{-3/2} (\mathbf{x}_i^T \mathbf{u})^2 \geq \min_{\mathbf{w} \in \tilde{S}_{1/p}} \frac{1}{n} \sum_{i=1}^n (1 + \epsilon_i^2 + (\mathbf{x}_i^T \mathbf{w})^2)^{-3/2} (\mathbf{x}_i^T \mathbf{w})^2 - \frac{20\kappa_2}{\sqrt{p}}.$$

on C_n . It follows by (26) and Assumption A1 that

$$\begin{aligned}
&P_0\left(\inf_{\mathbf{u}: \|\mathbf{u}\|=1} \frac{1}{n} \sum_{i=1}^n (1 + \epsilon_i^2 + (\mathbf{x}_i^T \mathbf{u})^2)^{-3/2} (\mathbf{x}_i^T \mathbf{u})^2 < \frac{\kappa_1 M_1}{2} - \frac{20\kappa_2}{\sqrt{p}}\right) \\
&\leq P_0\left(\min_{\mathbf{w} \in \tilde{S}_{1/p}} \frac{1}{n} \sum_{i=1}^n (1 + \epsilon_i^2 + (\mathbf{x}_i^T \mathbf{w})^2)^{-3/2} (\mathbf{x}_i^T \mathbf{w})^2 < \frac{\kappa_1 M_1}{2}\right) + P_0(C_n^c)
\end{aligned}$$

$$\begin{aligned}
&\leq P_0(C_n^c) + \sum_{\mathbf{w} \in \tilde{S}_{1/p}} P_0 \left(\frac{1}{n} \sum_{i=1}^n (1 + \epsilon_i^2 + (\mathbf{x}_i^T \mathbf{w})^2)^{-3/2} (\mathbf{x}_i^T \mathbf{w})^2 < \frac{\kappa_1 M_1}{2} \right) \\
&\leq P_0(C_n^c) + 2(2p+1)^p \exp(-\min(M_2, M_3)n) \\
&= P_0(C_n^c) + 2 \times \exp(-\min(M_2, M_3)n + p \log(2p+1)) \rightarrow 0
\end{aligned} \tag{29}$$

as $n \rightarrow \infty$. For large enough n , $\frac{\kappa_1 M_1}{2} - \frac{20\kappa_2}{\sqrt{p}} > \frac{\kappa_1 M_1}{4}$. Using (19), (22), (29), and Assumption A4, we get

$$\begin{aligned}
&P_0 \left(\inf_{\mathbf{u}: \|\mathbf{u}\|=1} (Q_\alpha(\boldsymbol{\beta}_0 + \delta_n \mathbf{u}) - Q_\alpha(\boldsymbol{\beta}_0)) > \frac{\sqrt{1 + \alpha^{-2}} \delta_n^2 \kappa_1 M_1}{8\alpha} - (K_1 \sqrt{1 + \alpha^{-2}} + 2) \delta_n \sqrt{\frac{p}{n}} \right) \\
&\geq 1 - \left(2 \exp\left(-\frac{2np}{3}\right) + \exp\left(-\left\{\frac{81K_1^2}{400\kappa_2} - \log 21\right\} p\right) + 2 \times \exp(-\min(M_2, M_3)n + p \log(2p+1)) \right)
\end{aligned}$$

for large enough n . Since $\delta_n = \tilde{M} \alpha_n \sqrt{\frac{p}{n}}$, it follows that

$$P_0 \left(\inf_{\mathbf{u}: \|\mathbf{u}\|=1} (Q_\alpha(\boldsymbol{\beta}_0 + \delta_n \mathbf{u}) - Q_\alpha(\boldsymbol{\beta}_0)) > \sqrt{1 + \alpha^{-2}} (K_1 + 2) \delta_n \sqrt{\frac{p}{n}} \right) \rightarrow 1$$

for a large enough choice of \tilde{M} . \square

C.2 Proof of Theorem 2

We first establish that the posterior asymptotically places all of its mass in a neighborhood of radius $K''\alpha$ around $\boldsymbol{\beta}_0$, for an appropriate K'' . Note that

$$\begin{aligned}
\Pi(\|\boldsymbol{\beta} - \boldsymbol{\beta}_0\| > K''\alpha \mid \mathbf{Y}) &= \frac{\int_{\|\mathbf{u}\| > K''\alpha} \exp(-n\alpha Q_\alpha(\boldsymbol{\beta}_0 + \mathbf{u})) d\mathbf{u}}{\int_{\mathbb{R}^p} \exp(-n\alpha Q_\alpha(\hat{\boldsymbol{\beta}}_{pm} + \mathbf{v})) d\mathbf{v}} \\
&= \exp(n\alpha Q_\alpha(\hat{\boldsymbol{\beta}}_{pm})) \frac{\int_{\|\mathbf{u}\| > K''\alpha} \exp(-n\alpha Q_\alpha(\boldsymbol{\beta}_0 + \mathbf{u})) d\mathbf{u}}{\int_{\mathbb{R}^p} \exp(-n\alpha \{Q_\alpha(\hat{\boldsymbol{\beta}}_{pm} + \mathbf{v}) - Q_\alpha(\hat{\boldsymbol{\beta}}_{pm})\}) d\mathbf{v}}
\end{aligned} \tag{30}$$

for any $K'' > 0$. A specific choice of K'' will be made later. Using the second order Taylor expansion of $\tilde{f}_{\mathbf{v}}(t) = Q_\alpha(\hat{\boldsymbol{\beta}}_{pm} + t\mathbf{v})$ around $t = 0$, we get

$$\begin{aligned}
&n\alpha \left(Q_\alpha(\hat{\boldsymbol{\beta}}_{pm} + \mathbf{v}) - Q_\alpha(\hat{\boldsymbol{\beta}}_{pm}) \right) \\
&= n\alpha \left(\tilde{f}_{\mathbf{v}}(1) - \tilde{f}_{\mathbf{v}}(0) \right) \\
&= \left\{ 2\tau^2 \hat{\boldsymbol{\beta}}_{pm}^T + \sum_{i=1}^n \ell'_\alpha(Y_i - \mathbf{x}_i^T \hat{\boldsymbol{\beta}}_{pm}) \mathbf{x}_i^T \right\} \mathbf{v} + \frac{1}{2} \sum_{i=1}^n \ell''_\alpha(Y_i - \mathbf{x}_i^T \hat{\boldsymbol{\beta}}_{pm} - t^*(\mathbf{u}) \mathbf{x}_i^T \mathbf{v}) (\mathbf{x}_i^T \mathbf{v})^2 + \tau^2 \mathbf{v}^T \mathbf{v}
\end{aligned}$$

where $t^*(\mathbf{v}) \in (0, 1)$. Since $\hat{\boldsymbol{\beta}}_{pm}$ is the unique minimizer of Q_α , it follows that

$$n\alpha \left(Q_\alpha(\hat{\boldsymbol{\beta}}_{pm} + \mathbf{v}) - Q_\alpha(\hat{\boldsymbol{\beta}}_{pm}) \right) = \frac{1}{2} \sum_{i=1}^n \ell''_\alpha(Y_i - \mathbf{x}_i^T \hat{\boldsymbol{\beta}}_{pm} - t^*(\mathbf{v}) \mathbf{x}_i^T \mathbf{v}) (\mathbf{x}_i^T \mathbf{v})^2 + \tau^2 \mathbf{v}^T \mathbf{v}. \tag{31}$$

Since $0 \leq \ell''_\alpha(y) \leq 1$ for every $y \in \mathbb{R}$, it follows that

$$\frac{n\alpha}{\sqrt{1+\alpha^{-2}}} \left(Q_\alpha(\hat{\beta}_{pm} + \mathbf{v}) - Q_\alpha(\hat{\beta}_{pm}) \right) \leq \mathbf{v}^T \frac{\sum_{i=1}^n \mathbf{x}_i \mathbf{x}_i^T}{2} \mathbf{v} + \tau^2 \mathbf{v}^T \mathbf{v} \quad (32)$$

for every $\mathbf{u} \in \mathbb{R}^p$. It follows from (30) that

$$\begin{aligned} & \Pi(\|\beta - \beta_0\| > K''\alpha \mid \mathbf{Y}) \\ & \leq \exp(n\alpha Q_\alpha(\hat{\beta}_{pm})) \frac{\int_{\|\mathbf{u}\| > K''\alpha} \exp(-n\alpha Q_\alpha(\beta_0 + \mathbf{u})) d\mathbf{u}}{\int_{\mathbb{R}^p} \exp\left(-\sqrt{1+\alpha^{-2}} \mathbf{v}^T \frac{\sum_{i=1}^n \mathbf{x}_i \mathbf{x}_i^T}{2} \mathbf{u} - \sqrt{1+\alpha^{-2}} \tau^2 \mathbf{v}^T \mathbf{v}\right) d\mathbf{u}}. \end{aligned} \quad (33)$$

Now, let $\mathbf{v} \in \mathbb{R}^p$ with $\|\mathbf{v}\| = 1$. Then

$$\mathbf{v}^T \left(\frac{1}{n} \sum_{i=1}^n \mathbf{x}_i \mathbf{x}_i^T \right) \mathbf{v} = \frac{1}{n} \mathbf{Z}^T Q \mathbf{Z},$$

where $\mathbf{Z} \sim \mathcal{N}_n(\mathbf{0}, I_n)$ under P_0 , and the $(r, s)^{th}$ element of Q is given by $\mathbf{v}^T \Gamma_n(r-s)\mathbf{v}$. Using $\|Q\|_F^2 \leq n\|Q\|$, $E_0 \left[\frac{1}{n} \mathbf{Z}^T Q \mathbf{Z} \right] = \mathbf{v}^T \Gamma_n(0)\mathbf{v}$, along with the Hanson-Wright inequality of Rudelson and Vershynin (2013), we obtain

$$P_0 \left(\left| \mathbf{v}^T \left(\frac{1}{n} \sum_{i=1}^n \mathbf{x}_i \mathbf{x}_i^T \right) \mathbf{v} - \mathbf{v}^T \Gamma_n(0)\mathbf{v} \right| > \|Q\|\eta \right) \leq 2 \exp(-cn \min(\eta^2, \eta))$$

for every $\eta > 0$. By a very similar argument to the one at the end of Page 1547 in Basu and Michailidis (2015), it follows that $\|Q\| \leq \|\Theta_n\| \leq 2\kappa_2$. Hence,

$$P_0 \left(\left| \mathbf{v}^T \left(\frac{1}{n} \sum_{i=1}^n \mathbf{x}_i \mathbf{x}_i^T \right) \mathbf{v} - \mathbf{v}^T \Gamma_n(0)\mathbf{v} \right| > \frac{10\kappa_2}{\sqrt{c}} \sqrt{\frac{p}{n}} \right) \leq 2 \exp(-25p).$$

Using Lemma B.2 in Ghosh et al. (2019), it follows that

$$P_0 \left(\left\| \frac{1}{n} \sum_{i=1}^n \mathbf{x}_i \mathbf{x}_i^T - \Gamma_n(0) \right\| > \frac{10\kappa_2}{\sqrt{c}} \sqrt{\frac{p}{n}} \right) \leq 2 \exp(-p(25 - 2 \log(21))) \rightarrow 0 \quad (34)$$

as $n \rightarrow \infty$. It follows by Assumption A1, Assumption A2 and (33) that on an event with P_0 -probability converging to one, we have

$$\Pi(\|\beta - \beta_0\| > K''\alpha \mid \mathbf{Y}) \leq \left(\frac{3\tau^2 + 3\kappa_1^{-1}n}{2\pi} \right)^{p/2} \exp(n\alpha Q_\alpha(\hat{\beta}_{pm})) \int_{\|\mathbf{u}\| > K''\alpha} \exp(-n\alpha Q_\alpha(\beta_0 + \mathbf{u})) d\mathbf{u}. \quad (35)$$

Note that for any $t \in \mathbb{R}$ we have

$$\sqrt{1+\alpha^2}(|t| - \alpha) \leq \ell_\alpha(t) \leq \sqrt{1+\alpha^2}|t|.$$

Since $y_i - \mathbf{x}_i^T(\beta_0 + \mathbf{u}) = \epsilon_i - \mathbf{x}_i^T \mathbf{u}$, $y_i - \mathbf{x}_i^T \hat{\beta}_{pm} = \epsilon_i - \mathbf{x}_i^T(\hat{\beta}_{pm} - \beta_0)$ and $|\epsilon_i - \mathbf{x}_i^T \mathbf{u}| \geq |\mathbf{x}_i^T \mathbf{u}| - |\epsilon_i|$, it follows after straightforward calculations that

$$\exp(n\alpha Q_\alpha(\hat{\beta}_{pm})) \int_{\|\mathbf{u}\| > K''\alpha} \exp(-n\alpha Q_\alpha(\beta_0 + \mathbf{u})) d\mathbf{u}$$

$$\begin{aligned}
&\leq \exp\left(n\alpha\sqrt{1+\alpha^2} + 2\sqrt{1+\alpha^2}\sum_{i=1}^n|\epsilon_i| + \sqrt{1+\alpha^2}\sum_{i=1}^n|\mathbf{x}_i^T(\hat{\boldsymbol{\beta}}_{pm} - \boldsymbol{\beta}_0)| + \tau^2\|\hat{\boldsymbol{\beta}}_{pm}\|^2 - \tau^2\|\boldsymbol{\beta}_0\|^2\right) \times \\
&\quad \int_{\|\mathbf{u}\|>K''\alpha} \exp\left(-\alpha\sum_{i=1}^n|\mathbf{x}_i^T\mathbf{u}| - 2\tau^2\mathbf{u}^T\boldsymbol{\beta}_0\right) d\mathbf{u} \\
&\leq \exp\left(n\alpha\sqrt{1+\alpha^2} + 2\sqrt{1+\alpha^2}\sum_{i=1}^n|\epsilon_i| + \sqrt{1+\alpha^2}\sum_{i=1}^n|\mathbf{x}_i^T(\hat{\boldsymbol{\beta}}_{pm} - \boldsymbol{\beta}_0)| + \tau^2\|\hat{\boldsymbol{\beta}}_{pm}\|^2 - \tau^2\|\boldsymbol{\beta}_0\|^2\right) \times \\
&\quad \int_{\|\mathbf{u}\|>K''\alpha} \exp\left(-n\alpha\|\mathbf{u}\|\left(\frac{1}{n}\sum_{i=1}^n|\mathbf{x}_i^T\tilde{\mathbf{u}}| - \frac{2\tau^2\|\boldsymbol{\beta}_0\|}{n\alpha}\right)\right) d\mathbf{u}, \tag{36}
\end{aligned}$$

where $\tilde{\mathbf{u}} = \mathbf{u}/\|\mathbf{u}\|$. By the Cauchy-Schwarz inequality, Assumption 2, (34) and Theorem 1 it follows that

$$\sum_{i=1}^n|\mathbf{x}_i^T(\hat{\boldsymbol{\beta}}_{pm} - \boldsymbol{\beta}_0)| \leq \sqrt{n}\sqrt{\sum_{i=1}^n(\hat{\boldsymbol{\beta}}_{pm} - \boldsymbol{\beta}_0)^T\mathbf{x}_i\mathbf{x}_i^T(\hat{\boldsymbol{\beta}}_{pm} - \boldsymbol{\beta}_0)} \leq \sqrt{2\kappa_1}\alpha\tilde{M}\sqrt{np}$$

on a set with P_0 probability converging to 1. Also, by the strong law of large numbers, Assumption A4' and Theorem 1, we get

$$2\sqrt{1+\alpha^2}\sum_{i=1}^n|\epsilon_i| + \tau^2\|\hat{\boldsymbol{\beta}}_{pm}\|^2 - \tau^2\|\boldsymbol{\beta}_0\|^2 \leq 4nE_0|\epsilon_1| + 2\tau^2\|\boldsymbol{\beta}_0\|\|\hat{\boldsymbol{\beta}}_{pm} - \boldsymbol{\beta}_0\| + \tau^2\|\hat{\boldsymbol{\beta}}_{pm} - \boldsymbol{\beta}_0\|^2 \leq K_2n\alpha^2$$

for an appropriate constant K_2 on an event with P_0 probability converging to 1. It follows by (36) that

$$\begin{aligned}
&\exp(n\alpha Q_\alpha(\hat{\boldsymbol{\beta}}_{pm})) \int_{\|\mathbf{u}\|>K''\alpha} \exp(-n\alpha Q_\alpha(\boldsymbol{\beta}_0 + \mathbf{u})) d\mathbf{u} \\
&\leq \exp(2(K_2 + 1)n\alpha^2) \int_{\|\mathbf{u}\|>K''\alpha} \exp\left(-n\|\mathbf{u}\|\left(\frac{\alpha}{n}\sum_{i=1}^n|\mathbf{x}_i^T\tilde{\mathbf{u}}| - \frac{2\tau^2\|\boldsymbol{\beta}_0\|}{n}\right)\right) d\mathbf{u} \tag{37}
\end{aligned}$$

on an event with P_0 probability converging to 1. Let $c := \frac{\log 2\pi}{8\sqrt{\kappa_2}}$. Fix \mathbf{v} with $\|\mathbf{v}\| = 1$ arbitrarily. Then, by Markov's inequality

$$\begin{aligned}
P_0\left(\sum_{i=1}^n|\mathbf{x}_i^T\mathbf{v}| < nc\right) &\leq P_0\left(\exp\left(-2\sqrt{\kappa_2}\sum_{i=1}^n|\mathbf{x}_i^T\mathbf{v}|\right) > \exp(-nc)\right) \\
&\leq \exp(2\sqrt{\kappa_2}nc)E_0\left[\exp\left(-2\sqrt{\kappa_2}\sum_{i=1}^n|\mathbf{x}_i^T\mathbf{v}|\right)\right]. \tag{38}
\end{aligned}$$

Recall that $\mathbf{x} \in \mathbb{R}^{np}$ is the vector obtained by stacking $\mathbf{x}_1, \mathbf{x}_2, \dots, \mathbf{x}_n$ on top of each other, and \mathbf{x} has a multivariate distribution with mean $\mathbf{0}$ and covariance matrix Θ_n . It follows that $X\mathbf{v} = (I_n \otimes \mathbf{v}^T)\mathbf{x}$ has a multivariate normal distribution with mean $\mathbf{0}$ and covariance matrix $(I_n \otimes \mathbf{v}^T)\Theta_n(I_n \otimes \mathbf{v})$. It follows by Assumptions A2 and A5 that

$$\kappa_3 \leq \lambda_{\min}((I_n \otimes \mathbf{v}^T)\Theta_n(I_n \otimes \mathbf{v})) \leq \lambda_{\max}((I_n \otimes \mathbf{v}^T)\Theta_n(I_n \otimes \mathbf{v})) \leq \kappa_2.$$

Combining this fact with (38), we get

$$P_0\left(\sum_{i=1}^n |\mathbf{x}_i^T \mathbf{v}| < nc\right) \leq \exp(2\sqrt{\kappa_2}nc) \left(\frac{\kappa_2}{\kappa_3}\right)^{p/2} E_0 \left[\exp\left(-2 \sum_{i=1}^n |Z_i|\right) \right],$$

where $\{Z_i\}_{i=1}^n$ have an i.i.d. standard normal distribution under P_0 . Using the Mills ratio identity, it follows that

$$\begin{aligned} P_0\left(\sum_{i=1}^n |\mathbf{x}_i^T \mathbf{v}| < nc\right) &\leq \exp(2\sqrt{\kappa_2}nc) \left(\frac{\kappa_2}{\kappa_3}\right)^{p/2} (E_0[\exp(-2|Z_1|)])^n \\ &\leq \exp(2\sqrt{\kappa_2}nc) \left(\frac{\kappa_2}{\kappa_3}\right)^{p/2} (2 \exp(-2) P_0(Z_1 > 2))^n \\ &\leq \exp(2\sqrt{\kappa_2}nc) \left(\frac{\kappa_2}{\kappa_3}\right)^{p/2} \left(\sqrt{\frac{1}{2\pi}}\right)^n \\ &= \exp\left(-\frac{n \log 2\pi}{4}\right) \left(\frac{\kappa_2}{\kappa_3}\right)^{p/2}. \end{aligned} \quad (39)$$

Recall the construction of the set $S_{1/p}$ (in the proof of Theorem 1) with the property that $S_{1/p} \subseteq \{\mathbf{v} : \|\mathbf{v}\| \leq 1\}$, $|S_{1/p}| \leq (2p+1)^p$, and for any \mathbf{v} with $\|\mathbf{v}\| \leq 1$, there exists $\mathbf{w}_{(\mathbf{v})} \in S_{1/p}$ such that $\|\mathbf{v} - \mathbf{w}_{(\mathbf{v})}\| \leq p^{-1}$. Recall also, the construction $\tilde{\mathbf{w}}_{(\mathbf{v})} = (1/\|\mathbf{w}_{(\mathbf{v})}\|)\mathbf{w}_{(\mathbf{v})}$ (so that $\|\tilde{\mathbf{w}}_{(\mathbf{v})}\| = 1$) with the property

$$\|\mathbf{v} - \tilde{\mathbf{w}}_{(\mathbf{v})}\| \leq \frac{2}{p},$$

and that $\tilde{S}_{1/p}$ denotes the collection of all $\tilde{\mathbf{w}}_{(\mathbf{v})}$ (as \mathbf{v} varies over $\{\mathbf{v} : \|\mathbf{v}\| \leq 1\}$). Now, for any \mathbf{v} with $\|\mathbf{v}\| \leq 1$, we have

$$\sum_{i=1}^n |\mathbf{x}_i^T \mathbf{v}| \geq \sum_{i=1}^n |\mathbf{x}_i^T \tilde{\mathbf{w}}_{(\mathbf{v})}| - \sum_{i=1}^n |\mathbf{x}_i^T (\mathbf{v} - \tilde{\mathbf{w}}_{(\mathbf{v})})|.$$

It follows that

$$\begin{aligned} \inf_{\mathbf{v}: \|\mathbf{v}\| \leq 1} \sum_{i=1}^n |\mathbf{x}_i^T \mathbf{v}| &\geq \inf_{\mathbf{w} \in \tilde{S}_{1/p}} \sum_{i=1}^n |\mathbf{x}_i^T \tilde{\mathbf{w}}| - \frac{2}{p} \sum_{i=1}^n \|\mathbf{x}_i\| \\ &\geq \inf_{\mathbf{v}: \|\mathbf{v}\| \leq 1} \sum_{i=1}^n |\mathbf{x}_i^T \mathbf{v}| - \frac{4n\sqrt{\kappa_2}}{\sqrt{p}} \end{aligned} \quad (40)$$

on an event with P_0 -probability converging to 1 (see the definition of the set C_n in the proof of Theorem 1). Using Assumption A1 and (40), for large enough n , we get

$$\begin{aligned} &P_0\left(\inf_{\mathbf{v}: \|\mathbf{v}\| \leq 1} \sum_{i=1}^n |\mathbf{x}_i^T \mathbf{v}| < \frac{nc}{2}\right) \\ &\leq P_0\left(\inf_{\mathbf{w} \in \tilde{S}_{1/p}} \sum_{i=1}^n |\mathbf{x}_i^T \tilde{\mathbf{w}}| < \frac{nc}{2} + \frac{4n\sqrt{\kappa_2}}{\sqrt{p}}\right) + P_0(C_n^c) \end{aligned}$$

$$\begin{aligned}
&\leq P_0 \left(\inf_{\mathbf{w} \in \tilde{S}_{1/p}} \sum_{i=1}^n |\mathbf{x}_i^T \tilde{\mathbf{w}}| < nc \right) + P_0(C_n^c) \\
&\leq \sum_{\mathbf{w} \in \tilde{S}_{1/p}} P_0 \left(\sum_{i=1}^n |\mathbf{x}_i^T \tilde{\mathbf{w}}| < nc \right) + P_0(C_n^c) \\
&\leq \exp \left(-\frac{n \log 2\pi}{4} \right) \left(\frac{\kappa_2}{\kappa_3} \right)^{p/2} (2p+1)^p + P_0(C_n^c) \rightarrow 0
\end{aligned} \tag{41}$$

as $n \rightarrow \infty$. By (35), (37), (41) and Assumption A4, it follows that

$$\begin{aligned}
&\Pi \left(\|\boldsymbol{\beta} - \hat{\boldsymbol{\beta}}_{pm}\| > K''\alpha \mid \mathbf{Y} \right) \\
&\leq \left(\frac{3\tau^2 + 3\kappa_1^{-1}n}{2\pi} \right)^{p/2} \exp(2(K_2 + 1)n\alpha^2) \int_{\|\mathbf{u}\| > K''\alpha} \exp \left(-\frac{n\alpha c \|\mathbf{u}\|}{4} \right) d\mathbf{u} \\
&\leq \left(\frac{3\tau^2 + 3\kappa_1^{-1}n}{2\pi} \right)^{p/2} \exp(2(K_2 + 1)n\alpha^2) \exp \left(-\frac{ncK''\alpha^2}{8} \right) \int_{\|\mathbf{u}\| > K''\alpha} \exp \left(-\frac{n\alpha c \|\mathbf{u}\|}{8} \right) d\mathbf{u} \\
&\leq \left(\frac{3\tau^2 + 3\kappa_1^{-1}n}{2\pi} \right)^{p/2} \exp(2(K_2 + 1)n\alpha^2) \exp \left(-\frac{ncK''\alpha^2}{8} \right) \int_{\|\mathbf{u}\| > K''\alpha} \exp \left(-\frac{n\alpha c \sum_{i=1}^p |u_i|}{8\sqrt{p}} \right) d\mathbf{u} \\
&\leq \left(\frac{3\tau^2 + 3\kappa_1^{-1}n}{2\pi} \right)^{p/2} \exp(2(K_2 + 1)n\alpha^2) \exp \left(-\frac{ncK''\alpha^2}{8} \right) \left(\frac{16\sqrt{p}}{n\alpha c} \right)^p.
\end{aligned}$$

on an event with P_0 -probability converging to 1. By Assumptions A1 and A5, it follows that

$$E_0 \left[\Pi \left(\|\boldsymbol{\beta} - \hat{\boldsymbol{\beta}}_{pm}\| > K''\alpha \mid \mathbf{Y} \right) \right] \rightarrow 0 \tag{42}$$

for a suitably large constant K'' as $n \rightarrow \infty$. In light of (42), to prove the desired result, it is enough to show that

$$\Pi \left(\|\boldsymbol{\beta} - \boldsymbol{\beta}_0\| > M^*\delta_n, \|\boldsymbol{\beta} - \boldsymbol{\beta}_0\| \leq (K'' - 1)\alpha \mid \mathbf{Y} \right)$$

converges in P_0 -probability to zero as $n \rightarrow \infty$. Note that

$$\begin{aligned}
&\Pi \left(\|\boldsymbol{\beta} - \boldsymbol{\beta}_0\| > M^*\delta_n, \|\boldsymbol{\beta} - \boldsymbol{\beta}_0\| \leq (K'' - 1)\alpha \mid \mathbf{Y} \right) \\
&= \frac{\int_{\|\mathbf{u}\| \leq \tilde{K}\alpha, \|\mathbf{u}\| > M^*\delta_n} \exp(-n\alpha Q_\alpha(\boldsymbol{\beta}_0 + \mathbf{u})) d\mathbf{u}}{\int_{\mathbb{R}^p} \exp(-n\alpha Q_\alpha(\boldsymbol{\beta})) d\boldsymbol{\beta}} \\
&= \frac{\int_{\|\mathbf{u}\| \leq \tilde{K}\alpha, \|\mathbf{u}\| > M^*\delta_n} \exp(-n\alpha \{Q_\alpha(\boldsymbol{\beta}_0 + \mathbf{u}) - Q_\alpha(\boldsymbol{\beta}_0)\}) d\mathbf{u}}{\int_{\mathbb{R}^p} \exp(-n\alpha \{Q_\alpha(\hat{\boldsymbol{\beta}}_{pm} + \mathbf{u}) - Q_\alpha(\hat{\boldsymbol{\beta}}_{pm})\}) d\mathbf{u}} \times \exp \left(n\alpha \left(Q_\alpha(\boldsymbol{\beta}_0) - Q_\alpha(\hat{\boldsymbol{\beta}}_{pm}) \right) \right)
\end{aligned} \tag{43}$$

where $\tilde{K} = K'' - 1$. For any vector \mathbf{u} , the vector $\tilde{\mathbf{u}}$ denotes $\mathbf{u}/\|\mathbf{u}\|$. For every \mathbf{u} such that $\|\mathbf{u}\| \leq \tilde{K}\alpha, \|\mathbf{u}\| > M^*\delta_n$, (17) (without the δ_n term) and (18), along with (22) and Assumption A5 imply that on an event with P_0 -probability converging to one

$$Q_\alpha(\boldsymbol{\beta}_0 + \mathbf{u}) - Q_\alpha(\boldsymbol{\beta}_0) \geq \frac{1}{n\alpha} \sum_{i=1}^n \ell'_\alpha(\epsilon_i) \mathbf{x}_i^T \mathbf{u} - \frac{2\tau^2}{n\alpha} \|\mathbf{u}\| \|\boldsymbol{\beta}_0\| + \frac{\tau^2}{n\alpha} \mathbf{u}^T \mathbf{u} +$$

$$\begin{aligned}
& \frac{\sqrt{1+\alpha^{-2}}}{2n\alpha} \sum_{i=1}^n (1+2\alpha^{-2}\epsilon_i^2+2\alpha^{-2}(\mathbf{x}_i^T \mathbf{u})^2)^{-3/2} (\mathbf{x}_i^T \mathbf{u})^2 \\
&= \frac{\|\mathbf{u}\|}{n\alpha} \sum_{i=1}^n \ell'_\alpha(\epsilon_i) \mathbf{x}_i^T \tilde{\mathbf{u}} - \frac{2\tau^2}{n\alpha} \|\mathbf{u}\| \|\beta_0\| + \frac{\tau^2}{n\alpha} \mathbf{u}^T \mathbf{u} + \\
& \quad \frac{\sqrt{1+\alpha^{-2}} \|\mathbf{u}\|^2}{2n\alpha} \sum_{i=1}^n (1+2\alpha^{-2}\epsilon_i^2+2\alpha^{-2}\|\mathbf{u}\|^2(\mathbf{x}_i^T \tilde{\mathbf{u}})^2)^{-3/2} (\mathbf{x}_i^T \tilde{\mathbf{u}})^2 \\
&\geq -CM^*\delta_n \sqrt{\frac{p}{n}} + \frac{\tau^2}{n\alpha} \mathbf{u}^T \mathbf{u} + \\
& \quad + \frac{\sqrt{1+\alpha^{-2}} \|\mathbf{u}\|^2}{2n\alpha} \sum_{i=1}^n (1+2\epsilon_i^2+2\tilde{K}^2(\mathbf{x}_i^T \tilde{\mathbf{u}})^2)^{-3/2} (\mathbf{x}_i^T \tilde{\mathbf{u}})^2 \quad (44)
\end{aligned}$$

for an appropriate constant C . Now, by the exact argument starting from the end of (22) to (29) (adjusting for relevant constants in the definition of $Z_i(\mathbf{u})$), it follows that

$$P_0 \left(\inf_{\mathbf{u}: \|\mathbf{u}\|=1} \frac{1}{n} \sum_{i=1}^n (1+2\epsilon_i^2+2\tilde{K}^2(\mathbf{x}_i^T \mathbf{u})^2)^{-3/2} (\mathbf{x}_i^T \mathbf{u})^2 > \tilde{M} \right) \rightarrow 1 \quad (45)$$

as $n \rightarrow \infty$ for an appropriate constant \tilde{M} . It follows by (43), (44), (31), (32) and (45) that

$$\begin{aligned}
& \Pi(\|\beta - \beta_0\| > M^*\delta_n, \|\beta - \beta_0\| \leq (K'' - 1)\alpha \mid \mathbf{Y}) \\
&\leq \exp \left(CM^*\delta_n \alpha \sqrt{np} + \frac{\sqrt{1+\alpha^{-2}}}{2} \left\| \sum_{i=1}^n \mathbf{x}_i \mathbf{x}_i^T \right\| \|\hat{\beta}_{pm} - \beta_0\|^2 + \tau^2 \|\hat{\beta}_{pm} - \beta_0\|^2 \right) \times \\
& \quad \frac{\int_{\|\mathbf{u}\| > M^*\delta_n} \exp \left(-\frac{n\tilde{M}\sqrt{1+\alpha^{-2}}}{2} \mathbf{u}^T \mathbf{u} - \tau^2 \mathbf{u}^T \mathbf{u} \right)}{\int_{\mathbb{R}^p} \exp \left(-n\sqrt{1+\alpha^{-2}}\kappa_1 \mathbf{u}^T \mathbf{u} - \tau^2 \sqrt{1+\alpha^{-2}} \mathbf{u}^T \mathbf{u} \right) d\mathbf{u}}
\end{aligned}$$

on an event whose P_0 -probability converges to one as $n \rightarrow \infty$. It follows by (34) and Theorem 1 that

$$\begin{aligned}
& \Pi(\|\beta - \beta_0\| > M^*\delta_n, \|\beta - \beta_0\| \leq (K'' - 1)\alpha \mid \mathbf{Y}) \\
&\leq \exp \left(CM^*\delta_n \alpha \sqrt{np} + 2n\kappa_1 \delta_n^2 + \tau^2 \delta_n^2 - \frac{n\tilde{M}(M^*)^2}{4} \delta_n^2 - \frac{\tau^2(M^*)^2}{2} \delta_n^2 \right) \times \\
& \quad \frac{\int_{\|\mathbf{u}\| > M^*\delta_n} \exp \left(-\frac{n\tilde{M}\sqrt{1+\alpha^{-2}}}{2} \mathbf{u}^T \mathbf{u} - \tau^2 \mathbf{u}^T \mathbf{u} \right)}{\int_{\mathbb{R}^p} \exp \left(-n\sqrt{1+\alpha^{-2}}\kappa_1 \mathbf{u}^T \mathbf{u} - \tau^2 \sqrt{1+\alpha^{-2}} \mathbf{u}^T \mathbf{u} \right) d\mathbf{u}} \\
&\leq \exp \left(CM^*\delta_n \alpha \sqrt{np} + 2n\kappa_1 \delta_n^2 + \tau^2 \delta_n^2 - \frac{n\tilde{M}(M^*)^2}{4} \delta_n^2 - \frac{\tau^2(M^*)^2}{2} \delta_n^2 \right) \left(\frac{n\tilde{M} + 2\tau^2}{5n\kappa_1 + 5\tau^2} \right)^{-p/2} \\
&\leq \exp \left(CM^*\delta_n \alpha \sqrt{np} + 2n\kappa_1 \delta_n^2 + \tau^2 \delta_n^2 - \frac{n\tilde{M}(M^*)^2}{4} \delta_n^2 - \frac{\tau^2(M^*)^2}{2} \delta_n^2 + \frac{p}{2} \log \kappa_3 \right),
\end{aligned}$$

on an event whose P_0 -probability converges to one as $n \rightarrow \infty$, where $\kappa_3 = 5\kappa_1/\tilde{M} + 5/2$. Since $\delta_n \alpha \sqrt{np} = o(n\delta_n^2)$ and $p = o(n\delta_n^2)$, choosing $M^* = 4 \max \left(1, 2\kappa_1, \frac{C+1}{\tilde{M}} \right)$ ensures that

$$\Pi(\|\beta - \beta_0\| > M^*\delta_n, \|\beta - \beta_0\| \leq (K'' - 1)\alpha \mid \mathbf{Y})$$

converges to zero in P_0 -probability as $n \rightarrow \infty$. \square

C.3 Proof of Theorem 3

Let \mathbf{s} be any element of $\{0, 1\}^p$ which satisfies $|\mathbf{s}| \leq n/(\log(\max(n, p)))^{1+\delta} + |\mathbf{s}_0|$. Using the same arguments that led to (34), but replacing \mathbf{x}_i by $\mathbf{x}_{i,s}$, $\sqrt{p/n}$ by $\sqrt{\frac{|\mathbf{s}| \log p}{n}}$, $\Gamma_n(0)$ by $(\Gamma_n(0))_{ss}$, we get

$$P_0 \left(\left\| \frac{1}{n} \sum_{i=1}^n \mathbf{x}_{i,s} \mathbf{x}_{i,s}^T - (\Gamma_n(0))_{ss} \right\| > \frac{10\kappa_2}{\sqrt{c}} \sqrt{\frac{|\mathbf{s}| \log p}{n}} \right) \leq 2 \exp(-|\mathbf{s}| \log p (25 - 2 \log(21))) \quad (46)$$

Let

$$D_n := \bigcap_{\mathbf{s} \in \{0,1\}^p: \mathbf{s} \neq \mathbf{0}, |\mathbf{s}| \leq n/(\log(\max(n,p)))^{1+\delta} + |\mathbf{s}_0|} \left\{ \left\| \frac{1}{n} \sum_{i=1}^n \mathbf{x}_{i,s} \mathbf{x}_{i,s}^T - (\Gamma_n(0))_{ss} \right\| \leq \frac{10\kappa_2}{\sqrt{c}} \sqrt{\frac{|\mathbf{s}| \log p}{n}} \right\}.$$

It follows by (46) that

$$\begin{aligned} P(D_n) &\geq 1 - \sum_{\mathbf{s} \in \{0,1\}^p: \mathbf{s} \neq \mathbf{0}, |\mathbf{s}| \leq n/(\log(\max(n,p)))^{1+\delta} + |\mathbf{s}_0|} 2 \exp(-|\mathbf{s}| \log p (25 - 2 \log(21))) \\ &\geq 1 - \sum_{k=1}^{\infty} \binom{p}{k} 2 \exp(-k \log p (25 - 2 \log(21))) \\ &\geq 1 - 2 \sum_{k=1}^{\infty} p^k p^{-3k} \\ &= 1 - \frac{p^{-2}}{1 - p^{-2}} \rightarrow 1 \end{aligned}$$

as $n \rightarrow \infty$. We now derive bounds for the ratio of the posterior probability assigned to a given sparsity pattern \mathbf{s} and the posterior probability assigned to the true sparsity pattern \mathbf{s}_0 under different cases.

Case I: \mathbf{s} is a ‘superset’ of \mathbf{s}_0 with $|\mathbf{s}| \leq n/(\log(\max(n, p)))^{1+\delta}$. Let $\mathbf{s} \in \{0, 1\}^p$ be such that $\mathbf{s}_0 \subset \mathbf{s}$. Hence $s_j = 1$ whenever $s_{0j} = 1$. Prior to examining the ratio in (15), we need to establish consistency of the restricted posterior mode for $\boldsymbol{\beta}$ under the sparsity constraint imposed by \mathbf{s} . This posterior mode is denoted by $\hat{\boldsymbol{\beta}}_{pm,s}$. The proof goes along the same lines as the proof of Theorem 1, with some key changes that we highlight. Similar to the proof of Theorem 1, with $\delta_{n,s} := M^{**} \alpha \sqrt{\frac{|\mathbf{s}| \log p}{n}}$ (for an appropriately chosen M^{**} independent of n and \mathbf{s}), we aim to establish that

$$P_0 \left(\inf_{\mathbf{u} \in \mathbb{R}^{|\mathbf{s}|}: \|\mathbf{u}\|=1} Q_\alpha(\boldsymbol{\beta}_{0,s} + \delta_{n,s} \mathbf{u}) > Q_\alpha(\boldsymbol{\beta}_{0,s}) \right) \rightarrow 1$$

as $n \rightarrow \infty$. Since $\mathbf{s}_0 \subset \mathbf{s}$, it follows that for every $1 \leq i \leq n$

$$\epsilon_i = y_i - \mathbf{x}_i^T \boldsymbol{\beta}_0 = y_i - \mathbf{x}_{i,s_0}^T \boldsymbol{\beta}_{0,s_0} = y_i - \mathbf{x}_{i,s}^T \boldsymbol{\beta}_{0,s} \quad \text{and} \quad \|\boldsymbol{\beta}_0\| = \|\boldsymbol{\beta}_{0,s_0}\| = \|\boldsymbol{\beta}_{0,s}\|.$$

Using this fact along with similar arguments leading up to equation (18), we obtain

$$Q_\alpha(\boldsymbol{\beta}_{0,s} + \delta_{n,s} \mathbf{u}) - Q_\alpha(\boldsymbol{\beta}_{0,s})$$

$$\begin{aligned}
&\geq \frac{\delta_{n,s}}{n\alpha} \sum_{i=1}^n \ell'_\alpha(\epsilon_i) \mathbf{x}_{i,s}^T \mathbf{u} - \frac{2\tau^2 \delta_{n,s}}{n\alpha} \|\boldsymbol{\beta}_0\| + \\
&\quad \frac{\sqrt{1 + \alpha^{-2} \delta_{n,s}^2}}{2n\alpha} \sum_{i=1}^n (1 + 2\alpha^{-2} \epsilon_i^2 + 2\delta_{n,s}^2 \alpha^{-2} (\mathbf{x}_{i,s}^T \mathbf{u})^2)^{-3/2} (\mathbf{x}_{i,s}^T \mathbf{u})^2. \tag{47}
\end{aligned}$$

Again, repeating the exact same arguments between (18) and (22) replacing \mathbf{x}_i by $\mathbf{x}_{i,s}$, $\sqrt{p/n}$ by $\sqrt{\frac{|s| \log p}{n}}$, $\Gamma_n(k)$ by $(\Gamma_n(k))_s$, and 21^p by $21^{|s|}$, we get

$$\begin{aligned}
&P_0 \left(\sup_{\|\mathbf{u}\|=1} \left| \frac{1}{n\alpha \sqrt{1 + \alpha^{-2}}} \sum_{i=1}^n \ell'_\alpha(\epsilon_i) \mathbf{x}_i^T \mathbf{u} \right| > K_1 \sqrt{\frac{|s| \log p}{n}} \right) \\
&= \exp \left(- \left\{ \frac{81K_1^2}{400\kappa_2} - \log 21 \right\} |s| \log p \right) \rightarrow 0 \text{ as } n \rightarrow \infty \tag{48}
\end{aligned}$$

if K_1 is chosen to be sufficiently large. Now fix $\mathbf{u} \in \mathbb{R}^{|s|}$ with $\|\mathbf{u}\| = 1$ and define

$$Z_{i,s}(\mathbf{u}) := \left(1 + \epsilon_i^2 + \frac{(\mathbf{x}_{i,s}^T \mathbf{u})^2}{\kappa_1 \mathbf{u}^T (\Gamma_n(0))_{ss} \mathbf{u}} \right)^{-3/2} \frac{(\mathbf{x}_{i,s}^T \mathbf{u})^2}{\mathbf{u}^T (\Gamma_n(0))_{ss} \mathbf{u}} \quad \forall 1 \leq i \leq n.$$

It follows by Assumptions A2 and A3 that $\{Z_{i,s}(\mathbf{u})\}_{i=1}^n$ are i.i.d. random variables and are uniformly bounded by κ_1 . Note that $G_s(\mathbf{u}) := \mathbf{x}_{1,s}^T \mathbf{u} / \sqrt{\mathbf{u}^T (\Gamma_n(0))_{ss} \mathbf{u}}$ has a standard normal distribution and is independent of ϵ_1 , and $E_0[Z_{1,s}(\mathbf{u})] = E_0[Z_1(\mathbf{u})] = M_1$ (see proof of Theorem 1). Also, by the definition of the function g in Assumption A3, it follows that $g(\epsilon_i) = E[Z_{i,s}(\mathbf{u}) | \epsilon_i]$ (and $E_0[Z_{i,s}(\mathbf{u})] = E[g(\epsilon_i)]$ by tower property). Now, the entire argument from equation (23) to (26), can essentially be repeated verbatim (with \mathbf{x}_i replaced by $\mathbf{x}_{i,s}$ and $\Gamma_n(\cdot)$ replaced by $(\Gamma_n(\cdot))_s$), leading to the conclusion that

$$P_0 \left(\frac{1}{n} \sum_{i=1}^n (1 + \epsilon_i^2 + (\mathbf{x}_{i,s}^T \mathbf{u})^2)^{-3/2} (\mathbf{x}_{i,s}^T \mathbf{u})^2 < \frac{\kappa_1 M_1}{2} \right) \leq 2 \exp(-\min(M_2, M_3)n). \tag{49}$$

Again, by (Vershynin, 2011, Theorem 5.2), there exists a subset $\tilde{S}_{1/\max n,p}$ of $\{\mathbf{u} \in \mathbb{R}^{|s|} : \|\mathbf{u}\| = 1\}$ with the property that $|\tilde{S}_{1/\max(n,p)}| \leq (2 \max(n,p) + 1)^{|s|}$, and that for any $\mathbf{u} \in \mathbb{R}^{|s|}$ with $\|\mathbf{u}\| = 1$, there exists $\tilde{\mathbf{w}}(\mathbf{u}) \in \tilde{S}_{1/\max(n,p)}$ such that $\|\mathbf{u} - \tilde{\mathbf{w}}(\mathbf{u})\| \leq \frac{2}{\max(n,p)}$. Again, the entire argument from equation (27) to (28), can essentially be repeated verbatim (with \mathbf{x}_i replaced by $\mathbf{x}_{i,s}$ and Θ_n replaced by $(\Theta_n)_s$), leading to the conclusion that

$$\begin{aligned}
&\inf_{\mathbf{u} \in \mathbb{R}^{|s|} : \|\mathbf{u}\|=1} \frac{1}{n} \sum_{i=1}^n (1 + \epsilon_i^2 + (\mathbf{x}_i^T \mathbf{u})^2)^{-3/2} (\mathbf{x}_i^T \mathbf{u})^2 \\
&\geq \min_{\mathbf{w} \in \tilde{S}_{1/\max(p,n)}} \frac{1}{n} \sum_{i=1}^n (1 + \epsilon_i^2 + (\mathbf{x}_{i,s}^T \mathbf{w})^2)^{-3/2} (\mathbf{x}_{i,s}^T \mathbf{w})^2 - \frac{20\sqrt{|s|\kappa_2}}{\max(n,p)} \\
&\geq \min_{\mathbf{w} \in \tilde{S}_{1/\max(p,n)}} \frac{1}{n} \sum_{i=1}^n (1 + \epsilon_i^2 + (\mathbf{x}_{i,s}^T \mathbf{w})^2)^{-3/2} (\mathbf{x}_{i,s}^T \mathbf{w})^2 - \frac{20\sqrt{\kappa_2}}{\sqrt{n}}
\end{aligned}$$

on an event with P_0 -probability converging to one. In particular, for appropriately chosen constants K_1 and M^{**} (independent of s), and for n large enough to satisfy $\sqrt{n}\kappa_1 M_1 > 80\kappa_2$ and

$\min(M_2, M_3)(\log \max(n, p))^{1+\delta} > 2 \log(2n + 1)$, we obtain

$$\begin{aligned}
& P_0 \left(\inf_{\mathbf{u} \in \mathbb{R}^{|\mathbf{s}|}: \|\mathbf{u}\|=1} Q_\alpha(\boldsymbol{\beta}_{0,s} + \delta_{n,s} \mathbf{u}) > Q_\alpha(\boldsymbol{\beta}_{0,s}) \right) \\
& \geq 1 - \left(2 \exp\left(-\frac{2n|\mathbf{s}|}{3}\right) + \exp\left(-\left\{\frac{81K_1^2}{400\kappa_2} - \log 21\right\} |\mathbf{s}| \log p\right) \right) - \\
& \quad 2 \times \exp(-\min(M_2, M_3)n + |\mathbf{s}| \log(2|\mathbf{s}| + 1)) \\
& \geq 1 - \left(2 \exp\left(-\frac{2n|\mathbf{s}|}{3}\right) + \exp(-3|\mathbf{s}| \log p) + 2 \times \exp\left(-\frac{\min(M_2, M_3)n}{2}\right) \right) \quad (50)
\end{aligned}$$

Let $C_{n,s} := \{\inf_{\mathbf{u} \in \mathbb{R}^{|\mathbf{s}|}: \|\mathbf{u}\|=1} Q_\alpha(\boldsymbol{\beta}_{0,s} + \delta_{n,s} \mathbf{u}) > Q_\alpha(\boldsymbol{\beta}_{0,s})\}$. It follows that $\|\hat{\boldsymbol{\beta}}_{pm,s} - \boldsymbol{\beta}_0\| \leq \delta_{n,s}$ on the event $C_{n,s}$. Now, by second order Taylor series expansion and the fact that $0 \leq \ell''(y) \leq 1$, it follows that for every $\mathbf{u} \in \mathbb{R}^{|\mathbf{s}|}$

$$n\alpha \left(Q_\alpha(\hat{\boldsymbol{\beta}}_{pm,s} + \mathbf{u}) - Q_\alpha(\hat{\boldsymbol{\beta}}_{pm,s}) \right) \geq \tau^2 \mathbf{u}^T \mathbf{u}, \quad (51)$$

and for every $\mathbf{v} \in \mathbb{R}^{|\mathbf{s}_0|}$

$$\begin{aligned}
& n\alpha \left(Q_\alpha(\hat{\boldsymbol{\beta}}_{pm,s_0} + \mathbf{v}) - Q_\alpha(\hat{\boldsymbol{\beta}}_{pm,s_0}) \right) \\
& \leq \sqrt{1 + \alpha^{-2}} \mathbf{v}^T \frac{\sum_{i=1}^n \mathbf{x}_{i,s_0} \mathbf{x}_{i,s_0}^T}{2} \mathbf{v} + \tau^2 \mathbf{v}^T \mathbf{v} \\
& \leq \kappa_1^{-1} \mathbf{v}^T \mathbf{v} + \tau^2 \mathbf{v}^T \mathbf{v} \quad (52)
\end{aligned}$$

on the event D_n defined at the beginning of this proof when n is large enough so that

$$\frac{\sqrt{1 + \alpha^{-2}}}{2 - \sqrt{1 + \alpha^{-2}}} \frac{10\kappa_2}{\sqrt{c}} \left(\frac{1}{(\log \max(n, p))^{\delta/2}} + \sqrt{\frac{|\mathbf{s}_0| \log p}{n}} \right) < \frac{1}{\kappa_1}.$$

Note by Assumption B1 that the LHS of the above inequality converges to zero as $n \rightarrow \infty$, hence this inequality eventually holds for all n above a relevant threshold. Combining (15), (51) and (52), we now get

$$\begin{aligned}
\frac{\Pi(\mathbf{s} | \mathbf{Y})}{\Pi(\mathbf{s}_0 | \mathbf{Y})} & \leq \left(\frac{q\tau}{(1-q)} \right)^{|\mathbf{s}|-|\mathbf{s}_0|} \frac{(\tau^2 + \kappa_1^{-1})^{|\mathbf{s}_0|/2}}{\tau^{|\mathbf{s}|}} \exp\left(n\alpha \left(Q_\alpha(\hat{\boldsymbol{\beta}}_{pm,s_0}) - Q_\alpha(\hat{\boldsymbol{\beta}}_{pm,s}) \right)\right) \\
& = \left(\frac{q}{(1-q)} \right)^{|\mathbf{s}|-|\mathbf{s}_0|} \left(1 + \frac{1}{\kappa_1 \tau^2} \right)^{|\mathbf{s}_0|} \exp\left(n\alpha \left(Q_\alpha(\hat{\boldsymbol{\beta}}_{pm,s_0}) - Q_\alpha(\hat{\boldsymbol{\beta}}_{pm,s}) \right)\right). \quad (53)
\end{aligned}$$

Again, noting that \mathbf{s} is a superset of \mathbf{s}_0 , and by repeating the arguments between (33) and (34) with appropriate changes, we get

$$\begin{aligned}
n\alpha(Q_\alpha(\hat{\boldsymbol{\beta}}_{pm,s_0}) - Q_\alpha(\hat{\boldsymbol{\beta}}_{pm,s})) & \leq (\kappa_1^{-1} + \tau^2) \|\hat{\boldsymbol{\beta}}_{fill,pm,s_0} - \hat{\boldsymbol{\beta}}_{fill,pm,s}\|^2 \\
& \leq (M^{**})^2 \alpha^2 (\kappa_1^{-1} + \tau^2) \frac{(|\mathbf{s}| + |\mathbf{s}_0|) \log p}{n}
\end{aligned}$$

on the event $C_{n,s} \cap C_{n,s_0} \cap D_n$. Note that

$$\frac{|\mathbf{s}| + |\mathbf{s}_0|}{|\mathbf{s}| - |\mathbf{s}_0|} = 1 + \frac{2|\mathbf{s}_0|}{|\mathbf{s}| - |\mathbf{s}_0|} \leq 1 + 2|\mathbf{s}_0|.$$

Let N_0 be such that $\alpha^\delta = \alpha_n^\delta > 4(1 + 2|\mathbf{s}_0|)$ for $n > N_0$. Then

$$(|\mathbf{s}| + |\mathbf{s}_0|)\alpha^2 \log p \leq 0.25 (|\mathbf{s}| - |\mathbf{s}_0|) \alpha^{2+\delta} \log p$$

for $n > N_0$. It follows by (53) and the definition of q that on $C_{n,s} \cap C_{n,s_0} \cap D_n$

$$\frac{\Pi_{SS}(\mathbf{s} \mid \mathbf{Y})}{\Pi_{SS}(\mathbf{s}_0 \mid \mathbf{Y})} \leq K_0 q^{\frac{|\mathbf{s}| - |\mathbf{s}_0|}{2}} \quad (54)$$

for large enough n (cutoff not depending on \mathbf{s}) and an appropriate constant K_0 (not depending on n and \mathbf{s}).

Case II: \mathbf{s} is a ‘subset’ of \mathbf{s}_0 . Let $\mathbf{s} \in \{0, 1\}^p$ be such that $\mathbf{s} \subset \mathbf{s}_0$. Note that under the true model P_0 , we have

$$\begin{aligned} y_i &= \mathbf{x}_i^T \boldsymbol{\beta}_0 + \epsilon_i \\ &= \mathbf{x}_{i,s}^T \boldsymbol{\beta}_{0,s} + \mathbf{x}_{i,s_0 \setminus s}^T \boldsymbol{\beta}_{0,s_0 \setminus s} + \epsilon_i \\ &= \mathbf{x}_{i,s}^T (\boldsymbol{\beta}_{0,s} + (\Gamma_n(0))_{ss} (\Gamma_n(0))_{s,s_0 \setminus s} \boldsymbol{\beta}_{0,s_0 \setminus s}) + \\ &\quad (\mathbf{x}_{i,s_0 \setminus s} - (\Gamma_n(0))_{s_0 \setminus s, s} (\Gamma_n(0))_{ss} \mathbf{x}_{i,s})^T \boldsymbol{\beta}_{0,s_0 \setminus s} + \epsilon_i \\ &= \mathbf{x}_{i,s}^T \tilde{\boldsymbol{\beta}}_{0,s} + \tilde{\epsilon}_{i,s} \end{aligned}$$

where

$$\tilde{\boldsymbol{\beta}}_{0,s} := \boldsymbol{\beta}_{0,s} + (\Gamma_n(0))_{ss} (\Gamma_n(0))_{s,s_0 \setminus s} \boldsymbol{\beta}_{0,s_0 \setminus s}$$

and

$$\tilde{\epsilon}_{i,s} := (\mathbf{x}_{i,s_0 \setminus s} - (\Gamma_n(0))_{s_0 \setminus s, s} (\Gamma_n(0))_{ss} \mathbf{x}_{i,s})^T \boldsymbol{\beta}_{0,s_0 \setminus s} + \epsilon_i.$$

Note that by construction $\tilde{\epsilon}_{i,s}$ is independent of $\mathbf{x}_{i,s}$. For any $\mathbf{u} \in \mathbb{R}^{|\mathbf{s}|}$ with $\|\mathbf{u}\| = 1$, define the random variables

$$\tilde{Z}_{i,s}(\mathbf{u}) := \left(1 + \tilde{\epsilon}_{i,s}^2 + \frac{(\mathbf{x}_{i,s}^T \mathbf{u})^2}{\kappa_1 \mathbf{u}^T (\Gamma_n(0))_{ss} \mathbf{u}} \right)^{-3/2} \frac{(\mathbf{x}_{i,s}^T \mathbf{u})^2}{\mathbf{u}^T (\Gamma_n(0))_{ss} \mathbf{u}} \quad \forall 1 \leq i \leq n.$$

Now, note that

$$\begin{aligned} & \left| \sum_{i=1}^n Z_i(\mathbf{u}) - nE_0[Z_1(\mathbf{u})] \right| \\ & \leq \left| \sum_{i=1}^n Z_i(\mathbf{u}) - \sum_{i=1}^n g(\tilde{\epsilon}_i) \right| + \left| \sum_{i=1}^n g(\epsilon_i) - nE_0[Z_1(\mathbf{u})] \right| \\ & \leq \left| \sum_{i=1}^n Z_i(\mathbf{u}) - \sum_{i=1}^n g(\tilde{\epsilon}_i) \right| + \left| \sum_{i=1}^n g(\tilde{\epsilon}_i) - \sum_{i=1}^n E_0[g(\tilde{\epsilon}_i) \mid \boldsymbol{\epsilon}] \right| + \left| \sum_{i=1}^n E_0[g(\tilde{\epsilon}_i) \mid \boldsymbol{\epsilon}] - nE_0[Z_1(\mathbf{u})] \right|, \end{aligned}$$

where $g(\tilde{\epsilon}_i) = E_0[Z_i(\mathbf{u}) \mid \tilde{\epsilon}_i]$. Using the independence of $\tilde{\epsilon}_{i,s}$ and $\mathbf{x}_{i,s}$, and observing that $\tilde{Z}_{i,s}(\mathbf{u})$ is a uniformly bounded function of $\mathbf{x}_{i,s}^T \mathbf{u}$ (conditional on $\tilde{\epsilon}_i$), a parallel argument to the one right after equation (23) leads to the bound

$$V\left(\sum_{i=1}^n \tilde{Z}_{i,s}(\mathbf{u}) \mid \tilde{\boldsymbol{\epsilon}}\right) \leq 4n\kappa_1\kappa_2.$$

Similarly, using independence of ϵ_i and \mathbf{x}_i , and observing that $g(\tilde{\epsilon}_i)$ is a uniformly bounded function of $(\mathbf{x}_{i,s_0 \setminus s} - (\Gamma_n(0))_{s_0 \setminus s, s} (\Gamma_n(0))_{ss} \mathbf{x}_{i,s})^T \boldsymbol{\beta}_{0,s_0 \setminus s}$ (conditional on ϵ_i), it can be shown that $n^{-1}V(\sum_{i=1}^n g(\tilde{\epsilon}_i) \mid \boldsymbol{\epsilon})$ is uniformly bounded (in $\boldsymbol{\epsilon}$ and \mathbf{s}). Finally Assumption B3 can be used to show that $n^{-1}V(\sum_{i=1}^n E_0[g(\tilde{\epsilon}_i) \mid \boldsymbol{\epsilon}])$ is uniformly bounded (in \mathbf{s}). The above facts can be leveraged to repeat the arguments in the proof of Theorem 1 with straightforward changes/adjustments to conclude that there exists a constant M^{***} (not depending on \mathbf{s}) such that

$$\|\hat{\boldsymbol{\beta}}_{pm,s} - \tilde{\boldsymbol{\beta}}_{0,s}\| \leq M^{***} \alpha \sqrt{\frac{|\mathbf{s}| \log p}{n}}$$

on a set $C_{n,s}$ with $P_0(C_{n,s}) \rightarrow 1$ as $n \rightarrow \infty$. Let $\mathbf{v} \in \mathbb{R}^{|\mathbf{s}_0|}$ be such that $\hat{\boldsymbol{\beta}}_{pm,s_0} + \mathbf{v}$ corresponds to the filled version of $\hat{\boldsymbol{\beta}}_{pm,s}$ in $\mathbb{R}^{|\mathbf{s}_0|}$ (with zeros appended in relevant places). It follows that for large enough n , there exists a constant K^* such that $\|\mathbf{v}\| \leq K^*$ on $C_{n,s}$. By a second order Taylor series expansion around the restricted mode $\hat{\boldsymbol{\beta}}_{pm,s_0}$, we get

$$\begin{aligned} & \alpha \left(Q_\alpha(\hat{\boldsymbol{\beta}}_{pm,s_0} + \mathbf{v}) - Q_\alpha(\hat{\boldsymbol{\beta}}_{pm,s_0}) \right) \\ & \geq \frac{\|\mathbf{v}\|^2}{2n} \sum_{i=1}^n (1 + 2\epsilon_i^2 + 2\|\mathbf{v}\|^2 (\mathbf{x}_{i,s_0}^T \tilde{\mathbf{v}})^2)^{-3/2} (\mathbf{x}_{i,s_0}^T \tilde{\mathbf{v}})^2 - \frac{2\tau^2}{n} \|\mathbf{v}\| \|\boldsymbol{\beta}_0\| \\ & \geq \frac{\|\mathbf{v}\|^2}{2n} \sum_{i=1}^n (1 + 2\epsilon_i^2 + 2(K^*)^2 (\mathbf{x}_{i,s_0}^T \tilde{\mathbf{v}})^2)^{-3/2} (\mathbf{x}_{i,s_0}^T \tilde{\mathbf{v}})^2 - \frac{2\tau^2}{n} K^* \|\boldsymbol{\beta}_0\| \end{aligned}$$

with $\tilde{\mathbf{v}} = \mathbf{v}/\|\mathbf{v}\|$. By a similar argument as the one leading to (45), there exists a constant \bar{M} such that

$$P_0 \left(\inf_{\mathbf{v}: \|\mathbf{v}\|=1} \frac{1}{n} \sum_{i=1}^n (1 + 2\epsilon_i^2 + 2(K^*)^2 (\mathbf{x}_{i,s_0}^T \mathbf{v})^2)^{-3/2} (\mathbf{x}_{i,s_0}^T \mathbf{v})^2 > \bar{M} \right) \rightarrow 1 \quad (55)$$

Note that the bound in (53) holds for any $\mathbf{s} \in \{0, 1\}^p$. Also, by construction of \mathbf{v} , it follows that $\|\mathbf{v}\|^2 \geq (|\mathbf{s}_0| - |\mathbf{s}|)S^2$, where $S = \min_{1 \leq i \leq |\mathbf{s}_0|} |\beta_{s_0,i}|$. Combining everything, we get

$$\begin{aligned} \frac{\Pi_{SS}(\mathbf{s} \mid \mathbf{Y})}{\Pi_{SS}(\mathbf{s}_0 \mid \mathbf{Y})} & \leq \left(\frac{q}{(1-q)} \right)^{|\mathbf{s}| - |\mathbf{s}_0|} \left(1 + \frac{1}{\kappa_1 \tau^2} \right)^{|\mathbf{s}_0|} \exp \left(n\alpha \left(Q_\alpha(\hat{\boldsymbol{\beta}}_{pm,s_0}) - Q_\alpha(\hat{\boldsymbol{\beta}}_{pm,s}) \right) \right) \\ & \leq K_1 q^{|\mathbf{s}| - |\mathbf{s}_0|} \exp \left(-0.25n(|\mathbf{s}_0| - |\mathbf{s}|)\bar{M}S^2 \right) \\ & \leq K_1 \exp \left(-0.125n(|\mathbf{s}_0| - |\mathbf{s}|)\bar{M}S^2 \right) \end{aligned} \quad (56)$$

for large enough n (cutoff not depending on \mathbf{s}) on a set, say $\tilde{C}_{n,s}$, with P_0 -probability converging to 1 as $n \rightarrow \infty$. Here K_1 is a constant which does not depend on n or \mathbf{s} . The last inequality follows from Assumption B4.

Case III: \mathbf{s} satisfies $\mathbf{s} \not\subseteq \mathbf{s}_0$, $\mathbf{s}_0 \not\subseteq \mathbf{s}$, $|\mathbf{s}| \leq n/(\log(\max(n,p)))^{1+\delta}$ and $|\mathbf{s}| > |\mathbf{s}_0|$. Let $\tilde{\mathbf{s}} := \mathbf{s} \cup \mathbf{s}_0$. Note that $\tilde{\mathbf{s}}$ is a superset of \mathbf{s}_0 . By repeating the arguments in Case I up to equation (50) verbatim, and noting $|\tilde{\mathbf{s}}| \leq n/(\log(\max(n,p)))^{1+\delta} + |\mathbf{s}_0| = o(n/\log n)$, there exists a set $C_{n,s}$ such that

$$P_0(C_{n,s}) \geq 1 - \left(2 \exp \left(-\frac{2n|\tilde{\mathbf{s}}|}{3} \right) + \exp(-3|\tilde{\mathbf{s}}| \log p) + 2 \times \exp \left(-\frac{\min(M_2, M_3)n}{2} \right) \right)$$

$$\geq 1 - \left(2 \exp\left(-\frac{2n|\mathbf{s}|}{3}\right) + \exp(-3|\mathbf{s}| \log p) + 2 \times \exp\left(-\frac{\min(M_2, M_3)n}{2}\right) \right),$$

for large enough n (cutoff not depending on \mathbf{s}), and $\|\hat{\boldsymbol{\beta}}_{pm, \bar{s}} - \boldsymbol{\beta}_0\| \leq \delta_{n, \bar{s}}$ on $C_{n, s}$. It follows that

$$\begin{aligned} n\alpha(Q_\alpha(\hat{\boldsymbol{\beta}}_{pm, s_0}) - Q_\alpha(\hat{\boldsymbol{\beta}}_{pm, \bar{s}})) &\leq (\kappa_1^{-1} + \tau^2) \|\hat{\boldsymbol{\beta}}_{fill, pm, s_0} - \hat{\boldsymbol{\beta}}_{fill, pm, \bar{s}}\|^2 \\ &\leq (M^{**})^2 \alpha^2 (\kappa_1^{-1} + \tau^2) \frac{(|\bar{\mathbf{s}}| + |\mathbf{s}_0|) \log p}{n} \\ &\leq (M^{**})^2 \alpha^2 (\kappa_1^{-1} + \tau^2) \frac{(|\mathbf{s}| + 2|\mathbf{s}_0|) \log p}{n} \end{aligned}$$

on the event $C_{n, s} \cap C_{n, s_0} \cap D_n$ for large enough n (cutoff not depending on \mathbf{s}). Note that

$$\frac{|\mathbf{s}| + 2|\mathbf{s}_0|}{|\mathbf{s}| - |\mathbf{s}_0|} = 1 + \frac{3|\mathbf{s}_0|}{|\mathbf{s}| - |\mathbf{s}_0|} \leq 1 + 3|\mathbf{s}_0|.$$

Let N_0^* be such that $\alpha^\delta = \alpha_n^\delta > 4|\mathbf{s}_0|(1 + 3|\mathbf{s}_0|)$ for $n > N_0^*$. Then

$$(|\mathbf{s}| + 2|\mathbf{s}_0|) \alpha^2 \log p \leq \frac{1}{4|\mathbf{s}_0|} (|\mathbf{s}| - |\mathbf{s}_0|) \alpha^{2+\delta} \log p$$

for $n > N_0^*$. Let $d(\mathbf{s}, \mathbf{s}_0) = |\mathbf{s} \cap \mathbf{s}_0^c| + |\mathbf{s}_0 \cap \mathbf{s}^c|$ denote the number of disagreements between \mathbf{s} and \mathbf{s}_0 . Since $|\mathbf{s}| - |\mathbf{s}_0| \geq 1$ and $|\mathbf{s}_0| \geq 1$, we get

$$\begin{aligned} d(\mathbf{s}, \mathbf{s}_0) &= |\mathbf{s} \cap \mathbf{s}_0^c| + |\mathbf{s}_0 \cap \mathbf{s}^c| \\ &= |\mathbf{s} \cap \mathbf{s}_0^c| - |\mathbf{s}_0 \cap \mathbf{s}^c| + 2|\mathbf{s}_0 \cap \mathbf{s}^c| \\ &= |\mathbf{s}| - |\mathbf{s}_0| + 2|\mathbf{s}_0 \cap \mathbf{s}^c| \\ &\leq |\mathbf{s}| - |\mathbf{s}_0| + 2|\mathbf{s}_0|(|\mathbf{s}| - |\mathbf{s}_0|) \\ &\leq 3|\mathbf{s}_0|(|\mathbf{s}| - |\mathbf{s}_0|). \end{aligned}$$

It follows by (53) and the definition of q that on $C_{n, s} \cap C_{n, s_0} \cap D_n$

$$\frac{\Pi_{SS}(\mathbf{s} | \mathbf{Y})}{\Pi_{SS}(\mathbf{s}_0 | \mathbf{Y})} \leq K_0^* \left(q^{1/|\mathbf{s}_0|} \right)^{\frac{|\mathbf{s}_0|(|\mathbf{s}| - |\mathbf{s}_0|)}{2}} \leq K_0^* \left(q^{1/(6|\mathbf{s}_0|)} \right)^{d(\mathbf{s}, \mathbf{s}_0)} \quad (57)$$

for large enough n (cutoff not depending on \mathbf{s}) and an appropriate constant K_0^* (not depending on \mathbf{s} as well).

Case IV: \mathbf{s} satisfies $\mathbf{s} \not\subseteq \mathbf{s}_0$, $\mathbf{s}_0 \not\subseteq \mathbf{s}$, $|\mathbf{s}| \leq n/(\log(\max(n, p)))^{1+\delta}$ and $|\mathbf{s}| \leq |\mathbf{s}_0|$. Let $\bar{\mathbf{s}} := \mathbf{s} \cap \mathbf{s}_0$. Note that $\bar{\mathbf{s}}$ is a subset of both \mathbf{s} and \mathbf{s}_0 . It follows by (53) that

$$\begin{aligned} \frac{\Pi_{SS}(\mathbf{s} | \mathbf{Y})}{\Pi_{SS}(\mathbf{s}_0 | \mathbf{Y})} &\leq \left(\frac{q}{(1-q)} \right)^{|\mathbf{s}| - |\mathbf{s}_0|} \left(1 + \frac{1}{\kappa_1 \tau^2} \right)^{|\mathbf{s}_0|} \exp\left(n\alpha \left(Q_\alpha(\hat{\boldsymbol{\beta}}_{pm, s_0}) - Q_\alpha(\hat{\boldsymbol{\beta}}_{pm, s}) \right) \right) \\ &= \left(\frac{q}{(1-q)} \right)^{|\mathbf{s}| - |\mathbf{s}_0|} \left(1 + \frac{1}{\kappa_1 \tau^2} \right)^{|\mathbf{s}_0|} \exp\left(n\alpha \left(Q_\alpha(\hat{\boldsymbol{\beta}}_{pm, s_0}) - Q_\alpha(\boldsymbol{\beta}_{0, s_0}) \right) \right) \\ &\quad \times \exp\left(n\alpha \left(Q_\alpha(\boldsymbol{\beta}_{0, s_0}) - Q_\alpha(\hat{\boldsymbol{\beta}}_{pm, s}) \right) \right) \\ &\leq \left(\frac{q}{(1-q)} \right)^{|\mathbf{s}| - |\mathbf{s}_0|} \left(1 + \frac{1}{\kappa_1 \tau^2} \right)^{|\mathbf{s}_0|} \exp\left(n\alpha \left(Q_\alpha(\boldsymbol{\beta}_{0, s_0}) - Q_\alpha(\hat{\boldsymbol{\beta}}_{pm, s}) \right) \right). \quad (58) \end{aligned}$$

Let

$$\mathbf{s}^* := \mathbf{s}_0 \cup \mathbf{s} = \mathbf{s}_0 \uplus (\mathbf{s} \setminus \bar{\mathbf{s}}) = \mathbf{s} \uplus (\mathbf{s}_0 \setminus \bar{\mathbf{s}}).$$

Let $\hat{\boldsymbol{\beta}}_{pm,s,fill(s^*)}$ denote the s^* -dimensional vector obtained by appending relevant zeros to $\hat{\boldsymbol{\beta}}_{pm,s}$. Noting that $|\mathbf{s}^*| \leq 2|\mathbf{s}_0|$, and repeating the analysis in Case I (replacing \mathbf{s} by \mathbf{s}^*), we get

$$\begin{aligned} & Q_\alpha(\hat{\boldsymbol{\beta}}_{pm,s}) - Q_\alpha(\boldsymbol{\beta}_{0,s_0}) \\ &= Q_\alpha(\hat{\boldsymbol{\beta}}_{pm,s,fill(s^*)}) - Q_\alpha(\boldsymbol{\beta}_{0,s^*}) \\ &\geq \|\hat{\boldsymbol{\beta}}_{pm,s,fill(s^*)} - \boldsymbol{\beta}_{0,s^*}\|^2 \frac{\kappa_1 M_1}{8\alpha} - \|\hat{\boldsymbol{\beta}}_{pm,s,fill(s^*)} - \boldsymbol{\beta}_{0,s^*}\| \left(K_1 \sqrt{\frac{|\mathbf{s}^*| \log p}{n}} + \frac{2\tau^2 \|\boldsymbol{\beta}_0\|}{n\alpha} \right) \end{aligned}$$

on an event with P_0 -probability converging to 1. Also, note that

$$\begin{aligned} y_i &= \mathbf{x}_i^T \boldsymbol{\beta}_0 + \epsilon_i \\ &= \mathbf{x}_{i,s^*}^T \boldsymbol{\beta}_{0,s^*} + \epsilon_i \\ &= \mathbf{x}_{i,s}^T \boldsymbol{\beta}_{0,s} + \mathbf{x}_{i,s^* \setminus s}^T \boldsymbol{\beta}_{0,s^* \setminus s} + \epsilon_i \\ &= \mathbf{x}_{i,s}^T (\boldsymbol{\beta}_{0,s} + (\Gamma_n(0))_{ss}^{-1} (\Gamma_n(0))_{s,s^* \setminus s} \boldsymbol{\beta}_{0,s^* \setminus s}) + (\mathbf{x}_{i,s^* \setminus s} - (\Gamma_n(0))_{s^* \setminus s,s} (\Gamma_n(0))_{ss}^{-1} \mathbf{x}_{i,s})^T \boldsymbol{\beta}_{0,s^* \setminus s} + \epsilon_i \\ &= \mathbf{x}_{i,s}^T (\boldsymbol{\beta}_{0,s} + (\Gamma_n(0))_{ss}^{-1} (\Gamma_n(0))_{s,s_0 \setminus \bar{\mathbf{s}}} \boldsymbol{\beta}_{0,s_0 \setminus \bar{\mathbf{s}}}) + (\mathbf{x}_{i,s_0 \setminus \bar{\mathbf{s}}} - (\Gamma_n(0))_{s_0 \setminus \bar{\mathbf{s}},s} (\Gamma_n(0))_{ss}^{-1} \mathbf{x}_{i,s})^T \boldsymbol{\beta}_{0,s_0 \setminus \bar{\mathbf{s}}} + \epsilon_i \\ &= \mathbf{x}_{i,s}^T \tilde{\boldsymbol{\beta}}_{0,s} + \tilde{\epsilon}_{i,s} \end{aligned}$$

where

$$\tilde{\boldsymbol{\beta}}_{0,s} := \boldsymbol{\beta}_{0,s} + (\Gamma_n(0))_{ss}^{-1} (\Gamma_n(0))_{s,s_0 \setminus \bar{\mathbf{s}}} \boldsymbol{\beta}_{0,s_0 \setminus \bar{\mathbf{s}}}$$

and

$$\tilde{\epsilon}_{i,s} := (\mathbf{x}_{i,s_0 \setminus \bar{\mathbf{s}}} - (\Gamma_n(0))_{s_0 \setminus \bar{\mathbf{s}},s} (\Gamma_n(0))_{ss}^{-1} \mathbf{x}_{i,s})^T \boldsymbol{\beta}_{0,s_0 \setminus \bar{\mathbf{s}}} + \epsilon_i.$$

By repeating the arguments in Case II (with \mathbf{s} replaced by $\bar{\mathbf{s}}$) up to equation (56), we get

$$\|\hat{\boldsymbol{\beta}}_{pm,s} - \tilde{\boldsymbol{\beta}}_{0,s}\| \leq M^{***} \alpha \sqrt{\frac{|\mathbf{s}| \log p}{n}}$$

on an event with P_0 -probability converging to one as $n \rightarrow \infty$. Since the true model \mathbf{s}_0 does not vary with n , and $|\mathbf{s}^*| \leq 2|\mathbf{s}_0|$, it follows that

$$\begin{aligned} & Q_\alpha(\hat{\boldsymbol{\beta}}_{pm,s,fill(s^*)}) - Q_\alpha(\boldsymbol{\beta}_{0,s^*}) \\ &\geq \|\hat{\boldsymbol{\beta}}_{pm,s,fill(s^*)} - \boldsymbol{\beta}_{0,s^*}\|^2 \frac{\kappa_1 M_1}{8\alpha} - \\ &\quad \|\hat{\boldsymbol{\beta}}_{pm,s,fill(s^*)} - \boldsymbol{\beta}_{0,s^*}\| \left(K_1 \sqrt{\frac{(1 + \alpha^{-2})|\mathbf{s}^*| \log p}{n}} + \frac{2\tau^2 \|\boldsymbol{\beta}_0\|}{n\alpha} \right) \\ &\geq \left(\|\boldsymbol{\beta}_{0,s} - \hat{\boldsymbol{\beta}}_{pm,s}\|^2 + \|\boldsymbol{\beta}_{0,s_0 \setminus \bar{\mathbf{s}}}\|^2 \right) \frac{\kappa_1 M_1}{8\alpha} - \left(\|\boldsymbol{\beta}_{0,s} - \tilde{\boldsymbol{\beta}}_{0,s}\| + \|\boldsymbol{\beta}_{0,s_0 \setminus \bar{\mathbf{s}}}\| + M^{***} \alpha \sqrt{\frac{2|\mathbf{s}_0| \log p}{n}} \right) \times \\ &\quad \left(K_1 \sqrt{\frac{2(1 + \alpha^{-2})|\mathbf{s}_0| \log p}{n}} + \frac{2\tau^2 \|\boldsymbol{\beta}_0\|}{n\alpha} \right) \\ &\geq \frac{(|\mathbf{s}_0| - |\bar{\mathbf{s}}|) S^2 \kappa_1 M_1}{16\alpha} \end{aligned}$$

for large enough n (cutoff not depending on \mathbf{s}), on an event with P_0 -probability converging to one as $n \rightarrow \infty$. Using (58), we conclude that

$$\begin{aligned} \frac{\Pi_{SS}(\mathbf{s} \mid \mathbf{Y})}{\Pi_{SS}(\mathbf{s}_0 \mid \mathbf{Y})} &\leq \bar{K}_1 q^{|\mathbf{s}| - |\mathbf{s}_0|} \exp\left(-\frac{(|\mathbf{s}_0| - |\bar{\mathbf{s}}|)nS^2\kappa_1 M_1}{16}\right) \\ &\leq \bar{K}_1 q^{-|\mathbf{s}_0|} \exp\left(-\frac{nS^2\kappa_1 M_1}{16}\right) \\ &\leq \bar{K}_1 \exp\left(-\frac{nS^2\kappa_1 M_1}{32}\right) \end{aligned} \quad (59)$$

$$\leq \bar{K}_1 \left(\exp\left(-\frac{nS^2\kappa_1 M_1}{64|\mathbf{s}_0|}\right)\right)^{d(\mathbf{s}, \mathbf{s}_0)} \quad (60)$$

for large enough n (cutoff not depending on \mathbf{s}) on a set with P_0 -probability converging to 1 as $n \rightarrow \infty$. Here \bar{K}_1 is a constant which does not depend on n or \mathbf{s} . The second to last inequality follows from Assumptions B1 and B4, and the last inequality uses $d(\mathbf{s}, \mathbf{s}_0) \leq 2|\mathbf{s}_0|$.

We now gather the results from all the four scenarios above to establish strong selection consistency. Note that

$$\begin{aligned} &\sum_{\mathbf{s}: |\mathbf{s}| > |\mathbf{s}_0|, |\mathbf{s}| \leq n/(\log(\max(n, p)))^{1+\delta}} P_0(C_{n, \mathbf{s}}^c) \\ &\leq \sum_{\mathbf{s}: |\mathbf{s}| > |\mathbf{s}_0|, |\mathbf{s}| \leq n/(\log(\max(n, p)))^{1+\delta}} \left(2 \exp\left(-\frac{2n|\mathbf{s}|}{3}\right) + \exp(-3|\mathbf{s}| \log p) + 2 \exp\left(-\frac{\min(M_2, M_3)n}{2}\right)\right) \\ &\leq \sum_{j=1}^{\infty} 2p^j \exp\left(-\frac{2nj}{3}\right) + \sum_{j=1}^{\infty} p^j \exp(-3j \log p) + \\ &\quad 2 \exp\left(n/(\log(\max(n, p)))^\delta + \log p - \frac{\min(M_2, M_3)n}{2}\right) \\ &\leq \frac{p \exp\left(-\frac{2n}{3}\right)}{1 - p \exp\left(-\frac{2n}{3}\right)} + \frac{1}{p^2 - 1} + 2 \exp\left(n/(\log(\max(n, p)))^\delta + \log p - \frac{\min(M_2, M_3)n}{2}\right) \rightarrow 0 \end{aligned}$$

as $n \rightarrow \infty$. Note that the number of sparsity patterns satisfying the conditions in Case II and Case IV are uniformly bounded in n (since the indices in \mathbf{s}_0 which are one do not change with n). It follows that the inequalities in (54), (56), (57) and (60) hold jointly on a common event whose P_0 -probability converges to 1 as $n \rightarrow \infty$. On this common set, denoted by \tilde{C}_n , we have that for every $\mathbf{s} \neq \mathbf{s}_0$ with $|\mathbf{s}| \leq n/(\log(\max(n, p)))^{1+\delta}$

$$\frac{\Pi_{SS}(\mathbf{s} \mid \mathbf{Y})}{\Pi_{SS}(\mathbf{s}_0 \mid \mathbf{Y})} \leq K^{**} f_n^{d(\mathbf{s}, \mathbf{s}_0)}$$

where

$$f_n = \min\left(q_n^{1/2}, q_n^{1/(6|\mathbf{s}_0|)}, \exp(-0.125n\bar{M}S^2), \exp\left(-\frac{nS^2\kappa_1 M_1}{64|\mathbf{s}_0|}\right)\right)$$

and K^{**} is a constant not depending on \mathbf{s} or on n . By Assumptions B1 and B4, it follows that $pf_n \rightarrow 0$ as $n \rightarrow \infty$. Hence

$$\sum_{\mathbf{s}: \mathbf{s} \neq \mathbf{s}_0, |\mathbf{s}| \leq n/(\log(\max(n, p)))^{1+\delta}} \frac{\Pi(\mathbf{s} \mid \mathbf{Y})}{\Pi(\mathbf{s}_0 \mid \mathbf{Y})}$$

$$\begin{aligned}
&\leq K^{**} \sum_{\mathbf{s}:\mathbf{s}\neq\mathbf{s}_0, |\mathbf{s}|\leq n/(\log(\max(n,p)))^{1+\delta}} f_n^{d(\mathbf{s},\mathbf{s}_0)} \\
&\leq K^{**} \sum_{j=1}^p \sum_{\mathbf{s}:d(\mathbf{s},\mathbf{s}_0)=j} f_n^{d(\mathbf{s},\mathbf{s}_0)} \\
&\leq K^{**} \sum_{j=1}^p (pf_n)^j \\
&\leq K^{**} \frac{pf_n}{1-pf_n} \rightarrow 0
\end{aligned}$$

as $n \rightarrow \infty$. □

D Detailed information on simulation settings

Table A3: Simulation settings for scenarios with data generated from extremely heavy-tailed error distributions and models fitted with a ridge prior on the regression parameters.

Setting	n	p	Correlation	Error Distribution
Setting-1	50	10	$x: 0; \varepsilon: 0$	discrete mix $\mathcal{N}(0, 1)$ and $\mathcal{U}(-10^{10}, 10^{10})$ (90%; 10%)
Setting-2	100	10	$x: 0; \varepsilon: 0$	discrete mix $\mathcal{N}(0, 1)$ and $\mathcal{U}(-10^{10}, 10^{10})$ (90%; 10%)
Setting-3	200	10	$x: 0; \varepsilon: 0$	discrete mix $\mathcal{N}(0, 1)$ and $\mathcal{U}(-10^{10}, 10^{10})$ (90%; 10%)
Setting-4	500	10	$x: 0; \varepsilon: 0$	discrete mix $\mathcal{N}(0, 1)$ and $\mathcal{U}(-10^{10}, 10^{10})$ (90%; 10%)
Setting-5	1,000	10	$x: 0; \varepsilon: 0$	discrete mix $\mathcal{N}(0, 1)$ and $\mathcal{U}(-10^{10}, 10^{10})$ (90%; 10%)
Setting-6	2,000	10	$x: 0; \varepsilon: 0$	discrete mix $\mathcal{N}(0, 1)$ and $\mathcal{U}(-10^{10}, 10^{10})$ (90%; 10%)
Setting-7	5,000	10	$x: 0; \varepsilon: 0$	discrete mix $\mathcal{N}(0, 1)$ and $\mathcal{U}(-10^{10}, 10^{10})$ (90%; 10%)
Setting-8	10,000	10	$x: 0; \varepsilon: 0$	discrete mix $\mathcal{N}(0, 1)$ and $\mathcal{U}(-10^{10}, 10^{10})$ (90%; 10%)
Setting-9	20,000	10	$x: 0; \varepsilon: 0$	discrete mix $\mathcal{N}(0, 1)$ and $\mathcal{U}(-10^{10}, 10^{10})$ (90%; 10%)
Setting-10	50	10	$x: 0; \varepsilon: 0$	discrete mix $\mathcal{N}(0, 1)$ and $\mathcal{U}(-10^{10}, 10^{10})$ (50%; 50%)
Setting-11	100	10	$x: 0; \varepsilon: 0$	discrete mix $\mathcal{N}(0, 1)$ and $\mathcal{U}(-10^{10}, 10^{10})$ (50%; 50%)
Setting-12	200	10	$x: 0; \varepsilon: 0$	discrete mix $\mathcal{N}(0, 1)$ and $\mathcal{U}(-10^{10}, 10^{10})$ (50%; 50%)
Setting-13	500	10	$x: 0; \varepsilon: 0$	discrete mix $\mathcal{N}(0, 1)$ and $\mathcal{U}(-10^{10}, 10^{10})$ (50%; 50%)
Setting-14	1,000	10	$x: 0; \varepsilon: 0$	discrete mix $\mathcal{N}(0, 1)$ and $\mathcal{U}(-10^{10}, 10^{10})$ (50%; 50%)
Setting-15	2,000	10	$x: 0; \varepsilon: 0$	discrete mix $\mathcal{N}(0, 1)$ and $\mathcal{U}(-10^{10}, 10^{10})$ (50%; 50%)
Setting-16	5,000	10	$x: 0; \varepsilon: 0$	discrete mix $\mathcal{N}(0, 1)$ and $\mathcal{U}(-10^{10}, 10^{10})$ (50%; 50%)
Setting-17	10,000	10	$x: 0; \varepsilon: 0$	discrete mix $\mathcal{N}(0, 1)$ and $\mathcal{U}(-10^{10}, 10^{10})$ (50%; 50%)
Setting-18	20,000	10	$x: 0; \varepsilon: 0$	discrete mix $\mathcal{N}(0, 1)$ and $\mathcal{U}(-10^{10}, 10^{10})$ (50%; 50%)

Table A4: Simulation settings for scenarios with data generated from heavy-tailed error distributions and models fitted with a ridge prior on the regression parameters.

Setting	n	p	Correlation	Error Distribution
Setting-1	100	20	$x: 0.2; \varepsilon: 0.3$	discrete mix $\mathcal{N}(0, 1)$ and $\mathcal{N}(0, 10^2)$ (90%; 10%)
Setting-2	100	50	$x: 0.2; \varepsilon: 0.3$	discrete mix $\mathcal{N}(0, 1)$ and $\mathcal{N}(0, 10^2)$ (90%; 10%)
Setting-3	100	75	$x: 0.2; \varepsilon: 0.3$	discrete mix $\mathcal{N}(0, 1)$ and $\mathcal{N}(0, 10^2)$ (90%; 10%)
Setting-4	250	50	$x: 0.2; \varepsilon: 0.3$	discrete mix $\mathcal{N}(0, 1)$ and $\mathcal{N}(0, 10^2)$ (90%; 10%)
Setting-5	250	125	$x: 0.2; \varepsilon: 0.3$	discrete mix $\mathcal{N}(0, 1)$ and $\mathcal{N}(0, 10^2)$ (90%; 10%)
Setting-6	250	187	$x: 0.2; \varepsilon: 0.3$	discrete mix $\mathcal{N}(0, 1)$ and $\mathcal{N}(0, 10^2)$ (90%; 10%)
Setting-7	100	20	$x: 0.2; \varepsilon: 0.3$	continuous t with df=1
Setting-8	100	50	$x: 0.2; \varepsilon: 0.3$	continuous t with df=1
Setting-9	100	75	$x: 0.2; \varepsilon: 0.3$	continuous t with df=1
Setting-10	250	50	$x: 0.2; \varepsilon: 0.3$	continuous t with df=1
Setting-11	250	125	$x: 0.2; \varepsilon: 0.3$	continuous t with df=1
Setting-12	250	187	$x: 0.2; \varepsilon: 0.3$	continuous t with df=1
Setting-13	100	20	$x: 0.2; \varepsilon: 0.3$	continuous t with df=2
Setting-14	100	50	$x: 0.2; \varepsilon: 0.3$	continuous t with df=2
Setting-15	100	75	$x: 0.2; \varepsilon: 0.3$	continuous t with df=2
Setting-16	250	50	$x: 0.2; \varepsilon: 0.3$	continuous t with df=2
Setting-17	250	125	$x: 0.2; \varepsilon: 0.3$	continuous t with df=2
Setting-18	250	187	$x: 0.2; \varepsilon: 0.3$	continuous t with df=2
Setting-19	100	20	$x: 0.4; \varepsilon: 0.6$	continuous t with df=1
Setting-20	100	50	$x: 0.4; \varepsilon: 0.6$	continuous t with df=1
Setting-21	100	75	$x: 0.4; \varepsilon: 0.6$	continuous t with df=1
Setting-22	250	50	$x: 0.4; \varepsilon: 0.6$	continuous t with df=1
Setting-23	250	125	$x: 0.4; \varepsilon: 0.6$	continuous t with df=1
Setting-24	250	187	$x: 0.4; \varepsilon: 0.6$	continuous t with df=1
Setting-25	100	20	$x: 0.4; \varepsilon: 0.6$	continuous t with df=2
Setting-26	100	50	$x: 0.4; \varepsilon: 0.6$	continuous t with df=2
Setting-27	100	75	$x: 0.4; \varepsilon: 0.6$	continuous t with df=2
Setting-28	250	50	$x: 0.4; \varepsilon: 0.6$	continuous t with df=2
Setting-29	250	125	$x: 0.4; \varepsilon: 0.6$	continuous t with df=2
Setting-30	250	187	$x: 0.4; \varepsilon: 0.6$	continuous t with df=2
Setting-31	200	20	$x: 0.2; \varepsilon: 0.3$	discrete mix $\mathcal{N}(0, 1)$ and $\mathcal{N}(0, 10^2)$ (90%; 10%)
Setting-32	200	50	$x: 0.2; \varepsilon: 0.3$	discrete mix $\mathcal{N}(0, 1)$ and $\mathcal{N}(0, 10^2)$ (90%; 10%)
Setting-33	200	75	$x: 0.2; \varepsilon: 0.3$	discrete mix $\mathcal{N}(0, 1)$ and $\mathcal{N}(0, 10^2)$ (90%; 10%)
Setting-34	500	50	$x: 0.2; \varepsilon: 0.3$	discrete mix $\mathcal{N}(0, 1)$ and $\mathcal{N}(0, 10^2)$ (90%; 10%)
Setting-35	500	125	$x: 0.2; \varepsilon: 0.3$	discrete mix $\mathcal{N}(0, 1)$ and $\mathcal{N}(0, 10^2)$ (90%; 10%)
Setting-36	500	187	$x: 0.2; \varepsilon: 0.3$	discrete mix $\mathcal{N}(0, 1)$ and $\mathcal{N}(0, 10^2)$ (90%; 10%)
Setting-37	200	20	$x: 0.2; \varepsilon: 0.3$	continuous t with df=1
Setting-38	200	50	$x: 0.2; \varepsilon: 0.3$	continuous t with df=1
Setting-39	200	75	$x: 0.2; \varepsilon: 0.3$	continuous t with df=1
Setting-40	500	50	$x: 0.2; \varepsilon: 0.3$	continuous t with df=1

Table A4: Simulation settings for scenarios with data generated from heavy-tailed error distributions and models fitted with a ridge prior on the regression parameters. (*continued*)

Setting	n	p	Correlation	Error Distribution
Setting-41	500	125	$x: 0.2; \varepsilon: 0.3$	continuous t with df=1
Setting-42	500	187	$x: 0.2; \varepsilon: 0.3$	continuous t with df=1
Setting-43	200	20	$x: 0.2; \varepsilon: 0.3$	continuous t with df=2
Setting-44	200	50	$x: 0.2; \varepsilon: 0.3$	continuous t with df=2
Setting-45	200	75	$x: 0.2; \varepsilon: 0.3$	continuous t with df=2
Setting-46	500	50	$x: 0.2; \varepsilon: 0.3$	continuous t with df=2
Setting-47	500	125	$x: 0.2; \varepsilon: 0.3$	continuous t with df=2
Setting-48	500	187	$x: 0.2; \varepsilon: 0.3$	continuous t with df=2
Setting-49	200	20	$x: 0.4; \varepsilon: 0.6$	discrete mix $\mathcal{N}(0, 1)$ and $\mathcal{N}(0, 10^2)$ (90%; 10%)
Setting-50	200	50	$x: 0.4; \varepsilon: 0.6$	discrete mix $\mathcal{N}(0, 1)$ and $\mathcal{N}(0, 10^2)$ (90%; 10%)
Setting-51	200	75	$x: 0.4; \varepsilon: 0.6$	discrete mix $\mathcal{N}(0, 1)$ and $\mathcal{N}(0, 10^2)$ (90%; 10%)
Setting-52	500	50	$x: 0.4; \varepsilon: 0.6$	discrete mix $\mathcal{N}(0, 1)$ and $\mathcal{N}(0, 10^2)$ (90%; 10%)
Setting-53	500	125	$x: 0.4; \varepsilon: 0.6$	discrete mix $\mathcal{N}(0, 1)$ and $\mathcal{N}(0, 10^2)$ (90%; 10%)
Setting-54	500	187	$x: 0.4; \varepsilon: 0.6$	discrete mix $\mathcal{N}(0, 1)$ and $\mathcal{N}(0, 10^2)$ (90%; 10%)
Setting-55	200	20	$x: 0.4; \varepsilon: 0.6$	continuous t with df=1
Setting-56	200	50	$x: 0.4; \varepsilon: 0.6$	continuous t with df=1
Setting-57	200	75	$x: 0.4; \varepsilon: 0.6$	continuous t with df=1
Setting-58	500	50	$x: 0.4; \varepsilon: 0.6$	continuous t with df=1
Setting-59	500	125	$x: 0.4; \varepsilon: 0.6$	continuous t with df=1
Setting-60	500	187	$x: 0.4; \varepsilon: 0.6$	continuous t with df=1
Setting-61	200	20	$x: 0.4; \varepsilon: 0.6$	continuous t with df=2
Setting-62	200	50	$x: 0.4; \varepsilon: 0.6$	continuous t with df=2
Setting-63	200	75	$x: 0.4; \varepsilon: 0.6$	continuous t with df=2
Setting-64	500	50	$x: 0.4; \varepsilon: 0.6$	continuous t with df=2
Setting-65	500	125	$x: 0.4; \varepsilon: 0.6$	continuous t with df=2
Setting-66	500	187	$x: 0.4; \varepsilon: 0.6$	continuous t with df=2
Setting-67	50	10	$x: 0; \varepsilon: 0$	discrete mix $\mathcal{N}(0, 1)$ and $\mathcal{C}(0, 10)$ (90%; 10%)
Setting-68	100	10	$x: 0; \varepsilon: 0$	discrete mix $\mathcal{N}(0, 1)$ and $\mathcal{C}(0, 10)$ (90%; 10%)
Setting-69	200	10	$x: 0; \varepsilon: 0$	discrete mix $\mathcal{N}(0, 1)$ and $\mathcal{C}(0, 10)$ (90%; 10%)
Setting-70	500	10	$x: 0; \varepsilon: 0$	discrete mix $\mathcal{N}(0, 1)$ and $\mathcal{C}(0, 10)$ (90%; 10%)
Setting-71	1,000	10	$x: 0; \varepsilon: 0$	discrete mix $\mathcal{N}(0, 1)$ and $\mathcal{C}(0, 10)$ (90%; 10%)
Setting-72	2,000	10	$x: 0; \varepsilon: 0$	discrete mix $\mathcal{N}(0, 1)$ and $\mathcal{C}(0, 10)$ (90%; 10%)
Setting-73	5,000	10	$x: 0; \varepsilon: 0$	discrete mix $\mathcal{N}(0, 1)$ and $\mathcal{C}(0, 10)$ (90%; 10%)
Setting-74	10,000	10	$x: 0; \varepsilon: 0$	discrete mix $\mathcal{N}(0, 1)$ and $\mathcal{C}(0, 10)$ (90%; 10%)
Setting-75	20,000	10	$x: 0; \varepsilon: 0$	discrete mix $\mathcal{N}(0, 1)$ and $\mathcal{C}(0, 10)$ (90%; 10%)
Setting-76	50	10	$x: 0; \varepsilon: 0$	continuous t with df=1
Setting-77	100	10	$x: 0; \varepsilon: 0$	continuous t with df=1
Setting-78	200	10	$x: 0; \varepsilon: 0$	continuous t with df=1
Setting-79	500	10	$x: 0; \varepsilon: 0$	continuous t with df=1
Setting-80	1,000	10	$x: 0; \varepsilon: 0$	continuous t with df=1

Table A4: Simulation settings for scenarios with data generated from heavy-tailed error distributions and models fitted with a ridge prior on the regression parameters. (*continued*)

Setting	n	p	Correlation	Error Distribution
Setting-81	2,000	10	$x: 0; \varepsilon: 0$	continuous t with df=1
Setting-82	5,000	10	$x: 0; \varepsilon: 0$	continuous t with df=1
Setting-83	10,000	10	$x: 0; \varepsilon: 0$	continuous t with df=1
Setting-84	20,000	10	$x: 0; \varepsilon: 0$	continuous t with df=1
Setting-85	50	10	$x: 0; \varepsilon: 0$	continuous t with df=2
Setting-86	100	10	$x: 0; \varepsilon: 0$	continuous t with df=2
Setting-87	200	10	$x: 0; \varepsilon: 0$	continuous t with df=2
Setting-88	500	10	$x: 0; \varepsilon: 0$	continuous t with df=2
Setting-89	1,000	10	$x: 0; \varepsilon: 0$	continuous t with df=2
Setting-90	2,000	10	$x: 0; \varepsilon: 0$	continuous t with df=2
Setting-91	5,000	10	$x: 0; \varepsilon: 0$	continuous t with df=2
Setting-92	10,000	10	$x: 0; \varepsilon: 0$	continuous t with df=2
Setting-93	20,000	10	$x: 0; \varepsilon: 0$	continuous t with df=2

Table A5: Simulation settings for scenarios with data generated from moderate-tailed error distributions and models fitted with a ridge prior on the regression parameters.

Setting	n	p	Correlation	Error Distribution
Setting-1	100	20	$x: 0.2; \varepsilon: 0.3$	discrete mix $\mathcal{N}(0, 1)$ and $\mathcal{N}(0, 10^2)$ (99%; 1%)
Setting-2	100	50	$x: 0.2; \varepsilon: 0.3$	discrete mix $\mathcal{N}(0, 1)$ and $\mathcal{N}(0, 10^2)$ (99%; 1%)
Setting-3	100	75	$x: 0.2; \varepsilon: 0.3$	discrete mix $\mathcal{N}(0, 1)$ and $\mathcal{N}(0, 10^2)$ (99%; 1%)
Setting-4	250	50	$x: 0.2; \varepsilon: 0.3$	discrete mix $\mathcal{N}(0, 1)$ and $\mathcal{N}(0, 10^2)$ (99%; 1%)
Setting-5	250	125	$x: 0.2; \varepsilon: 0.3$	discrete mix $\mathcal{N}(0, 1)$ and $\mathcal{N}(0, 10^2)$ (99%; 1%)
Setting-6	250	187	$x: 0.2; \varepsilon: 0.3$	discrete mix $\mathcal{N}(0, 1)$ and $\mathcal{N}(0, 10^2)$ (99%; 1%)
Setting-7	100	20	$x: 0.2; \varepsilon: 0.3$	discrete mix $\mathcal{N}(0, 1)$ and $\mathcal{N}(0, 10^2)$ (95%; 5%)
Setting-8	100	50	$x: 0.2; \varepsilon: 0.3$	discrete mix $\mathcal{N}(0, 1)$ and $\mathcal{N}(0, 10^2)$ (95%; 5%)
Setting-9	100	75	$x: 0.2; \varepsilon: 0.3$	discrete mix $\mathcal{N}(0, 1)$ and $\mathcal{N}(0, 10^2)$ (95%; 5%)
Setting-10	250	50	$x: 0.2; \varepsilon: 0.3$	discrete mix $\mathcal{N}(0, 1)$ and $\mathcal{N}(0, 10^2)$ (95%; 5%)
Setting-11	250	125	$x: 0.2; \varepsilon: 0.3$	discrete mix $\mathcal{N}(0, 1)$ and $\mathcal{N}(0, 10^2)$ (95%; 5%)
Setting-12	250	187	$x: 0.2; \varepsilon: 0.3$	discrete mix $\mathcal{N}(0, 1)$ and $\mathcal{N}(0, 10^2)$ (95%; 5%)
Setting-13	100	20	$x: 0.2; \varepsilon: 0.3$	continuous t with df=4
Setting-14	100	50	$x: 0.2; \varepsilon: 0.3$	continuous t with df=4
Setting-15	100	75	$x: 0.2; \varepsilon: 0.3$	continuous t with df=4
Setting-16	250	50	$x: 0.2; \varepsilon: 0.3$	continuous t with df=4
Setting-17	250	125	$x: 0.2; \varepsilon: 0.3$	continuous t with df=4
Setting-18	250	187	$x: 0.2; \varepsilon: 0.3$	continuous t with df=4
Setting-19	100	20	$x: 0.2; \varepsilon: 0.3$	continuous t with df=8
Setting-20	100	50	$x: 0.2; \varepsilon: 0.3$	continuous t with df=8

Table A5: Simulation settings for scenarios with data generated from moderate-tailed error distributions and models fitted with a ridge prior on the regression parameters. (*continued*)

Setting	n	p	Correlation	Error Distribution
Setting-21	100	75	$x: 0.2; \varepsilon: 0.3$	continuous t with $df=8$
Setting-22	250	50	$x: 0.2; \varepsilon: 0.3$	continuous t with $df=8$
Setting-23	250	125	$x: 0.2; \varepsilon: 0.3$	continuous t with $df=8$
Setting-24	250	187	$x: 0.2; \varepsilon: 0.3$	continuous t with $df=8$
Setting-25	100	20	$x: 0.4; \varepsilon: 0.6$	discrete mix $\mathcal{N}(0, 1)$ and $\mathcal{N}(0, 10^2)$ (95%; 5%)
Setting-26	100	50	$x: 0.4; \varepsilon: 0.6$	discrete mix $\mathcal{N}(0, 1)$ and $\mathcal{N}(0, 10^2)$ (95%; 5%)
Setting-27	100	75	$x: 0.4; \varepsilon: 0.6$	discrete mix $\mathcal{N}(0, 1)$ and $\mathcal{N}(0, 10^2)$ (95%; 5%)
Setting-28	250	50	$x: 0.4; \varepsilon: 0.6$	discrete mix $\mathcal{N}(0, 1)$ and $\mathcal{N}(0, 10^2)$ (95%; 5%)
Setting-29	250	125	$x: 0.4; \varepsilon: 0.6$	discrete mix $\mathcal{N}(0, 1)$ and $\mathcal{N}(0, 10^2)$ (95%; 5%)
Setting-30	250	187	$x: 0.4; \varepsilon: 0.6$	discrete mix $\mathcal{N}(0, 1)$ and $\mathcal{N}(0, 10^2)$ (95%; 5%)
Setting-31	100	20	$x: 0.4; \varepsilon: 0.6$	continuous t with $df=4$
Setting-32	100	50	$x: 0.4; \varepsilon: 0.6$	continuous t with $df=4$
Setting-33	100	75	$x: 0.4; \varepsilon: 0.6$	continuous t with $df=4$
Setting-34	250	50	$x: 0.4; \varepsilon: 0.6$	continuous t with $df=4$
Setting-35	250	125	$x: 0.4; \varepsilon: 0.6$	continuous t with $df=4$
Setting-36	250	187	$x: 0.4; \varepsilon: 0.6$	continuous t with $df=4$
Setting-37	100	20	$x: 0.4; \varepsilon: 0.6$	continuous t with $df=8$
Setting-38	100	50	$x: 0.4; \varepsilon: 0.6$	continuous t with $df=8$
Setting-39	100	75	$x: 0.4; \varepsilon: 0.6$	continuous t with $df=8$
Setting-40	250	50	$x: 0.4; \varepsilon: 0.6$	continuous t with $df=8$
Setting-41	250	125	$x: 0.4; \varepsilon: 0.6$	continuous t with $df=8$
Setting-42	250	187	$x: 0.4; \varepsilon: 0.6$	continuous t with $df=8$
Setting-43	200	20	$x: 0.2; \varepsilon: 0.3$	discrete mix $\mathcal{N}(0, 1)$ and $\mathcal{N}(0, 10^2)$ (99%; 1%)
Setting-44	200	50	$x: 0.2; \varepsilon: 0.3$	discrete mix $\mathcal{N}(0, 1)$ and $\mathcal{N}(0, 10^2)$ (99%; 1%)
Setting-45	200	75	$x: 0.2; \varepsilon: 0.3$	discrete mix $\mathcal{N}(0, 1)$ and $\mathcal{N}(0, 10^2)$ (99%; 1%)
Setting-46	500	50	$x: 0.2; \varepsilon: 0.3$	discrete mix $\mathcal{N}(0, 1)$ and $\mathcal{N}(0, 10^2)$ (99%; 1%)
Setting-47	500	125	$x: 0.2; \varepsilon: 0.3$	discrete mix $\mathcal{N}(0, 1)$ and $\mathcal{N}(0, 10^2)$ (99%; 1%)
Setting-48	500	187	$x: 0.2; \varepsilon: 0.3$	discrete mix $\mathcal{N}(0, 1)$ and $\mathcal{N}(0, 10^2)$ (99%; 1%)
Setting-49	200	20	$x: 0.2; \varepsilon: 0.3$	discrete mix $\mathcal{N}(0, 1)$ and $\mathcal{N}(0, 10^2)$ (95%; 5%)
Setting-50	200	50	$x: 0.2; \varepsilon: 0.3$	discrete mix $\mathcal{N}(0, 1)$ and $\mathcal{N}(0, 10^2)$ (95%; 5%)
Setting-51	200	75	$x: 0.2; \varepsilon: 0.3$	discrete mix $\mathcal{N}(0, 1)$ and $\mathcal{N}(0, 10^2)$ (95%; 5%)
Setting-52	500	50	$x: 0.2; \varepsilon: 0.3$	discrete mix $\mathcal{N}(0, 1)$ and $\mathcal{N}(0, 10^2)$ (95%; 5%)
Setting-53	500	125	$x: 0.2; \varepsilon: 0.3$	discrete mix $\mathcal{N}(0, 1)$ and $\mathcal{N}(0, 10^2)$ (95%; 5%)
Setting-54	500	187	$x: 0.2; \varepsilon: 0.3$	discrete mix $\mathcal{N}(0, 1)$ and $\mathcal{N}(0, 10^2)$ (95%; 5%)
Setting-55	200	20	$x: 0.2; \varepsilon: 0.3$	continuous t with $df=4$
Setting-56	200	50	$x: 0.2; \varepsilon: 0.3$	continuous t with $df=4$
Setting-57	200	75	$x: 0.2; \varepsilon: 0.3$	continuous t with $df=4$
Setting-58	500	50	$x: 0.2; \varepsilon: 0.3$	continuous t with $df=4$
Setting-59	500	125	$x: 0.2; \varepsilon: 0.3$	continuous t with $df=4$
Setting-60	500	187	$x: 0.2; \varepsilon: 0.3$	continuous t with $df=4$

Table A5: Simulation settings for scenarios with data generated from moderate-tailed error distributions and models fitted with a ridge prior on the regression parameters. (*continued*)

Setting	n	p	Correlation	Error Distribution
Setting-61	200	20	$x: 0.2; \varepsilon: 0.3$	continuous t with $df=8$
Setting-62	200	50	$x: 0.2; \varepsilon: 0.3$	continuous t with $df=8$
Setting-63	200	75	$x: 0.2; \varepsilon: 0.3$	continuous t with $df=8$
Setting-64	500	50	$x: 0.2; \varepsilon: 0.3$	continuous t with $df=8$
Setting-65	500	125	$x: 0.2; \varepsilon: 0.3$	continuous t with $df=8$
Setting-66	500	187	$x: 0.2; \varepsilon: 0.3$	continuous t with $df=8$
Setting-67	200	20	$x: 0.4; \varepsilon: 0.6$	discrete mix $\mathcal{N}(0, 1)$ and $\mathcal{N}(0, 10^2)$ (99%; 1%)
Setting-68	200	50	$x: 0.4; \varepsilon: 0.6$	discrete mix $\mathcal{N}(0, 1)$ and $\mathcal{N}(0, 10^2)$ (99%; 1%)
Setting-69	200	75	$x: 0.4; \varepsilon: 0.6$	discrete mix $\mathcal{N}(0, 1)$ and $\mathcal{N}(0, 10^2)$ (99%; 1%)
Setting-70	500	50	$x: 0.4; \varepsilon: 0.6$	discrete mix $\mathcal{N}(0, 1)$ and $\mathcal{N}(0, 10^2)$ (99%; 1%)
Setting-71	500	125	$x: 0.4; \varepsilon: 0.6$	discrete mix $\mathcal{N}(0, 1)$ and $\mathcal{N}(0, 10^2)$ (99%; 1%)
Setting-72	500	187	$x: 0.4; \varepsilon: 0.6$	discrete mix $\mathcal{N}(0, 1)$ and $\mathcal{N}(0, 10^2)$ (99%; 1%)
Setting-73	200	20	$x: 0.4; \varepsilon: 0.6$	discrete mix $\mathcal{N}(0, 1)$ and $\mathcal{N}(0, 10^2)$ (95%; 5%)
Setting-74	200	50	$x: 0.4; \varepsilon: 0.6$	discrete mix $\mathcal{N}(0, 1)$ and $\mathcal{N}(0, 10^2)$ (95%; 5%)
Setting-75	200	75	$x: 0.4; \varepsilon: 0.6$	discrete mix $\mathcal{N}(0, 1)$ and $\mathcal{N}(0, 10^2)$ (95%; 5%)
Setting-76	500	50	$x: 0.4; \varepsilon: 0.6$	discrete mix $\mathcal{N}(0, 1)$ and $\mathcal{N}(0, 10^2)$ (95%; 5%)
Setting-77	500	125	$x: 0.4; \varepsilon: 0.6$	discrete mix $\mathcal{N}(0, 1)$ and $\mathcal{N}(0, 10^2)$ (95%; 5%)
Setting-78	500	187	$x: 0.4; \varepsilon: 0.6$	discrete mix $\mathcal{N}(0, 1)$ and $\mathcal{N}(0, 10^2)$ (95%; 5%)
Setting-79	200	20	$x: 0.4; \varepsilon: 0.6$	continuous t with $df=4$
Setting-80	200	50	$x: 0.4; \varepsilon: 0.6$	continuous t with $df=4$
Setting-81	200	75	$x: 0.4; \varepsilon: 0.6$	continuous t with $df=4$
Setting-82	500	50	$x: 0.4; \varepsilon: 0.6$	continuous t with $df=4$
Setting-83	500	125	$x: 0.4; \varepsilon: 0.6$	continuous t with $df=4$
Setting-84	500	187	$x: 0.4; \varepsilon: 0.6$	continuous t with $df=4$
Setting-85	200	20	$x: 0.4; \varepsilon: 0.6$	continuous t with $df=8$
Setting-86	200	50	$x: 0.4; \varepsilon: 0.6$	continuous t with $df=8$
Setting-87	200	75	$x: 0.4; \varepsilon: 0.6$	continuous t with $df=8$
Setting-88	500	50	$x: 0.4; \varepsilon: 0.6$	continuous t with $df=8$
Setting-89	500	125	$x: 0.4; \varepsilon: 0.6$	continuous t with $df=8$
Setting-90	500	187	$x: 0.4; \varepsilon: 0.6$	continuous t with $df=8$
Setting-91	50	10	$x: 0; \varepsilon: 0$	discrete mix $\mathcal{N}(0, 1)$ and $\mathcal{C}(0, 10)$ (99%; 1%)
Setting-92	100	10	$x: 0; \varepsilon: 0$	discrete mix $\mathcal{N}(0, 1)$ and $\mathcal{C}(0, 10)$ (99%; 1%)
Setting-93	200	10	$x: 0; \varepsilon: 0$	discrete mix $\mathcal{N}(0, 1)$ and $\mathcal{C}(0, 10)$ (99%; 1%)
Setting-94	500	10	$x: 0; \varepsilon: 0$	discrete mix $\mathcal{N}(0, 1)$ and $\mathcal{C}(0, 10)$ (99%; 1%)
Setting-95	1,000	10	$x: 0; \varepsilon: 0$	discrete mix $\mathcal{N}(0, 1)$ and $\mathcal{C}(0, 10)$ (99%; 1%)
Setting-96	2,000	10	$x: 0; \varepsilon: 0$	discrete mix $\mathcal{N}(0, 1)$ and $\mathcal{C}(0, 10)$ (99%; 1%)
Setting-97	5,000	10	$x: 0; \varepsilon: 0$	discrete mix $\mathcal{N}(0, 1)$ and $\mathcal{C}(0, 10)$ (99%; 1%)
Setting-98	10,000	10	$x: 0; \varepsilon: 0$	discrete mix $\mathcal{N}(0, 1)$ and $\mathcal{C}(0, 10)$ (99%; 1%)
Setting-99	20,000	10	$x: 0; \varepsilon: 0$	discrete mix $\mathcal{N}(0, 1)$ and $\mathcal{C}(0, 10)$ (99%; 1%)
Setting-100	50	10	$x: 0; \varepsilon: 0$	discrete mix $\mathcal{N}(0, 1)$ and $\mathcal{C}(0, 10)$ (95%; 5%)

Table A5: Simulation settings for scenarios with data generated from moderate-tailed error distributions and models fitted with a ridge prior on the regression parameters. (*continued*)

Setting	n	p	Correlation	Error Distribution
Setting-101	100	10	$x: 0; \varepsilon: 0$	discrete mix $\mathcal{N}(0, 1)$ and $\mathcal{C}(0, 10)$ (95%; 5%)
Setting-102	200	10	$x: 0; \varepsilon: 0$	discrete mix $\mathcal{N}(0, 1)$ and $\mathcal{C}(0, 10)$ (95%; 5%)
Setting-103	500	10	$x: 0; \varepsilon: 0$	discrete mix $\mathcal{N}(0, 1)$ and $\mathcal{C}(0, 10)$ (95%; 5%)
Setting-104	1,000	10	$x: 0; \varepsilon: 0$	discrete mix $\mathcal{N}(0, 1)$ and $\mathcal{C}(0, 10)$ (95%; 5%)
Setting-105	2,000	10	$x: 0; \varepsilon: 0$	discrete mix $\mathcal{N}(0, 1)$ and $\mathcal{C}(0, 10)$ (95%; 5%)
Setting-106	5,000	10	$x: 0; \varepsilon: 0$	discrete mix $\mathcal{N}(0, 1)$ and $\mathcal{C}(0, 10)$ (95%; 5%)
Setting-107	10,000	10	$x: 0; \varepsilon: 0$	discrete mix $\mathcal{N}(0, 1)$ and $\mathcal{C}(0, 10)$ (95%; 5%)
Setting-108	20,000	10	$x: 0; \varepsilon: 0$	discrete mix $\mathcal{N}(0, 1)$ and $\mathcal{C}(0, 10)$ (95%; 5%)
Setting-109	50	10	$x: 0; \varepsilon: 0$	continuous t with df=4
Setting-110	100	10	$x: 0; \varepsilon: 0$	continuous t with df=4
Setting-111	200	10	$x: 0; \varepsilon: 0$	continuous t with df=4
Setting-112	500	10	$x: 0; \varepsilon: 0$	continuous t with df=4
Setting-113	1,000	10	$x: 0; \varepsilon: 0$	continuous t with df=4
Setting-114	2,000	10	$x: 0; \varepsilon: 0$	continuous t with df=4
Setting-115	5,000	10	$x: 0; \varepsilon: 0$	continuous t with df=4
Setting-116	10,000	10	$x: 0; \varepsilon: 0$	continuous t with df=4
Setting-117	20,000	10	$x: 0; \varepsilon: 0$	continuous t with df=4
Setting-118	50	10	$x: 0; \varepsilon: 0$	continuous t with df=8
Setting-119	100	10	$x: 0; \varepsilon: 0$	continuous t with df=8
Setting-120	200	10	$x: 0; \varepsilon: 0$	continuous t with df=8
Setting-121	500	10	$x: 0; \varepsilon: 0$	continuous t with df=8
Setting-122	1,000	10	$x: 0; \varepsilon: 0$	continuous t with df=8
Setting-123	2,000	10	$x: 0; \varepsilon: 0$	continuous t with df=8
Setting-124	5,000	10	$x: 0; \varepsilon: 0$	continuous t with df=8
Setting-125	10,000	10	$x: 0; \varepsilon: 0$	continuous t with df=8
Setting-126	20,000	10	$x: 0; \varepsilon: 0$	continuous t with df=8

Table A6: Simulation settings for scenarios with data generated from thin-tailed error distributions and models fitted with a ridge prior on the regression parameters.

Setting	n	p	Correlation	Error Distribution
Setting-1	100	20	$x: 0.2; \varepsilon: 0.3$	continuous $\mathcal{N}(0, 1)$
Setting-2	100	50	$x: 0.2; \varepsilon: 0.3$	continuous $\mathcal{N}(0, 1)$
Setting-3	100	75	$x: 0.2; \varepsilon: 0.3$	continuous $\mathcal{N}(0, 1)$
Setting-4	250	50	$x: 0.2; \varepsilon: 0.3$	continuous $\mathcal{N}(0, 1)$
Setting-5	250	125	$x: 0.2; \varepsilon: 0.3$	continuous $\mathcal{N}(0, 1)$
Setting-6	250	187	$x: 0.2; \varepsilon: 0.3$	continuous $\mathcal{N}(0, 1)$
Setting-7	100	20	$x: 0.4; \varepsilon: 0.6$	continuous $\mathcal{N}(0, 1)$

Table A6: Simulation settings for scenarios with data generated from thin-tailed error distributions and models fitted with a ridge prior on the regression parameters. (*continued*)

Setting	n	p	Correlation	Error Distribution
Setting-8	100	50	$x: 0.4; \varepsilon: 0.6$	continuous $\mathcal{N}(0, 1)$
Setting-9	100	75	$x: 0.4; \varepsilon: 0.6$	continuous $\mathcal{N}(0, 1)$
Setting-10	250	50	$x: 0.4; \varepsilon: 0.6$	continuous $\mathcal{N}(0, 1)$
Setting-11	250	125	$x: 0.4; \varepsilon: 0.6$	continuous $\mathcal{N}(0, 1)$
Setting-12	250	187	$x: 0.4; \varepsilon: 0.6$	continuous $\mathcal{N}(0, 1)$
Setting-13	200	20	$x: 0.2; \varepsilon: 0.3$	continuous $\mathcal{N}(0, 1)$
Setting-14	200	50	$x: 0.2; \varepsilon: 0.3$	continuous $\mathcal{N}(0, 1)$
Setting-15	200	75	$x: 0.2; \varepsilon: 0.3$	continuous $\mathcal{N}(0, 1)$
Setting-16	500	50	$x: 0.2; \varepsilon: 0.3$	continuous $\mathcal{N}(0, 1)$
Setting-17	500	125	$x: 0.2; \varepsilon: 0.3$	continuous $\mathcal{N}(0, 1)$
Setting-18	500	187	$x: 0.2; \varepsilon: 0.3$	continuous $\mathcal{N}(0, 1)$
Setting-19	200	20	$x: 0.4; \varepsilon: 0.6$	continuous $\mathcal{N}(0, 1)$
Setting-20	200	50	$x: 0.4; \varepsilon: 0.6$	continuous $\mathcal{N}(0, 1)$
Setting-21	200	75	$x: 0.4; \varepsilon: 0.6$	continuous $\mathcal{N}(0, 1)$
Setting-22	500	50	$x: 0.4; \varepsilon: 0.6$	continuous $\mathcal{N}(0, 1)$
Setting-23	500	125	$x: 0.4; \varepsilon: 0.6$	continuous $\mathcal{N}(0, 1)$
Setting-24	500	187	$x: 0.4; \varepsilon: 0.6$	continuous $\mathcal{N}(0, 1)$
Setting-25	50	10	$x: 0; \varepsilon: 0$	continuous $\mathcal{N}(0, 1)$
Setting-26	100	10	$x: 0; \varepsilon: 0$	continuous $\mathcal{N}(0, 1)$
Setting-27	200	10	$x: 0; \varepsilon: 0$	continuous $\mathcal{N}(0, 1)$
Setting-28	500	10	$x: 0; \varepsilon: 0$	continuous $\mathcal{N}(0, 1)$
Setting-29	1,000	10	$x: 0; \varepsilon: 0$	continuous $\mathcal{N}(0, 1)$
Setting-30	2,000	10	$x: 0; \varepsilon: 0$	continuous $\mathcal{N}(0, 1)$
Setting-31	5,000	10	$x: 0; \varepsilon: 0$	continuous $\mathcal{N}(0, 1)$
Setting-32	10,000	10	$x: 0; \varepsilon: 0$	continuous $\mathcal{N}(0, 1)$
Setting-33	20,000	10	$x: 0; \varepsilon: 0$	continuous $\mathcal{N}(0, 1)$

Table A7: Simulation settings for scenarios with data generated from heavy-tailed error distributions and models fitted with a spike and slab prior on the regression parameters.

Setting	n	p	Correlation	Error Distribution
Setting-1	75	100	$x: 0; \varepsilon: 0$	discrete mix $\mathcal{N}(0, 1)$ and $\mathcal{C}(0, 10)$ (90%; 10%)
Setting-2	75	200	$x: 0; \varepsilon: 0$	discrete mix $\mathcal{N}(0, 1)$ and $\mathcal{C}(0, 10)$ (90%; 10%)
Setting-3	75	250	$x: 0; \varepsilon: 0$	discrete mix $\mathcal{N}(0, 1)$ and $\mathcal{C}(0, 10)$ (90%; 10%)
Setting-4	75	100	$x: 0; \varepsilon: 0$	continuous t with df=1
Setting-5	75	200	$x: 0; \varepsilon: 0$	continuous t with df=1
Setting-6	75	250	$x: 0; \varepsilon: 0$	continuous t with df=1
Setting-7	75	100	$x: 0; \varepsilon: 0$	continuous t with df=2

Table A7: Simulation settings for scenarios with data generated from heavy-tailed error distributions and models fitted with a spike and slab prior on the regression parameters. (*continued*)

Setting	n	p	Correlation	Error Distribution
Setting-8	75	200	$x: 0; \varepsilon: 0$	continuous t with $df=2$
Setting-9	75	250	$x: 0; \varepsilon: 0$	continuous t with $df=2$
Setting-10	75	100	$x: 0.2; \varepsilon: 0.3$	discrete mix $\mathcal{N}(0, 1)$ and $\mathcal{C}(0, 10)$ (90%; 10%)
Setting-11	75	200	$x: 0.2; \varepsilon: 0.3$	discrete mix $\mathcal{N}(0, 1)$ and $\mathcal{C}(0, 10)$ (90%; 10%)
Setting-12	75	250	$x: 0.2; \varepsilon: 0.3$	discrete mix $\mathcal{N}(0, 1)$ and $\mathcal{C}(0, 10)$ (90%; 10%)
Setting-13	100	100	$x: 0.2; \varepsilon: 0.3$	discrete mix $\mathcal{N}(0, 1)$ and $\mathcal{C}(0, 10)$ (90%; 10%)
Setting-14	100	200	$x: 0.2; \varepsilon: 0.3$	discrete mix $\mathcal{N}(0, 1)$ and $\mathcal{C}(0, 10)$ (90%; 10%)
Setting-15	100	250	$x: 0.2; \varepsilon: 0.3$	discrete mix $\mathcal{N}(0, 1)$ and $\mathcal{C}(0, 10)$ (90%; 10%)
Setting-16	75	100	$x: 0.2; \varepsilon: 0.3$	continuous t with $df=1$
Setting-17	75	200	$x: 0.2; \varepsilon: 0.3$	continuous t with $df=1$
Setting-18	75	250	$x: 0.2; \varepsilon: 0.3$	continuous t with $df=1$
Setting-19	100	100	$x: 0.2; \varepsilon: 0.3$	continuous t with $df=1$
Setting-20	100	200	$x: 0.2; \varepsilon: 0.3$	continuous t with $df=1$
Setting-21	100	250	$x: 0.2; \varepsilon: 0.3$	continuous t with $df=1$
Setting-22	75	100	$x: 0.2; \varepsilon: 0.3$	continuous t with $df=2$
Setting-23	75	200	$x: 0.2; \varepsilon: 0.3$	continuous t with $df=2$
Setting-24	75	250	$x: 0.2; \varepsilon: 0.3$	continuous t with $df=2$
Setting-25	100	100	$x: 0.2; \varepsilon: 0.3$	continuous t with $df=2$
Setting-26	100	200	$x: 0.2; \varepsilon: 0.3$	continuous t with $df=2$
Setting-27	100	250	$x: 0.2; \varepsilon: 0.3$	continuous t with $df=2$
Setting-28	75	100	$x: 0.4; \varepsilon: 0.6$	discrete mix $\mathcal{N}(0, 1)$ and $\mathcal{C}(0, 10)$ (90%; 10%)
Setting-29	75	200	$x: 0.4; \varepsilon: 0.6$	discrete mix $\mathcal{N}(0, 1)$ and $\mathcal{C}(0, 10)$ (90%; 10%)
Setting-30	75	250	$x: 0.4; \varepsilon: 0.6$	discrete mix $\mathcal{N}(0, 1)$ and $\mathcal{C}(0, 10)$ (90%; 10%)
Setting-31	100	100	$x: 0.4; \varepsilon: 0.6$	discrete mix $\mathcal{N}(0, 1)$ and $\mathcal{C}(0, 10)$ (90%; 10%)
Setting-32	100	200	$x: 0.4; \varepsilon: 0.6$	discrete mix $\mathcal{N}(0, 1)$ and $\mathcal{C}(0, 10)$ (90%; 10%)
Setting-33	100	250	$x: 0.4; \varepsilon: 0.6$	discrete mix $\mathcal{N}(0, 1)$ and $\mathcal{C}(0, 10)$ (90%; 10%)
Setting-34	75	100	$x: 0.4; \varepsilon: 0.6$	continuous t with $df=1$
Setting-35	75	200	$x: 0.4; \varepsilon: 0.6$	continuous t with $df=1$
Setting-36	75	250	$x: 0.4; \varepsilon: 0.6$	continuous t with $df=1$
Setting-37	100	100	$x: 0.4; \varepsilon: 0.6$	continuous t with $df=1$
Setting-38	100	200	$x: 0.4; \varepsilon: 0.6$	continuous t with $df=1$
Setting-39	100	250	$x: 0.4; \varepsilon: 0.6$	continuous t with $df=1$
Setting-40	75	100	$x: 0.4; \varepsilon: 0.6$	continuous t with $df=2$
Setting-41	75	200	$x: 0.4; \varepsilon: 0.6$	continuous t with $df=2$
Setting-42	75	250	$x: 0.4; \varepsilon: 0.6$	continuous t with $df=2$
Setting-43	100	100	$x: 0.4; \varepsilon: 0.6$	continuous t with $df=2$
Setting-44	100	200	$x: 0.4; \varepsilon: 0.6$	continuous t with $df=2$
Setting-45	100	250	$x: 0.4; \varepsilon: 0.6$	continuous t with $df=2$

Table A8: Simulation settings for scenarios with data generated from moderate-tailed error distributions and models fitted with a spike and slab prior on the regression parameters.

Setting	n	p	Correlation	Error Distribution
Setting-1	75	100	$x: 0; \varepsilon: 0$	discrete mix $\mathcal{N}(0, 1)$ and $\mathcal{C}(0, 10)$ (99%; 1%)
Setting-2	75	200	$x: 0; \varepsilon: 0$	discrete mix $\mathcal{N}(0, 1)$ and $\mathcal{C}(0, 10)$ (99%; 1%)
Setting-3	75	250	$x: 0; \varepsilon: 0$	discrete mix $\mathcal{N}(0, 1)$ and $\mathcal{C}(0, 10)$ (99%; 1%)
Setting-4	75	100	$x: 0; \varepsilon: 0$	discrete mix $\mathcal{N}(0, 1)$ and $\mathcal{C}(0, 10)$ (95%; 5%)
Setting-5	75	200	$x: 0; \varepsilon: 0$	discrete mix $\mathcal{N}(0, 1)$ and $\mathcal{C}(0, 10)$ (95%; 5%)
Setting-6	75	250	$x: 0; \varepsilon: 0$	discrete mix $\mathcal{N}(0, 1)$ and $\mathcal{C}(0, 10)$ (95%; 5%)
Setting-7	75	100	$x: 0; \varepsilon: 0$	continuous t with df=4
Setting-8	75	200	$x: 0; \varepsilon: 0$	continuous t with df=4
Setting-9	75	250	$x: 0; \varepsilon: 0$	continuous t with df=4
Setting-10	75	100	$x: 0; \varepsilon: 0$	continuous t with df=8
Setting-11	75	200	$x: 0; \varepsilon: 0$	continuous t with df=8
Setting-12	75	250	$x: 0; \varepsilon: 0$	continuous t with df=8
Setting-13	75	100	$x: 0.2; \varepsilon: 0.3$	discrete mix $\mathcal{N}(0, 1)$ and $\mathcal{C}(0, 10)$ (99%; 1%)
Setting-14	75	200	$x: 0.2; \varepsilon: 0.3$	discrete mix $\mathcal{N}(0, 1)$ and $\mathcal{C}(0, 10)$ (99%; 1%)
Setting-15	75	250	$x: 0.2; \varepsilon: 0.3$	discrete mix $\mathcal{N}(0, 1)$ and $\mathcal{C}(0, 10)$ (99%; 1%)
Setting-16	100	100	$x: 0.2; \varepsilon: 0.3$	discrete mix $\mathcal{N}(0, 1)$ and $\mathcal{C}(0, 10)$ (99%; 1%)
Setting-17	100	200	$x: 0.2; \varepsilon: 0.3$	discrete mix $\mathcal{N}(0, 1)$ and $\mathcal{C}(0, 10)$ (99%; 1%)
Setting-18	100	250	$x: 0.2; \varepsilon: 0.3$	discrete mix $\mathcal{N}(0, 1)$ and $\mathcal{C}(0, 10)$ (99%; 1%)
Setting-19	75	100	$x: 0.2; \varepsilon: 0.3$	discrete mix $\mathcal{N}(0, 1)$ and $\mathcal{C}(0, 10)$ (95%; 5%)
Setting-20	75	200	$x: 0.2; \varepsilon: 0.3$	discrete mix $\mathcal{N}(0, 1)$ and $\mathcal{C}(0, 10)$ (95%; 5%)
Setting-21	75	250	$x: 0.2; \varepsilon: 0.3$	discrete mix $\mathcal{N}(0, 1)$ and $\mathcal{C}(0, 10)$ (95%; 5%)
Setting-22	100	100	$x: 0.2; \varepsilon: 0.3$	discrete mix $\mathcal{N}(0, 1)$ and $\mathcal{C}(0, 10)$ (95%; 5%)
Setting-23	100	200	$x: 0.2; \varepsilon: 0.3$	discrete mix $\mathcal{N}(0, 1)$ and $\mathcal{C}(0, 10)$ (95%; 5%)
Setting-24	100	250	$x: 0.2; \varepsilon: 0.3$	discrete mix $\mathcal{N}(0, 1)$ and $\mathcal{C}(0, 10)$ (95%; 5%)
Setting-25	75	100	$x: 0.2; \varepsilon: 0.3$	continuous t with df=4
Setting-26	75	200	$x: 0.2; \varepsilon: 0.3$	continuous t with df=4
Setting-27	75	250	$x: 0.2; \varepsilon: 0.3$	continuous t with df=4
Setting-28	100	100	$x: 0.2; \varepsilon: 0.3$	continuous t with df=4
Setting-29	100	200	$x: 0.2; \varepsilon: 0.3$	continuous t with df=4
Setting-30	100	250	$x: 0.2; \varepsilon: 0.3$	continuous t with df=4
Setting-31	75	100	$x: 0.2; \varepsilon: 0.3$	continuous t with df=8
Setting-32	75	200	$x: 0.2; \varepsilon: 0.3$	continuous t with df=8
Setting-33	75	250	$x: 0.2; \varepsilon: 0.3$	continuous t with df=8
Setting-34	100	100	$x: 0.2; \varepsilon: 0.3$	continuous t with df=8
Setting-35	100	200	$x: 0.2; \varepsilon: 0.3$	continuous t with df=8
Setting-36	100	250	$x: 0.2; \varepsilon: 0.3$	continuous t with df=8
Setting-37	75	100	$x: 0.4; \varepsilon: 0.6$	discrete mix $\mathcal{N}(0, 1)$ and $\mathcal{C}(0, 10)$ (99%; 1%)
Setting-38	75	200	$x: 0.4; \varepsilon: 0.6$	discrete mix $\mathcal{N}(0, 1)$ and $\mathcal{C}(0, 10)$ (99%; 1%)
Setting-39	75	250	$x: 0.4; \varepsilon: 0.6$	discrete mix $\mathcal{N}(0, 1)$ and $\mathcal{C}(0, 10)$ (99%; 1%)
Setting-40	100	100	$x: 0.4; \varepsilon: 0.6$	discrete mix $\mathcal{N}(0, 1)$ and $\mathcal{C}(0, 10)$ (99%; 1%)

Table A8: Simulation settings for scenarios with data generated from moderate-tailed error distributions and models fitted with a spike and slab prior on the regression parameters. (*continued*)

Setting	n	p	Correlation	Error Distribution
Setting-41	100	200	$x: 0.4; \varepsilon: 0.6$	discrete mix $\mathcal{N}(0, 1)$ and $\mathcal{C}(0, 10)$ (99%; 1%)
Setting-42	100	250	$x: 0.4; \varepsilon: 0.6$	discrete mix $\mathcal{N}(0, 1)$ and $\mathcal{C}(0, 10)$ (99%; 1%)
Setting-43	75	100	$x: 0.4; \varepsilon: 0.6$	discrete mix $\mathcal{N}(0, 1)$ and $\mathcal{C}(0, 10)$ (95%; 5%)
Setting-44	75	200	$x: 0.4; \varepsilon: 0.6$	discrete mix $\mathcal{N}(0, 1)$ and $\mathcal{C}(0, 10)$ (95%; 5%)
Setting-45	75	250	$x: 0.4; \varepsilon: 0.6$	discrete mix $\mathcal{N}(0, 1)$ and $\mathcal{C}(0, 10)$ (95%; 5%)
Setting-46	100	100	$x: 0.4; \varepsilon: 0.6$	discrete mix $\mathcal{N}(0, 1)$ and $\mathcal{C}(0, 10)$ (95%; 5%)
Setting-47	100	200	$x: 0.4; \varepsilon: 0.6$	discrete mix $\mathcal{N}(0, 1)$ and $\mathcal{C}(0, 10)$ (95%; 5%)
Setting-48	100	250	$x: 0.4; \varepsilon: 0.6$	discrete mix $\mathcal{N}(0, 1)$ and $\mathcal{C}(0, 10)$ (95%; 5%)
Setting-49	75	100	$x: 0.4; \varepsilon: 0.6$	continuous t with df=4
Setting-50	75	200	$x: 0.4; \varepsilon: 0.6$	continuous t with df=4
Setting-51	75	250	$x: 0.4; \varepsilon: 0.6$	continuous t with df=4
Setting-52	100	100	$x: 0.4; \varepsilon: 0.6$	continuous t with df=4
Setting-53	100	200	$x: 0.4; \varepsilon: 0.6$	continuous t with df=4
Setting-54	100	250	$x: 0.4; \varepsilon: 0.6$	continuous t with df=4
Setting-55	75	100	$x: 0.4; \varepsilon: 0.6$	continuous t with df=8
Setting-56	75	200	$x: 0.4; \varepsilon: 0.6$	continuous t with df=8
Setting-57	75	250	$x: 0.4; \varepsilon: 0.6$	continuous t with df=8
Setting-58	100	100	$x: 0.4; \varepsilon: 0.6$	continuous t with df=8
Setting-59	100	200	$x: 0.4; \varepsilon: 0.6$	continuous t with df=8
Setting-60	100	250	$x: 0.4; \varepsilon: 0.6$	continuous t with df=8

Table A9: Simulation settings for scenarios with data generated from thin-tailed error distributions and models fitted with a spike and slab prior on the regression parameters.

Setting	n	p	Correlation	Error Distribution
Setting-1	75	100	$x: 0; \varepsilon: 0$	continuous $\mathcal{N}(0, 1)$
Setting-2	75	200	$x: 0; \varepsilon: 0$	continuous $\mathcal{N}(0, 1)$
Setting-3	75	250	$x: 0; \varepsilon: 0$	continuous $\mathcal{N}(0, 1)$
Setting-4	75	100	$x: 0.2; \varepsilon: 0.3$	continuous $\mathcal{N}(0, 1)$
Setting-5	75	200	$x: 0.2; \varepsilon: 0.3$	continuous $\mathcal{N}(0, 1)$
Setting-6	75	250	$x: 0.2; \varepsilon: 0.3$	continuous $\mathcal{N}(0, 1)$
Setting-7	100	100	$x: 0.2; \varepsilon: 0.3$	continuous $\mathcal{N}(0, 1)$
Setting-8	100	200	$x: 0.2; \varepsilon: 0.3$	continuous $\mathcal{N}(0, 1)$
Setting-9	100	250	$x: 0.2; \varepsilon: 0.3$	continuous $\mathcal{N}(0, 1)$
Setting-10	75	100	$x: 0.4; \varepsilon: 0.6$	continuous $\mathcal{N}(0, 1)$
Setting-11	75	200	$x: 0.4; \varepsilon: 0.6$	continuous $\mathcal{N}(0, 1)$
Setting-12	75	250	$x: 0.4; \varepsilon: 0.6$	continuous $\mathcal{N}(0, 1)$
Setting-13	100	100	$x: 0.4; \varepsilon: 0.6$	continuous $\mathcal{N}(0, 1)$

Table A9: Simulation settings for scenarios with data generated from thin-tailed error distributions and models fitted with a spike and slab prior on the regression parameters. (*continued*)

Setting	n	p	Correlation	Error Distribution
Setting-14	100	200	$x: 0.4; \varepsilon: 0.6$	continuous $\mathcal{N}(0, 1)$
Setting-15	100	250	$x: 0.4; \varepsilon: 0.6$	continuous $\mathcal{N}(0, 1)$